

---

Identification and characterisation of ependyma-  
specific genes and their proteins

Identifizierung und Charakterisierung von  
Ependym-spezifischen Genen und deren Proteine

DISSERTATION

der Fakultät für Chemie und Pharmazie  
der Eberhard-Karls-Universität Tübingen

zur Erlangung des Grades eines Doktors  
der Naturwissenschaften

2007

vorgelegt von

Wolfgang Hirschner

---

**Tag der mündlichen Prüfung: 13. 04. 2007**

**Dekan: Prof. Dr. Lars Wesemann**

**1. Berichterstatter: Prof. Dr. B. Hamprecht**

**2. Berichterstatter: Prof. Dr. H. Wiesinger**

---

## Danksagung

Herzlichen Dank an Prof. Dr. Bernd Hamprecht für seine permanente Diskussionsbereitschaft, die zahlreichen Anregungen und sein Engagement, das es mir ermöglicht hat mehrere internationale Kongresse besuchen zu dürfen.

Vielen Dank an Prof. Dr. Heinrich Wiesinger für die Übernahme des Koreferats und seine hoch interessante Vorlesung „Enzymologie des Nervensystems“.

Bei Dr. Stephan Verleysdonk bedanke ich mich herzlich für seine überaus engagierte Betreuung, das stetige Interesse am Erfolg des Projektes und für seine Motivationskünste, die mich auch in schwierigen Phasen der Arbeit nicht den Mut verlieren ließen. Der Erfolg dieser Arbeit basiert wesentlich auf seiner außergewöhnlichen Unterstützung

Danke an Carina Kramer und Dr. Hans-Martin Pogoda für die Durchführung der Zebrafisch Experimente, die entscheidend zum Erfolg des Projektes beigetragen haben.

Elke Maier danke ich für die perfekte Anfertigung der zahlreichen Hirn-Kryoschnitte.

Danke an Prof. Dr. Günther Jung und Prof. Dr. Karl-Heinz Wiesmüller für die Synthese der Peptide.

Dr. Matthias Lautner danke ich für die Bereitstellung des Bullenspermas.

Dr. Mirna Rapp sage ich Danke für die Bereitstellung des Thrombins.

Prof. Dr. Jürgen Seitz und Gerhard Jennemann sowie Prof. Dr. Andreas Reichenbach und Dr. Wolfgang Härtig danke ich für die freundliche Aufnahme

---

in ihren Arbeitsgruppen, ihr Interesse an meiner Arbeit und die wissenschaftliche Betreuung.

Dem Arbeitskreis von Prof. Dr. Gabriele Dodt, insbesondere Dr. Katja Nau sowie der Arbeitsgruppe von Prof. Dr. Frank Madeo, vor allem Dr. Eva Herker und Dr. Silke Wissing danke ich für tatkräftige Hilfe bei der Durchführung des Yeast-Two-Hybrid Screens.

Bei Dr. Brigitte Pfeiffer-Guglielmi bedanke ich mich für die Bereitstellung des Glycogenphosphorylase Antikörpers und die hilfreichen Ratschläge für die Anfertigung der Kryopräparate und die Durchführung der Immunhistochemie.

Ulrike Thiess danke ich für die professionelle technische Durchführung der Lightcycler - Analysen und ihren unermüdlichen Einsatz.

Danke an Barbara Birk für die exzellente technische Unterstützung und die zahlreichen am Wochenende durchgeführten Medienwechsel.

Mein Dank gilt Ruth Schmid für die Überlassung der selektionierten Astroglia Kultur.

Herzlichen Dank an die Doktoranden des Arbeitskreises von Dr. Stephan Verleysdonk, Bhawani Shankar Kowtharapu und Daniela Scheible für die gemeinsam initiierten und durchgeführten Projekte, sowie an meine weiteren Kollegen Dr. Benedikt Dolderer, Klaus Frommer, Steffen Kistner, Felix Tritschler und Annette Schwetzler für die hervorragende Zusammenarbeit.

Dr. Radovan Murin sage ich vielen Danke für die Fragen, Denkanstöße und Kommentare, sowie für seine Zeit und Geduld bei der Bewältigung der Tücken des Microsoft-Office-Paketes. Danke auch für die Bereitstellung des Druckers zum Ausdruck dieser Arbeit.

Danke an Dr. John Wellard für seine wissenschaftliche und mentale Unterstützung and for the demonstration how rich the english language can be.

---

Danke auch an Prof. Dr. Ralf Dringen und seinen Mitarbeitern Dr. Johannes Hirrlinger, Dr. Hans-Herrmann Höpken, Julia Hullmann, Tobias Minich, Petra Pawlowski, Dr. Cornelia Rüdiger und Jens Waak für ihre permanente Kooperationsbereitschaft.

Vielen Dank an die Mitarbeiter des Lehrstuhl I Claudia Heberle, Hermann Liggesmeyer, Erika Mikeler, Katharina Rehn und Heide Schmid für ihre ständige Hilfsbereitschaft und ihr offenes Ohr für meine Anliegen.

Einen Dank möchte ich auch an alle Mitarbeiter des Interfakultären Instituts für Biochemie für Ihre Unterstützung aussprechen und dem "Casino Team" ein Vergelt's Gott für die netten Stunden bei Kaffee und kostenlos gerauchten Zigaretten."

Vielen Dank an meine Eltern Berta und Alfred Hirschner und an meine Großeltern, die mich stets in jeglicher Hinsicht unterstützen und mir meinen bisherigen Lebensweg überhaupt erst ermöglicht haben.

Bei meiner Freundin Dr. Corinna Bähr bedanke ich mich herzlich dafür, daß sie trotz 5 ½ - jähriger Wochenendbeziehung - und ganz besonders in schwierigen Zeiten - zu mir gestanden hat.

## Abbreviations

The following list does not contain abbreviations that do not require definition according to the instructions for authors of FEBS Journal (available online at <http://www.blackwellpublishing.com/products/journals/suppmat/ejb/ejbt4.htm>).

Such abbreviations are used in the text and the legends of figures and tables without prior definition.

AMV	avian myeloblastosis virus
ANP	atrial natriuretic peptide
AP	alkaline phosphatase
Apaf	apoptotic protease-activating factor
APC	astroglial primary culture
APS	ammonium peroxodisulfate
AQP	aquaporin
ATCC	American Type Culture Collection
BBS	Bardet-Biedl syndrome
CIAP	calf intestine alkaline phosphatase
CNS	central nervous system
CP	crossing point
CSF	cerebrospinal fluid
Cy3	carbocyanin 3
DAPI	4',6-diamidino-2-phenylindole
ddH <sub>2</sub> O	doubly deionized water
DIG	digoxigenin
DMEM	Dulbecco's modified Eagle's medium
DMSO	dimethylsulfoxide
dNTP	deoxyribonucleoside triphosphate
DTT	dithiothreitol
E	efficiency of PCR reaction
ECL	enhanced chemiluminescence
EGFP	enhanced green fluorescent protein
EPC	ependymal primary culture
EST	expressed sequence tag

## Abbreviations

---

FCS	fetal calf serum
Fig	Figure
FITC	fluorescein isothiocyanate
g	earth's gravitational acceleration (9.81 m/s <sup>2</sup> )
GFP	green fluorescent protein
GP BB	brain isoform of glycogen phosphorylase
HBSS	Hank's balanced salt solution
hpf	hours post fertilisation
hyh	hydrocephaly with hop gait
IFIB	Interfaculty Institute for Biochemistry, University of Tuebingen
IFT	intraflagellar transport
JNK	c-Jun N-terminal kinase
KLH	keyhole limpet hemocyanin
LB	Lysogeny broth
MEM	Minimal Essential Medium
MOPS	3-(N-morpholino propanesulfonic acid)
NCBI	National Center for Biotechnology Information, Bethesda, USA
NPs	natriuretic peptides
NSF	N-ethylmaleimide-sensitive factor
OD	optical density (absorbance)
PBS	phosphate-buffered saline
PC	personal computer
PCP	planar cell polarity
PFA	paraformaldehyde
PS	penicillin/streptomycin
rpm	revolutions per minute
RT	1. reverse transcriptase 2. reverse transcription 3. room temperature
SCO	subcommissural organ
SOC	medium for bacterial liquid culture; super optimal broth, catabolite repression
$\alpha$ -SNAP	soluble NSF attachment protein
SNARE	soluble NSF attachment protein receptor

## Abbreviations

---

SOURCE	database name; see <a href="http://source.stanford.edu">http://source.stanford.edu</a>
Spag6	sperm-associated antigen 6
SVZ	subventricular zone
TEMED	N,N,N',N'-tetramethylethylenediamine
Tris	tris(hydroxymethyl)aminomethane
wdr16CoMO	wdr16 control morpholino
wdr16MO	wdr16 antisense morpholino



# Content

<b>1. Introduction</b> .....	<b>1</b>
1.1. The cerebral liquor system .....	1
1.2. The ependyma.....	2
1.2.1. Tanycytes.....	2
1.2.2. Normal ependymal cells .....	2
1.2.3. Ependymal development and proliferation.....	3
1.3. The subcommissural organ.....	3
1.4. Function of ependymal cells.....	3
1.4.1. Involvement of the ependyma in neuron generation .....	4
1.4.2. Involvement of ependymal cells in cerebral energy metabolism .....	4
1.4.3. Participation of the ependyma in brain water and osmoregulation .....	5
1.5. Hydrocephalus .....	5
1.6. Cilia .....	6
1.7. The WD40-repeat protein family .....	7
1.8. Subtractive cDNA libraries .....	7
1.9. Scope of the thesis .....	9
<b>2. Results</b> .....	<b>10</b>
2.1. Identification of ependyma-specific cDNA fragments.....	10
2.2. Bioinformatic characterisation of Epe10/Wdr16.....	11
2.2.1. Analyses of the primary and tertiary structure of Epe10/Wdr16.....	11
2.2.2. Identification of Epe10/Wdr16 orthologs.....	13
2.2.3. Analysis of the evolutionary relationship between Epe10/Wdr16 orthologs .....	15
2.2.4. Bioinformatic analysis of Wdr16 splice variants in human and rat .....	16
2.2.5. Evidence for gene orthology between rat wdr16 and its homologous zebrafish sequence.....	16
2.3. Analysis of the wdr16 transcription profile.....	17
2.3.1. Conventional RT-PCR.....	17
2.3.2. Real-time RT-PCR .....	18
2.3.3. Experimental investigation of putative Wdr16 splice variants in the rat .....	21
2.4. Determination of immunoreactivity and specificity for the Wdr16 antiserum.....	22
2.4.1. ELISA .....	22
2.4.2. Western blot.....	23
2.5. Analysis of tissue-specific Wdr16 protein expression by Western blotting.....	25
2.5.1. Rat tissues and cell cultures.....	25
2.5.2. Wdr16 in developing rat testis, ependymal primary culture and astroglial primary culture .....	25
2.5.3. Bull sperm.....	26
2.5.4. HepG2 cell line .....	27
2.6. Analysis of mammary gland for wdr16 expression.....	28
2.6.1. Real-time RT-PCR .....	28
2.6.2. Western blot.....	29
2.7. Comparison of transcription kinetics between wdr16, sperm-associated antigen 6, hydin and polaris .....	30
2.8. Antigen affinity and specificity of Wdr16 antiserum in immunostainings .....	32
2.9. Affinity purification of Wdr16 antibody .....	33
2.9.1. ELISA .....	33

## Content

---

2.9.2. Western Blot.....	35
2.10. Immunostaining of cell cultures .....	35
2.10.1. Immunostaining of ependymal primary culture for Wdr16.....	35
2.10.2. Immunocytochemical double stainings of ependymal primary cultures and astroglial primary cultures for Wdr16 and $\alpha$ -tubulin .....	36
2.10.3. Immunocytochemical double stainings of primary cultures for Wdr16 and the brain isoform of glycogen phosphorylase .....	37
2.11. Immunohistochemistry .....	38
2.11.1. Staining of rat testis for Wdr16 at different animal age .....	38
2.11.2. Staining of adult rat brain for Wdr16 .....	38
2.11.3. Double immunostaining of developing rat brain.....	40
2.11.3.1. Wdr16 and $\alpha$ -tubulin stainings of embryonic rat brain at day 19 of gestation.....	40
2.11.3.2. Staining of brain from newborn rat for Wdr16 and $\alpha$ -tubulin.....	41
2.11.3.3. Costaining of Wdr16 and either $\alpha$ -tubulin or the brain isoform of glycogen phosphorylase in the brain of two day-old rat .....	43
2.12. Zebrafish embryo as a suitable model organism for investigating possible Wdr16 functions .....	44
2.12.1. Analysis of the presence of Wdr16 mRNA in zebrafish embryo by in-situ hybridisation .....	44
2.12.2. Efficiency and specificity of the Wdr16 antisense morpholino .....	45
2.12.3. Consequences of Wdr16 knockdown in zebrafish embryos.....	46
2.13. Yeast-Two Hybrid Screen .....	48
<b>3. Discussion.....</b>	<b>49</b>
3.1. Potential of subtractive ependymal cDNA libraries .....	49
3.2. Comparison of Wdr16 with other WD40-repeat proteins .....	49
3.3. Congruence between Wdr16 and the expression of kinocilia .....	50
3.4. Expression of the wdr16 gene in the hepatocellular carcinoma cell line HepG2.....	53
3.5. Colocalisation of Wdr16 and the brain isoform of glycogen phosphorylase .....	53
3.6. Comparison of Wdr16 knockdown-associated hydrocephalus with other animal models of hydrocephalus.....	54
3.7. Impact of cilia on the generation of cell polarity and intracellular signalling.....	56
3.8. Putative function of Wdr16 .....	57
3.9. Outlook and perspectives.....	59
<b>4. Materials and methods .....</b>	<b>60</b>
4.1. Materials .....	60
4.1.1. Devices .....	60
4.1.2. General material .....	62
4.1.3. Chemicals .....	62
4.1.4. Kits.....	64
4.1.5. Reagents for molecular biology.....	65
4.1.6. Enzymes for molecular biology.....	65
4.1.7. Constituents and reagents for bacterial and mammalian cell culture media .....	66
4.1.8. Antigenic peptide.....	66
4.1.9. Antibodies.....	67
4.1.9.1. Primary antibodies.....	67
4.1.9.2. Secondary antibodies.....	67
4.1.10. Bacterial strains .....	67
4.1.11. Mammalian cells.....	68
4.1.12. Animals.....	68
4.1.13. Vectors.....	68

## Content

---

4.2. Methods	70
4.2.1. Cell culture techniques	70
4.2.1.1. Media and solutions for cell cultivation	70
4.2.1.2. Ependymal primary cultures	72
4.2.1.3. Astroglial primary cultures	73
4.2.1.4. Cultures of the mouse fibroblast cell line A9	74
4.2.1.5. Cultures of the human hepatocellular carcinoma cell line HepG2	75
4.2.2. Harvesting of rat organs and cells	76
4.2.2.1. Harvesting of rat organs for RNA isolation and for preparation of protein homogenates	76
4.2.2.2. Harvesting of rat organs for immunohistochemical stainings	76
4.2.2.3. Harvesting of cells from culture dishes 35 mm in diameter	76
4.2.2.4. Collecting of cells grown in 80 cm <sup>2</sup> culture flasks	77
4.2.3. Preparation of homogenates	77
4.2.3.1. Preparation of homogenates from rat organs	77
4.2.3.2. Preparation of homogenates from cultured cells	77
4.2.4. Preparation of cryosections from rat tissues	78
4.2.5. Subtracted ependymal cDNA libraries	78
4.2.5.1. Generation of a subtracted ventricular ependymal cDNA library and a subtracted bovine subcommissural cDNA library	78
4.2.5.2. Screening of subtracted ependymal cDNA libraries	79
4.2.6. Other molecular biology techniques	79
4.2.6.1. Preparation of medium for bacterial liquid cultures	79
4.2.6.2. Preparation of agar plates	79
4.2.6.3. Bacterial liquid cultures	79
4.2.6.4. "Mini" scale preparation of plasmid DNA from bacterial liquid cultures	80
4.2.6.5. Preparation of bacterial glycerol stocks	80
4.2.6.6. Photometric determination of nucleic acid concentration	80
4.2.6.7. Cloning of the Wdr16 PCR product into the pDNR-1r vector	80
4.2.6.8. Cloning of the Wdr16 PCR product into the pEGFP-N1 vector	82
4.2.6.9. Cutting of DNA with restriction endonucleases	83
4.2.6.10. Phenol/Chloroform/Isoamyl alcohol extraction of DNA with subsequent ethanol precipitation	84
4.2.6.11. Dephosphorylation of vector DNA	84
4.2.6.12. Agarose gel electrophoresis	84
4.2.6.13. DNA extraction from preparative agarose gels	85
4.2.6.14. Ligation of PCR fragments into vector DNA	85
4.2.6.15. Preparation of E. coli DH5 $\alpha$ competent cells	86
4.2.6.16. Transformation of competent bacterial cells with plasmid DNA	86
4.2.7. Bioinformatic tools	87
4.2.8. Reverse transcriptase reaction	87
4.2.9. Conventional RT-PCR	88
4.2.10. Real-time PCR	89
4.2.11. Generation of the Wdr16 peptide antibody	90
4.2.12. Affinity purification of the Wdr16 antibody	90
4.2.13. ELISA to determine antibody titer	91
4.2.14. Protein assay (Bradford assay)	92
4.2.15. Discontinuous SDS PAGE	92
4.2.16. Coomassie staining of polyacrylamide gels	93
4.2.17. Western blot analysis with chemiluminescence detection	94
4.2.18. Transfection of A9 fibroblasts	95

## Content

---

4.2.19. Immunofluorescent staining .....	96
4.2.19.1. Staining of A9 fibroblasts.....	96
4.2.19.2. Staining of rat tissues.....	97
4.2.19.3. Staining of ependymal primary cultures and astroglial .....	98
4.2.20. Separation of bull sperm into head and tail fractions .....	99
4.2.21. Analysis of Wdr16 in zebrafish embryos .....	100
4.2.21.1. Green fluorescent protein fusion control experiment .....	101
4.2.21.2. Procedure of Wdr16 knockdown.....	101
4.2.21.3. Analysis of ciliary beating.....	102
4.2.21.4. In-situ hybridisation.....	102
<b>5. References.....</b>	<b>103</b>
<b>6. Summary .....</b>	<b>120</b>

# 1.Introduction

## 1.1. The cerebral liquor system

The cerebral liquor system is filled with the cerebrospinal fluid (CSF) and can be classified into the inner and the outer liquor space. The outer space is confined outwardly by the arachnoidea and inwardly by the pia mater. The inner system is composed of two lateral ventricles that are connected to the third ventricle by the so-called interventricular foramina. The third ventricle, in turn, communicates with the fourth ventricle via the cerebral aqueduct. In the region of the fourth ventricle, the CSF passes via the median and lateral apertures into the outer liquor space, from where it ultimately drains into the venous canals of the subarachnoidal space via arachnoidal villi (Kahle et al., 1990).

The major sites of CSF production are the choroid plexus found in all four ventricles (Nicholson, 1999). These plexus, which include the choroidal epithelium, blood vessels and interstitial connective tissue, are the result of invaginations of the pia mater into the ventricular cavities (Fishman, 1992). The capillaries in the choroid plexus are fenestrated (Segal, 1993), while the choroidal ependymocytes are connected by tight junctions, thereby forming the blood/CSF barrier (Davson and Segal, 1996). A comparison of the constituents from both fluids demonstrates that the CSF is not just a plasma ultrafiltrate (Fishman, 1992). Rather, it is a product the secretion of which involves unidirectional ion transport processes that create an osmotic gradient which drives the flux of water. This is achieved by many different transporters on the apical and basolateral membranes of the cells of the choroid plexus, as well as by the expression of aquaporins (Brown et al., 2004).

Several functions are attributed to the CSF. For example, it may serve as a sink for metabolites and neurotransmitters from the brain parenchyma (Segal, 1993), or as a source for nutrients of brain cells (Johanson, 1999).

## **1.2. The ependyma**

The term “ependyma” originates from the greek word for upper garment (Daly et al., 1957). It is a single-layered epithelium that lines the ventricles of the brain and the central canal of the spinal cord (for review see Del Bigio, 1995) and mainly consists of two different cell types, namely tanycytes and “normal” ependymal cells.

### **1.2.1. Tanycytes**

In vertebrates, tanycytes are preferentially found in the developing brain (Bruni, 1998). In the adult mammalian brain they form the ventrolateral walls and the floor of the third ventricle (Akmayev et al., 1973). Characteristic for tanycytes of the ventricle floor are processes that project to the median eminence of the neurohypophysis, where they contact the blood vessel system via numerous endfeet, connecting the CSF and the vasculature of the neurohypophysis (Wittkowski, 1998). The tanycytes of the floor of the third ventricle exhibit numerous apical microvilli and membrane protrusions, but in general do not bear kinocilia (Rinne, 1966; Röhlich et al., 1965; Scott et al., 1972; Wittkowski, 1967).

### **1.2.2. Normal ependymal cells**

The quantitatively predominating “normal” ependymal cells of the ventricular epithelia, also called ependymocytes (Fleischhauer, 1972), are mostly of cuboidal, but in some regions also of columnar shape. Their most characteristic feature is a bundle of approximately 40 kinocilia on the apical cell surface (Manthorpe et al., 1977). The cilia are approximately 8  $\mu\text{m}$  long and project into the CSF, beating with a frequency of 40 Hz in the rat (O’ Callaghan et al., 1999; for further information about cilia, refer to section 1.6). In addition to the kinocilia, the apical surface of ependymocytes is often covered by microvilli. The basal end may occasionally extend cell processes that have to be considered rather short when compared to tanycytes (Junqueira and Carneiro, 1996). The ventricular ependymocytes of the adult rat brain do not express glial fibrillary acidic protein, but they contain the

intermediate filament protein vimentin (Wellard et al., 2006). Ependymocytes are connected via zonulae adherentes-type junctions (Brightman and Reese, 1969) as well as by gap junctions (Jarvis and Andrew, 1988; Yamamoto et al., 1992), which allows for a liquid exchange between the ventricular spaces and the interstitium of the brain.

### **1.2.3. Ependymal development and proliferation**

Ependymal cells emerge from radial glia (Spassky et al., 2005). Their differentiation begins after birth and progresses from the region of the cerebral aqueduct (Banizs et al., 2005). At gestational day 10, those neuroepithelial cells of the rat brain destined to become ependymal cells start to proliferate (Korr, 1980). Adult ependymal cells are postmitotic (Spassky et al., 2005) and lack regenerative capacity (Sarnat, 1995).

## **1.3. The subcommissural organ**

The subcommissural organ (SCO) is a small gland located in the dorso-caudal region of the third ventricle at the passage to the aqueduct. The cells of the SCO are arranged in two layers, namely the ependyma and the hypendyma, and they release glycoproteins into the CSF (Leonhardt, 1980; Rodriguez et al., 1992). These glycoproteins have a high molecular weight (Nualart et al., 1991) and aggregate to form the so-called Reissner's fibre (Sterba, 1969). The function of this thread-like structure is unknown, as is the physiological function of the entire SCO (Rodriguez et al., 1998).

## **1.4. Function of ependymal cells**

The precise roles of ependymal cells in health and disease have not yet been elucidated and remain mostly speculative. Nevertheless, a number of putative functions have been postulated and investigated, including the local mixing of the

CSF (Roth et al., 1985), the movement of cellular debris in the direction of CSF bulk flow (Cathcart and Worthington, 1964) and the secretion of components into the CSF (Manthorpe et al., 1977). Furthermore, the ependyma has been implicated in additional roles as detailed below.

### **1.4.1. Involvement of the ependyma in neuron generation**

The idea that ependymal cells are neural precursors in the adult mammalian brain (Johansson et al., 1999) has been dismissed, since this stem cell function is now attributed to astrocytes of the subventricular zone (SVZ) located in the lateral walls of the lateral ventricles (Doetsch et al., 1999). These SVZ astrocytes give rise to neuroblasts (Doetsch et al., 1999) that migrate in the SVZ (Doetsch and Alvarez-Buylla, 1996) in the direction of the CSF flow (Sawamoto et al., 2006). Neuroblast migration is directed by a spacial gradient of guidance molecules that in turn is created by the coordinated beating of ependymal cilia bundles (Sawamoto et al., 2006). The migrating neuroblasts enter the olfactory bulb via the rostral migratory pathway, where they finally differentiate into interneurons (Doetsch and Alvarez-Buylla, 1996; Lois and Alvarez-Buylla, 1994; Luskin, 1993). A further auxiliary function of ependymal cells in the process of neuron generation might be that they supply fuel molecules to neuronal precursors, as postulated by Verleysdonk et al. (2004).

### **1.4.2. Involvement of ependymal cells in cerebral energy metabolism**

Ependymal cells exhibit the highest glycogen content among all cell types in the central nervous system (CNS; Cataldo and Broadwell, 1986; Prothmann et al., 2001), in conjunction with a high protein level and activity of glycogen phosphorylase (Cataldo and Broadwell, 1986; Pfeiffer et al., 1990). In an ependymal cell culture model, glycogen is degraded after addition of serotonin or noradrenaline (Prothmann et al., 2001). Ependymal glycogen may serve as an internal energy store that is mobilised in times of increased cellular energy demand. The elevated ciliary beating



frequency observed after serotonergic stimulation of the ependyma (Nguyen et al., 2001) would be an example thereof. Since ependymal cells coexpress the facilitative glucose transporters GLUT2 and GLUT4 besides GLUT1, as well as the enzyme glucokinase, they have been postulated to play a role in the brain glucose sensing mechanism (Maekawa et al., 2000). Cell culture experiments indeed confirmed an insulin-sensitive ependymal glucose uptake, although this process was found to be mediated by GLUT1, with insulin-like growth factor-1 as the most probable physiological regulator molecule (Verleysdonk et al., 2004).

### **1.4.3. Participation of the ependyma in brain water and osmoregulation**

The expression of the water transport proteins aquaporin (AQP) 4 and AQP9 on ependymal cells (Lehmann et al., 2004) warrants the assumption that the ependyma may be involved in water homeostasis of the CNS (Del Bigio, 1995). AQP4 has been implicated in the formation of cerebral edema after ischemic injuries to the brain (e.g. stroke; summarised by Papadopoulos et al., 2002), because AQP4 knockout mice exhibit reduced susceptibility for brain edema under this condition (Manley et al., 2000). In addition to aquaporins, natriuretic peptides (NPs) are considered to modulate osmoregulation in the brain. The application of NPs to cultured ependymal cells or to the ependyma *ex vivo* elicits a rise of intracellular guanosine 3',5'-cyclic monophosphate levels (Wellard et al., 2003; 2006), indicating a responsiveness of the ependyma toward NPs. The atrial natriuretic peptide (ANP) present in the CSF (Marumo et al., 1987) mainly stems from the anteroventral third ventricle (Geiger et al., 1989; Gundlach and Knobe, 1992) and ANP levels were observed to be augmented in obstructive hydrocephalus (Diringer et al., 1990).

## **1.5. Hydrocephalus**

Hydrocephalus, the pathological dilation of the brain ventricles at the expense of brain parenchyma, can be classified into a communicating and a non-communicating form. The communicating variant is characterised by a general increase of CSF

volume in the ventricles due to either augmented production or impaired absorption. The non-communicating form can be regarded as a pathophysiological obstruction of the Sylvian aqueduct. It may be caused by congenital insults, tumors or infections (summarised by Crews et al., 2004). The medical consequences associated with hydrocephalus are white matter atrophy and axon damage (Gadsdon et al., 1979). The incidence of hydrocephalus is about 3 to 4 cases per 1000 live births (Pattisapu, 2001), with aqueductal stenosis contributing nearly 20 % of all cases (Menkes and Sarnat, 2000). Several animal models are under investigation in order to discover genes associated with hydrocephalus (Banizs et al., 2005; Ibanez-Tallon et al., 2002; 2004; Sapiro et al., 2002). Translation products of such genes are either direct constituents of the ciliary axonemal apparatus, e.g sperm-associated antigen 6 (Spag6; Sapiro et al., 2002), polaris (Banizs et al., 2005) and Mdnah5 (Ibanez-Tallon et al., 2004), or they are associated with the formation and maintenance of cilia or cilia-bearing cells in general, as assumed for hydin (Davy and Robinson, 2003). Furthermore, a defect in the gene encoding the vesicular trafficking protein soluble N-ethylmaleimide-sensitive factor (NSF)-attachment protein  $\alpha$  ( $\alpha$ -SNAP) is also known to evoke hydrocephalus (Hong et al., 2004).

### **1.6. Cilia**

The motile ependymal cilia show the 9+2 axonemal architecture, like most other kinocilia and eukaryotic flagella. This structure is characterised by 9 outer microtubule doublets (each doublet consists of an A and a B tubule) that surround a central apparatus. The central apparatus is composed of two bridged, single microtubules encircled by the central sheath. The outer microtubule doublets are connected to each other by nexin links. Dynein arms attached to the A tubules generate the driving force for ciliary movement by cleavage of ATP. Radial spokes project from the outer microtubule doublets toward the center of the axoneme. They are equipped with several kinases and appear to be involved in the regulation of the ciliary beat (Lindemann and Kanous, 1997).

Cilia are rooted in basal bodies, which are derived from either centrosomes (Wheatley et al., 1996) or a single centriole anchored to the plasma membrane

(Beisson and Wright, 2003). The assembly and maintenance of cilia is accomplished by a process called intraflagellar transport (IFT), in which cargo particles move from the proximal end to the distal tip and back, driven by kinesin and dynein motor proteins, respectively (Rosenbaum and Witman, 2002; Snell et al., 2004).

In contrast to kinocilia, immotile primary cilia lack the central apparatus and are devoid of force-generating constituents. They are generally assumed to have sensory functions (Afzelius, 2004; Ibanez-Tallon et al., 2003).

## **1.7. The WD40-repeat protein family**

The members of the WD40-repeat protein family are characterised by the presence of conserved, approximately 40 amino acids long repetitive sequences in their primary structure, which tend to end with the amino acids tryptophan and aspartate (WD). These motifs, termed WD40 repeats, usually also bear the characteristic dipeptide glycyl-histidine (GH) 11-24 residues distant from the N-terminal start of the repeat sequence (Smith et al., 1999). The tertiary structure is characterised by the so-called  $\beta$ -propeller fold, comprising up to seven four-stranded  $\beta$ -propeller blades. One such blade of four  $\beta$ -strands is assembled from the first three  $\beta$ -strands of one WD40-sequence repeat and the last  $\beta$ -strand of the previous WD repeat (Li and Roberts, 2001). The propeller region of the WD proteins does not possess any catalytic activity (Neer et al., 1994). Rather, the function of WD proteins is to provide a structure capable of mediating protein-protein interactions (Smith et al., 1999). Thus, proteins of the WD-repeat family show a high degree of functional diversity despite the common motif (summarised in Li and Roberts, 2001).

## **1.8. Subtractive cDNA libraries**

Suppression subtractive hybridisation is an established tool for identifying genes that are differentially transcribed in one tissue but not another. It can be used to generate subtractive cDNA libraries. To this end, mRNA from two different sources is

converted into cDNA. The cDNA obtained from the source to be analysed for differentially expressed mRNA species is named “tester” cDNA, while the cDNA obtained from the reference source is designated as “driver” cDNA. The driver cDNA is “subtracted” from the tester cDNA by hybridisation. Target cDNA sequences in the tester fraction are enriched by exponential PCR amplification, while the exponential amplification of cDNA fragments present in the tester and in the driver portion is prevented. The effect of suppression subtractive hybridisation is based on the cDNA adaptor-sequences that are ligated to the tester cDNA. Suppression PCR kinetics favour the attachment of PCR primers at the differentially expressed cDNA fragments, while non-target cDNAs either do not bear primer binding sites, only allow linear amplification or favour the formation of intramolecular hair-pin like structures hampering primer attachment and subsequently PCR amplification. For further molecular detail, refer to Diatchenko et al. (1996) or to the instruction manual of the PCR Select™ cDNA subtraction kit. After ligation of the amplified cDNA sequences into plasmid vector DNA and transfection into bacteria, the resulting cDNA library represents gene fragments differentially transcribed in the target mRNA source.

Screening of a subtractive cDNA library is accomplished by a dot blot array. The DNA of randomly picked clones from the library is transferred in duplicate onto nylon membranes and hybridised with forward and reverse-subtracted cDNA probes, respectively, in which digoxigenin (DIG) has been incorporated. The probe for the forward hybridisation is derived from the subtracted cDNA used to construct the library (source minus reference), whereas the probe for reverse hybridisation is made from subtracted cDNA for the production of which driver and tester cDNA had been exchanged (reference minus source). Dots of differentially expressed cDNAs are visualised by an anti-DIG antibody conjugated to alkaline phosphatase (AP). AP converts an applied chemiluminescent substrate to its reaction product accompanied by the emission of light that is detected on an X-ray film. Only colonies which give a clear signal with the forward subtracted, but not with the reverse subtracted probe are considered to represent differentially expressed sequences. For details refer to the instruction manual of the PCR-Select differential screening kit.

## **1.9. Scope of the thesis**

While the existence of ependymal cells is known since 1836 (Purkinje, 1836), their specific roles in health and disease are not yet precisely understood. The identification of ependyma-specific gene expression is expected to help in elucidating ependymal functions. Therefore, subtractive ependymal cDNA libraries were to be constructed and screened in order to find differentially transcribed mRNA species. Candidate sequences and the respective encoded proteins were to be further analysed for their expression patterns and putative functions.

## 2.Results

### 2.1. Identification of ependyma-specific cDNA fragments

In order to identify genes specifically transcribed in the ependyma, a subtractive bovine ependymal cDNA library of ependyma minus brain and SCO minus brain was generated and screened as described in 1.8. and in 4.2.5. The obtained sequences of putative differentially expressed targets were subjected to bioinformatic analysis using computerized databases from the National Center for Biotechnology Information, Bethesda, USA (NCBI). Initially promising candidates are listed in Table 1, whereas unambiguous false-positives, like self-ligated vector, genomic DNA and clones without an ORF, are omitted.

Member 1 of the solute carrier family 14 (a urea transporter; clone F3) is highly expressed in ependymal cells, but also in astrocytes (Berger et al., 1998). It has therefore not been considered further. The EF-hand domain protein corresponding to clone C2 is encoded by database clones from various tissues and has therefore also been dismissed. The protein represented by clone S38, carbonic anhydrase II, is predicted by SOURCE (a unification tool which dynamically collects and compiles data from many scientific databases, and therefore attempts to encapsulate the genetics and molecular biology of genes from the genomes of *Homo sapiens*, *Mus musculus*, *Rattus norvegicus* into easy to navigate gene reports; <http://source.stanford.edu>) analysis to be expressed throughout the brain and not exclusively in the ependyma. It was therefore not studied further. Clone E68 was excluded from further investigation due to the presence of Alu elements (SOURCE analysis), which are mobile retroposons in the human genome (El-Sawy and Deininger, 2005). The most promising candidate clones from the subtractive library screens, in terms of the aim of this thesis, are those encoding previously unknown ependyma-specific proteins. Since Spag6 is a known constituent of kinocilia in general, only E81 and C10 remain as candidates for subsequent analysis. None of them was chosen for further work within the scope of the present thesis, because an

even more interesting target had been identified in the laboratory before. Its encoded amino acid sequence was found to contain WD40 repeats (see 1.7). This structural motif mediates protein-protein interactions, and members of the WD40-repeat protein family exert diverse physiological functions (Smith et al, 1999; Li and Roberts, 2001). The underlying clone, provisionally designated Epe10, had been encountered multiple times in the course of several screenings of the subtracted libraries. The chance for it to be a false-positive was therefore deemed to be low, and it was selected for analysis within the work of this thesis in preference over E81 and C10.

**Table 1.** Sequencing results from clones identified by screening the subtractive ependymal cDNA libraries. False-positive sequences are not listed. *Rattus norveg.*: *Rattus norvegicus*.

Clone No	Name	Accession number	Species	Identification
1	E68	AAH30277 BAB30207	Homo sapiens Mus musculus	cDNA clone MGC40178, adult medulla hypothetical protein, testis
2	E81	T43445	Homo sapiens	hypothetical protein DKFZp434A2017.1, testis
3	C2	NP_60570 BAB24614	Homo sapiens Mus musculus	EF-hand domain (C-terminal) containing 1 unnamed protein product, EF-hand motif, testis
4	C10	NP_078963	Homo sapiens	hypothetical protein LOC79740(FLJ23049), testis
5	F3	NP_062219	<i>Rattus norveg.</i>	solute carrier family 14 (urea transporter), member 1
6	A1	NP_056588	Mus musculus	Spag6
7	S38	NP_00058	Homo sapiens	carbonic anhydrase II

## 2.2. Bioinformatic characterisation of Epe10/Wdr16

### 2.2.1. Analyses of the primary and tertiary structure of Epe10/Wdr16

The full length sequence of the rat Epe10 cDNA was obtained by 5' and 3' RACE and can be found in the Gene Bank database under the accession number DQ445463. The Epe10 ORF encodes a protein of 620 amino acids and a relative molecular mass

of 68,300. Protein motif scans reveal the Epe10 protein to bear at least eleven WD repeats, placing it into the WD-repeat protein family. A tertiary structure model obtained by threading predicts the Epe10 protein to be organised into two seven-bladed  $\beta$ -propellers that are covalently linked to each other as depicted in Fig. 1.

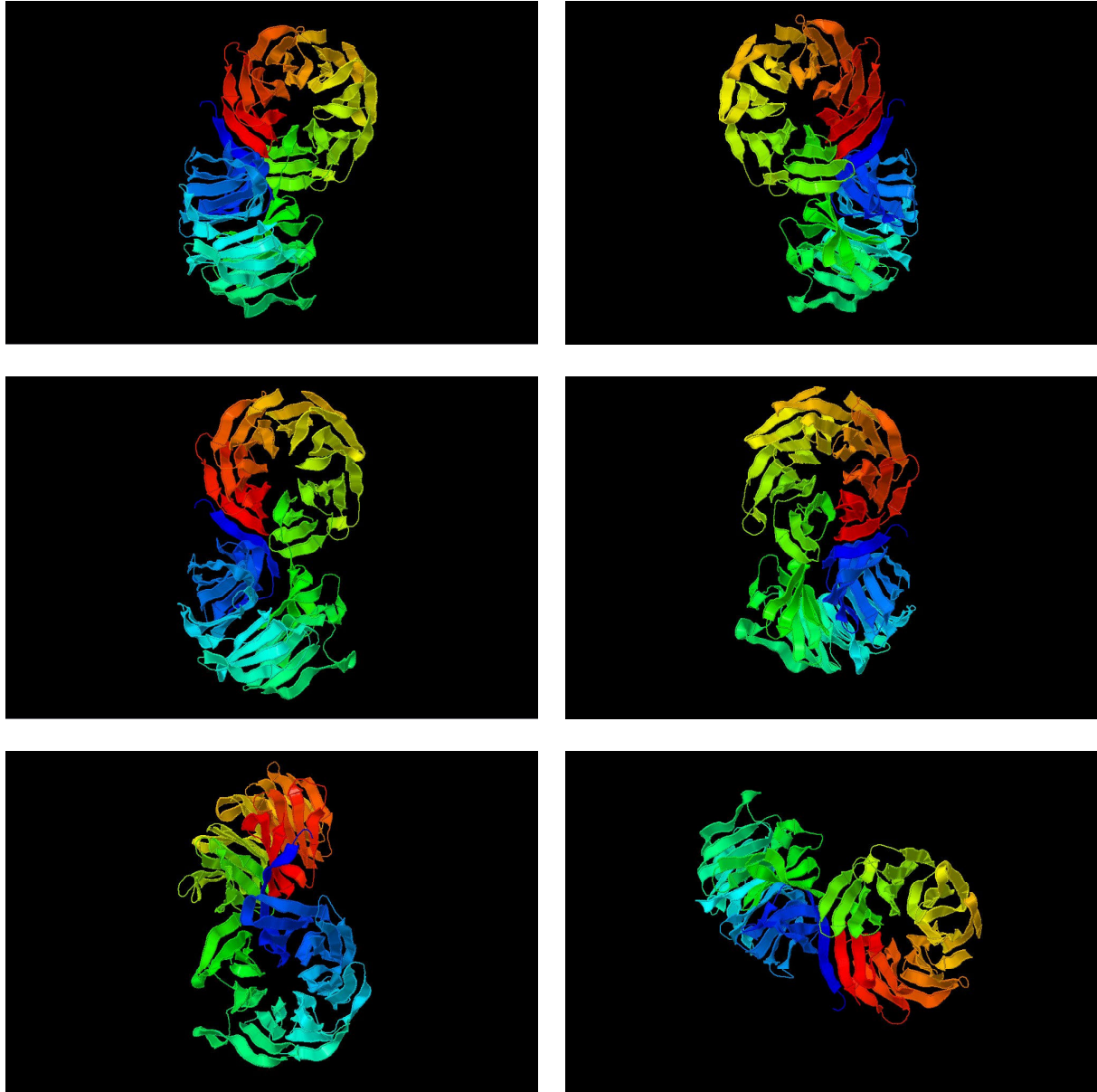


**Fig. 1.** Tertiary structure prediction for Epe10 by threading, featuring an architecture of two covalently linked seven-bladed  $\beta$ -propellers. The structure is depicted from 6 different perspectives. Each blade, represented by a different colour, is made up of four antiparallel  $\beta$ -strands.



### **2.2.2. Identification of Epe10/Wdr16 orthologs**

In order to identify homologs of Epe10, the nucleotide sequence databases deposited at the NCBI were screened with the TBLASTN program. This algorithm takes a protein query sequence and compares it against NCBI nucleotide databases translated in all six possible reading frames. The identified sequences were aligned on the protein level by the CLUSTALW algorithm, and the result is depicted in Fig. 2. In such cases where detected sequences homologous to Epe10 were not present as a continuous entity in the database, the full length cDNA sequences were inferred from those expressed sequence tags (ESTs) deposited at the NCBI that matched the hypothetical cDNA sequences derived from gene prediction algorithms and the known sequence for Epe10. In a gap-free alignment, the sequence of the human Wdr16 protein turns out to be identical to Epe10 in 561 out of 620 amino acids (90 %). In order to check for further similar genes, the human genome was scanned with either the Epe10 protein sequence via TBLASTN or with the human Wdr16 mRNA sequence via BLASTN. The latter algorithm takes a nucleotide sequence and compares it against the NCBI nucleotide data base. The protein with the second highest homology after Wdr16 encoded by the human genome, as present in the database, corresponds to Wdr5B, the product of a gene predicted by automatic computational analysis. Wdr5B, although a member of the WD-repeat protein family, shares only 25 % identity with Epe10 on the amino acid level, a similarity exclusively attributable to the presence of WD repeats in both molecules. The high degree of similarity between rat Epe10 and human Wdr16 protein, combined with the absence of other sequences with a similar level of homology in the respective genomes, indicates orthology between these two proteins. The same is true for all proteins listed in Fig. 2, the minimal mutual amino acid identity of which is 40 %. Therefore they can be regarded as orthologs of rat Epe10 and human Wdr16. Putative Wdr16 orthologs are found to be absent from the genomes of fungi, nematodes, Dictyosteliida, Entamoebidae and angiosperms. These bioinformatics-based findings suggest that the occurrence of Epe10 homologs is restricted to kinocilia-possessing organisms.



## Results

**Fig. 2.** Multiple protein sequence alignment by CLUSTALW (default parameters) of putative Wdr16 orthologs. Genera designations are followed by the GeneBank accession numbers of the underlying sequences. In cases where no complete sequence was present in the database, it was assembled from expressed sequence tags (ESTs), indicated by “assembled”. In those cases where the database sequence was only predicted (GNOMON etc.), it was edited to best fit all available ESTs and the known sequence of Wdr16, indicated by “edited”. The Rattus sequence was determined experimentally. The Drosophila sequence is truncated at amino acid 684.

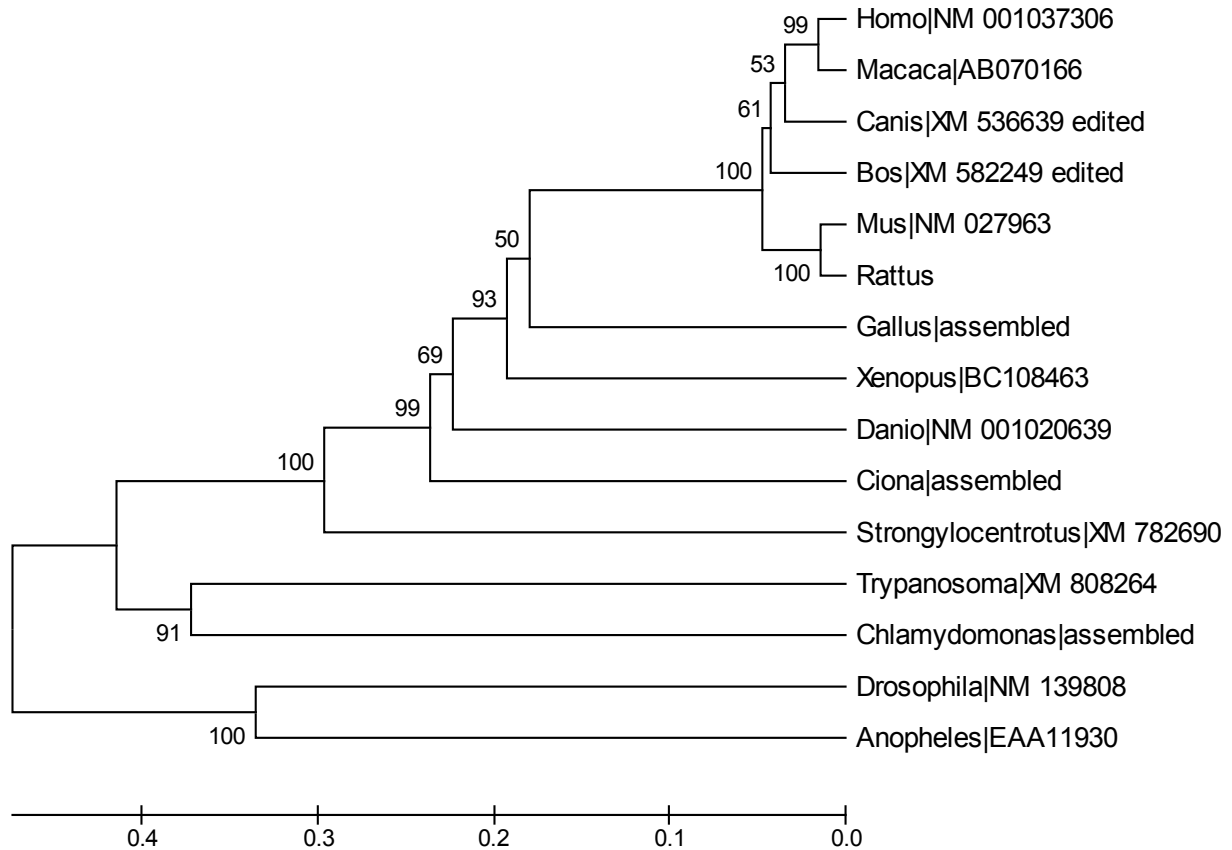


**Fig. 3.** Phylogenetic tree of putative Wdr16 orthologs inferred by the unweighted pair group method with arithmetic mean (Sneath and Snokal, 1973) from the multiple protein sequence alignment depicted in Fig. 2. Poisson correction and pairwise gap deletion were chosen as options. Homogeneous patterns among lineages and uniform mutation rates among sites were assumed. The depicted tree is the bootstrap consensus tree of 1000 replicates. The scale bar indicates substitutions per nucleotide position.

### 2.2.3. Analysis of the evolutionary relationship between Epe10/Wdr16 orthologs

The evolutionary relationship between the orthologs of Epe10 was analysed by constructing a phylogenetic tree using the unweighted pair group method with arithmetic mean (Sneath and Snokal, 1973). The consensus tree of 1000 bootstrap replicates (Fig. 3) for the Epe10 orthologs from 15 species reproduces the commonly accepted evolutionary relationship between the included genera, further confirming

orthology for all aligned sequences. Due to the implicated gene orthology, rat Epe10 will be referred to as Wdr16 from now on.

#### **2.2.4. Bioinformatic analysis of Wdr16 splice variants in human and rat**

In human beings, the wdr16 gene is located on chromosome 17 (17p12-17p13) and comprises 15 exons, the transcription products of which are differentially arranged in three splice variants identified in the nucleotide sequence database at the NCBI. The standard splice variant (GenBank sequence NM\_001037306) that is completely homologous to the Epe10 cDNA sequence (accession number DQ445463) is termed “transcript variant 2” and comprises exons 1 - 14. The second splice variant represented by EST clones, exclusively derived from human lung (accession numbers DA541452, BI824877 and DA269991), is devoid of exon 2 and is, for that reason, formed from only 13 exons. A third mRNA isoform, designated as “transcript variant 1” (accession number NM\_145054), uses, apart from exons 2 - 14, an alternative exon 1 that is contained in the EST sequence DA260431. In the rat genome, the wdr16 ortholog localises to chromosome 10 (10q23-10q24) and contains only 14 exons, with the alternative exon 1 missing. While this excludes “transcript variant 1” from occurring in rat, the presence or absence of mRNA species devoid of exon 2 had to be probed experimentally (2.3.3.).

#### **2.2.5. Evidence for gene orthology between rat wdr16 and its homologous zebrafish sequence**

Since the experiments described in 2.12. are conducted in zebrafish embryos, it was desirable to obtain additional evidence for orthology between the rat and the zebrafish wdr16 gene.

A screening of the zebrafish (*Danio rerio*) genome with the rat wdr16 sequence as the query identifies the candidate for the orthologous gene on the minus strand of chromosome 18 (LOC553666). The corresponding mRNA sequence can be found

under Gene Bank accession number NM\_001020639. On the protein level, zebrafish and rat Wdr16 are identical in 390 out of 608 amino acids (64 %) of a gap-free alignment. No other sequences with comparable similarity on the protein level are detectable in the zebrafish genome. Regarding the organisation of Danio chromosome 18, LOC553666 (corresponding to wdr16) on the minus strand is separated by less than 5000 nucleotides from the downstream locus of syntaxin 8 (accession number NP\_956669), which in turn is located on the plus strand of the chromosome. This head-to-head orientation of wdr16 and syntaxin 8 is also observed on the respective human, rat, mouse, dog, cow and chicken chromosomes. Beyond the high sequence similarity, the described synteny, also found in several other species, lends additional support to the postulated orthology of rat wdr16 and the zebrafish sequence at LOC553666.

## **2.3. Analysis of the wdr16 transcription profile**

### **2.3.1. Conventional RT-PCR**

The tissue-specific transcription profile of the wdr16 gene was analysed by RT-PCR in several rat organs and cell culture systems (Fig. 4). High levels of wdr16 transcript were detected in 13 day-old rat ependymal primary cultures (EPC) and in testis. A weak signal for Wdr16 mRNA was found to be present in 21 day-old astroglial primary cultures (APC), lung and brain. The wdr16 transcript was not observed in liver, spleen, kidney, small intestine, heart or in the mouse neuroblastoma x rat glioma hybrid cell line with neuronal properties, 108CC15 (Hamprecht et al., 1985).

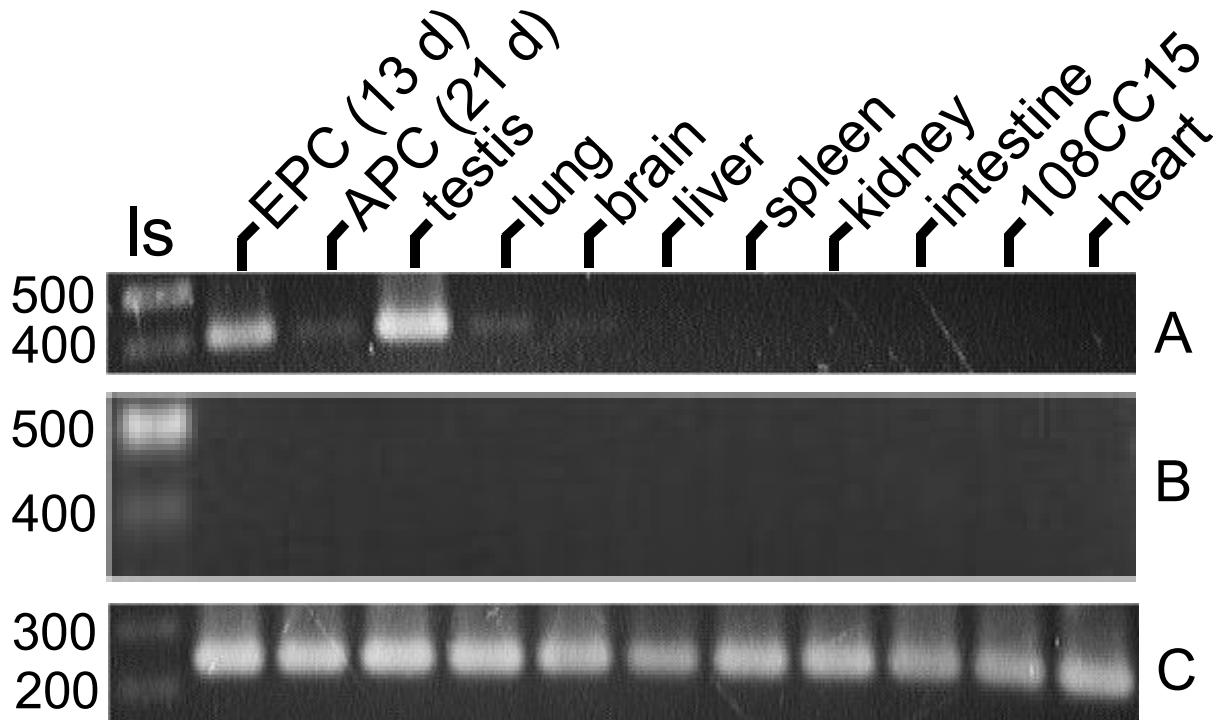


**Fig. 4.** Ethidium bromide-stained agarose gel demonstrating the presence or absence of Wdr16 mRNA in indicated rat tissues and in cell cultures. One microgram of total RNA was reverse-transcribed and subjected to a PCR reaction over 30 cycles (**A**). As a negative control, reverse transcriptase was omitted (**B**). As a positive control, RT-PCR was carried out with primers for  $\beta$ -actin (**C**). The annealing temperature was 58°C for each primer pair. APC, astroglial primary culture (age indicated); EPC, ependymal primary culture (age indicated); 108CC15, mouse neuroblastoma x rat glioma hybrid cell line with neuronal properties (Hamprecht et al., 1985); ls, length standard in base pairs.

### 2.3.2. Real-time RT-PCR

The amount of Wdr16 mRNA present in various rat organs and cell cultures was further probed by real-time RT-PCR. The specificity of the individual reactions was verified by agarose gel electrophoresis and melting point analysis (not shown). A Wdr16-specific PCR product was obtained with RNA from brain, lung, testis, APC and EPC, whilst no signal was seen with samples from liver, spleen, kidney, small intestine and the cell line 108CC15 (not shown).

In order to meaningfully compare the relative concentrations of Wdr16 mRNA in the different materials, the efficiencies (E) of target amplification had to be experimentally determined for each RNA source. For this, a dilution series was prepared from each RNA preparation and subjected to real-time PCR analysis. The fluorescence intensity

## Results

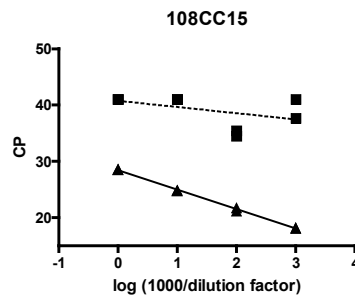
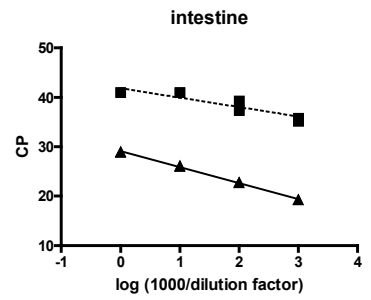
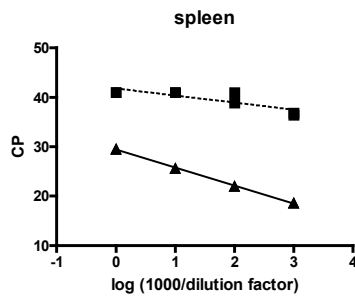
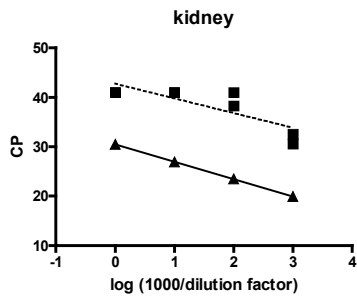
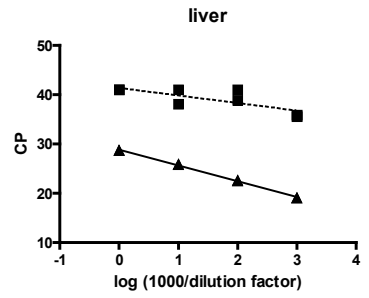
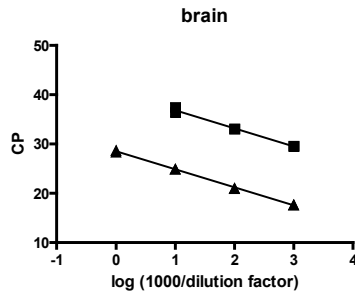
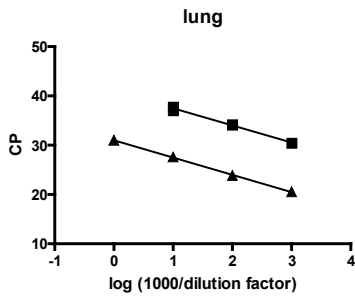
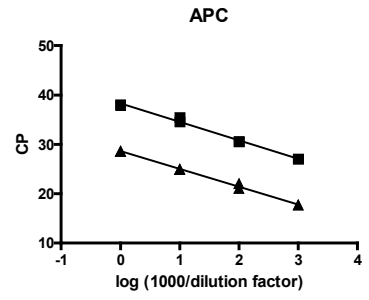
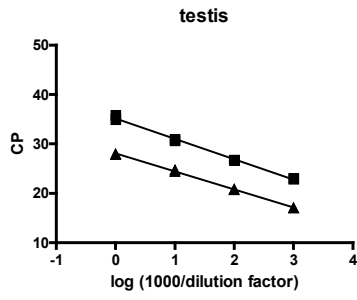
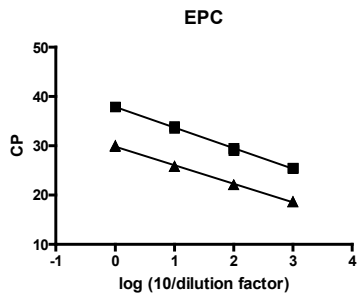
threshold crossing points (CPs) obtained from these experiments were plotted against the logarithms of the respective dilutions in one diagram per RNA source, and a straight line was obtained from these plots by linear regression analysis (Fig. 5). The PCR amplification efficiencies were then calculated from the slopes of the regression lines according to the equation  $E = 10^{-1/\text{slope}}$  (Table 2). In those cases in which the Wdr16-specific PCR product could not be obtained from the majority of the dilutions, the squared linear correlation coefficient ( $R^2$ ) remains below 0.98, indicating that no PCR efficiency is obtainable for the RNA source and that the target Wdr16 mRNA has to be assumed to be absent (Table 2; Fig. 5).

PCR efficiencies derived from regression lines with  $R^2 \geq 0.98$  were used to calculate the amounts of Wdr16 mRNA relative to that of the mRNA for cyclophilin as the standard (see Methods). The highest relative levels of Wdr16 mRNA were found in testis and EPC, while low amounts were detected in lung, brain and APC (Table 3).

**Table 2.** Goodness of fit ( $R^2$ ) and efficiencies (E) for Wdr16 and cyclophilin directed RT-PCR resulting from regression lines depicted in Fig. 5. The housekeeping gene cyclophilin encodes a peptidyl-prolyl isomerase that is transcribed constitutively and independently from the analysed tissue and can therefore be used as a positive control to demonstrate the integrity of the cDNA.  $R^2$  values < 0.98 indicate that the efficiency is not determinable (-). Efficiencies are calculated from the slope of the respective regression line via the equation  $E = 10^{(-1/\text{slope})}$ .

Tissue	$R^2$ regression line (Wdr16)	Efficiency Wdr16	$R^2$ regression line (cyclophilin)	Efficiency cyclophilin
EPC	0.99	1.74	0.99	1.84
Testis	0.99	1.75	0.99	1.88
APC	0.99	1.85	0.99	1.89
Lung	0.99	1.94	0.99	1.93
Brain	0.98	1.87	0.99	1.88
Liver	0.61	-	0.99	2.04
Kidney	0.68	-	0.99	1.92
Spleen	0.71	-	0.99	1.88
Intestine	0.84	-	0.99	2.00
108CC15	0.22	-	0.99	1.95

# Results





## Results

**Fig. 5.** Results of real-time PCR analysis reflecting the presence or absence of Wdr16 mRNA in the indicated rat organs and cell cultures. A cDNA dilution series was generated in duplicate from each tissue, and each dilution was analysed by real-time PCR using Wdr16-specific (■) and cyclophilin-specific primers (▲), respectively. The housekeeping gene cyclophilin encodes a peptidyl-prolyl isomerase that is transcribed constitutively and independently from the analysed tissue and can therefore be used as a positive control to demonstrate the integrity of the employed cDNA. Recorded crossing points were plotted against  $\log(1000/\text{dilution factor})$  and subjected to a linear regression. Solid line, linear regression line with a goodness of fit ( $R^2 \geq 0.98$ ), indicating that an RT-PCR efficiency could be determined and the target message was present. Dotted line, linear regression line with  $R^2 < 0.98$ , indicating that no RT-PCR efficiency was obtainable and the target message was absent. The values for  $R^2$  are listed in Table 2. EPC, ependymal primary culture; APC, astroglial primary culture; CP, crossing point; 108CC15, mouse neuroblastoma x rat glioma hybrid cell line with neuronal properties (Hamprrecht et al., 1985). Slopes of regression lines are listed in the order Wdr16, cyclophilin. Slopes of regression lines with  $R^2 < 0.98$  were considered as not determinable (n.d.). EPC: -4.169, -3.764; testis: -4.129, -3.645; APC: -3.736, -3.608; lung: -3.485, -3.504; brain: -3.687, -3.645; liver: n.d., -3.213; kidney: n.d., -3.526; spleen: n.d., -3.651; intestine: n.d., -3.227; 1008CC15: n.d., -3.443.

**Table 3.** Relative quantification of rat Wdr16 mRNA in tissues and cells cultures, as determined by real-time PCR. Values are the mean  $\pm$  standard error of the mean of at least 3 independent determinations with separate RNA sources and expressed as % abundance of cyclophilin mRNA. The housekeeping gene cyclophilin encodes a peptidyl-prolyl isomerase that is transcribed constitutively and independently from the analysed tissue and can therefore be used as a reference to which the Wdr16 mRNA levels can be referred to.

Testis	EPC	Brain	Lung	APC (13 d)	APC (21 d)
9.9 $\pm$ 0.9	6.6 $\pm$ 1.2	0.07 $\pm$ 0.04	0.13 $\pm$ 0.01	0.4 $\pm$ 0.1	0.71 $\pm$ 0.04

### 2.3.3. Experimental investigation of putative Wdr16 splice variants in the rat

Due to the occurrence of splice variants in humans (2.2.4.), Wdr16 mRNA from rat lung, testis and EPC was analysed for the inclusion of exon 2 by RT-PCR. The selected primer pair was expected to yield a PCR product of 170 bp in the absence and one of 369 bp in the presence of exon 2. Only the longer amplicate was detected in lung, testis and EPC (Fig. 6). For negative controls demonstrating RNA preparations to be free of genomic DNA, the reverse transcriptase (RT) was omitted in the reverse transcription (RT) reaction for each respective sample. The absence of an exon 2-devoid splice variant confirms the bioinformatic data (2.2.4.), indicating that alternative splicing, as observed in humans, is undeveloped in *Rattus*.

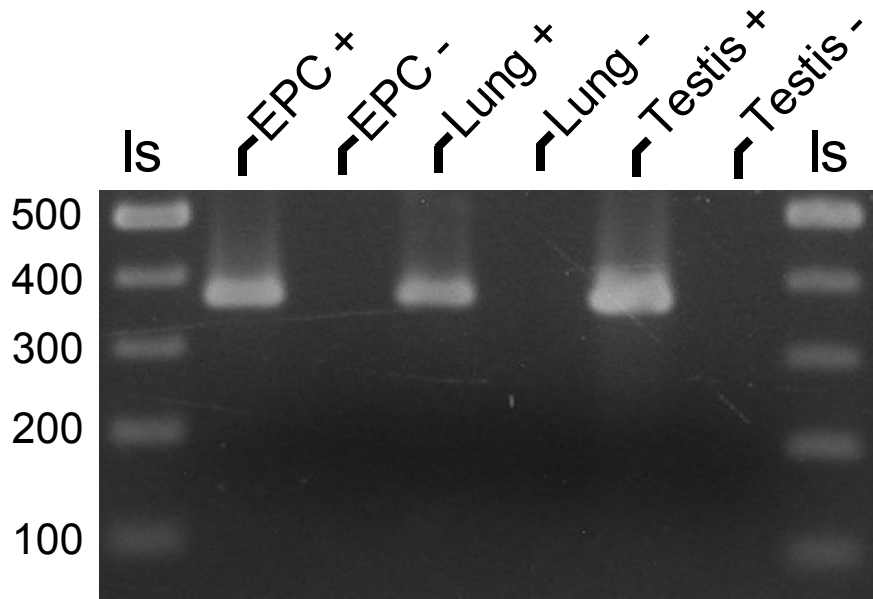


**Fig. 6.** Ethidium bromide-stained agarose gel, indicating the presence of exon 2 in Wdr16 mRNA from the probed rat organs and ependymal primary culture (EPC). One microgram of total RNA was reverse-transcribed and subsequently amplified in a PCR over 30 cycles using primers spanning intron 2 of wdr16. The annealing temperature was 55°C. In the presence of exon 2 the expected product size is 369 bp, whereas a band of 170 bp would indicate the absence of exon 2. + represents the addition, – the omission of reverse transcriptase from the RT reaction. ls, length standard in base pairs.

## 2.4. Determination of immunoreactivity and specificity for the Wdr16 antiserum

Since it was desirable to analyse the expression of Wdr16 on the protein level, an antibody was raised against a peptide, the sequence of which was derived from the primary structure of the rat Wdr16 ortholog. The antigenic peptide CQAINTEQNFLHGHGN was coupled to the immunogenic compound keyhole limpet hemocyanin (KLH) and sent to Charles River Laboratories for immunisation of guinea pigs.

### 2.4.1. ELISA

Only one of the two guinea pigs immunised with the peptide conjugate produced a Wdr16-specific antibody. The titer of the resulting antiserum was monitored by an ELISA over the time of the immunisation procedure. This ELISA revealed an increase of the antiserum titer from the first to the second immunisation that persisted until the

final bleeding of the animal. The preimmune serum, obtained from the animal prior to injection of the antigenic peptide, exhibits no affinity for Wdr16 (Fig. 7).

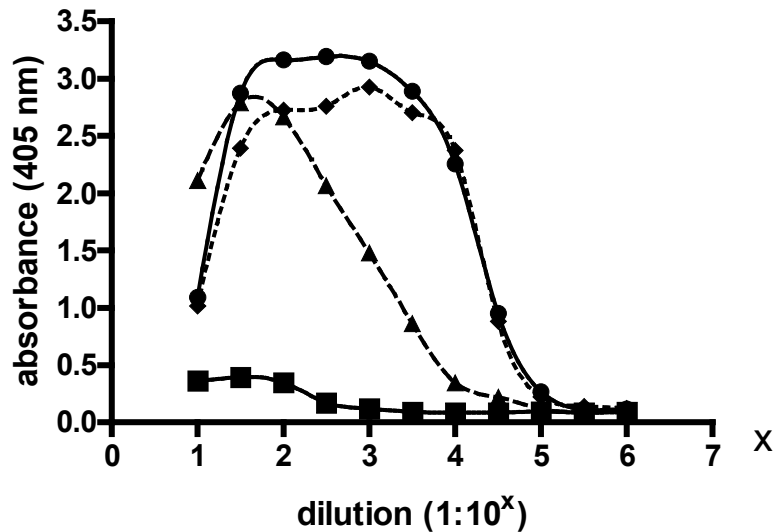


**Fig. 7.** ELISA demonstrating the immunoreactivity of the guinea pig Wdr16 antiserum. A 96 well plate was coated with BSA conjugated to 250 ng peptide against which the antiserum was raised. Serum samples resulting from immunisation of a guinea pig with keyhole limpet hemocyanin-conjugated antigenic peptide were applied to the BSA-conjugated peptide in a dilution series ranging from 1:10 up to 1:10<sup>6</sup>. Incubation time was 2 h. Goat anti-guinea pig IgG-alkaline phosphatase conjugate (1:1,000) was applied as secondary antibody for 1 h. The conjugated phosphatase converted p-nitrophenylphosphate into the p-nitrophenolate ion, the absorbance of which was measured at a wavelength of 405 nm in an ELISA reader. The inflection point of the curve connecting the individual data points represents the titer of the respective antigenic sample. ■, preimmune serum, taken from the animal before immunisation; ▲, antiserum after first boost; ◆, antiserum after second boost; ●, antiserum after final bleeding.

## 2.4.2. Western blot

In the next step, the Wdr16 antiserum was checked for reactivity and specificity in immunoblotting experiments. Since it had been learned from PCR analyses that the Wdr16 mRNA is present in EPC, homogenates from this source were probed with the Wdr16 antiserum. Western blot analysis resulted in a single band at the relative molecular mass of approximately 68,000, as to be expected for Wdr16 (Fig. 8). The band disappeared when the antiserum was omitted, when the antiserum was substituted by preimmune serum, or when it was preabsorbed with the antigenic peptide against which it had been raised (Fig. 8).

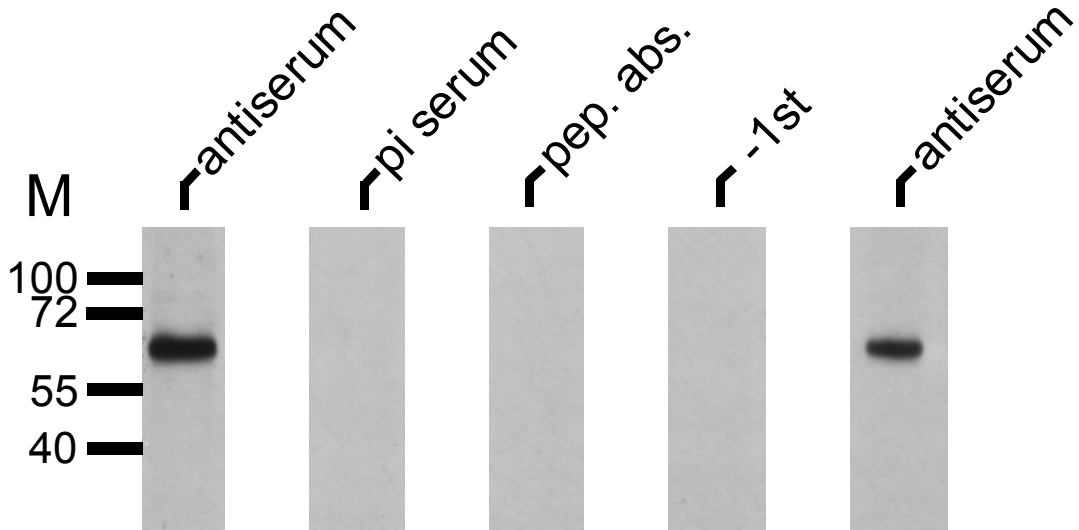


**Fig. 8.** Western blot demonstrating the monospecificity of the Wdr16 antiserum. Each lane of the gel was loaded with 30  $\mu$ g protein from ependymal primary culture. Proteins were separated by SDS PAGE and transferred to a nitrocellulose membrane by electroblotting. The membrane was probed for 1 h with guinea pig Wdr16 antiserum diluted 1:10,000 (antiserum), preimmune serum diluted 1:10,000 (pi serum) and antiserum diluted 1:10,000 and preabsorbed with antigenic peptide (pep. abs.). In the “-1<sup>st</sup>” control, the antiserum was omitted. The secondary antibody used was donkey anti-guinea pig IgG-peroxidase conjugate diluted 1:120,000. Incubation time was 1 h. Detection was performed with an enhanced chemiluminescence system. M, relative molecular mass  $\times 10^{-3}$ .

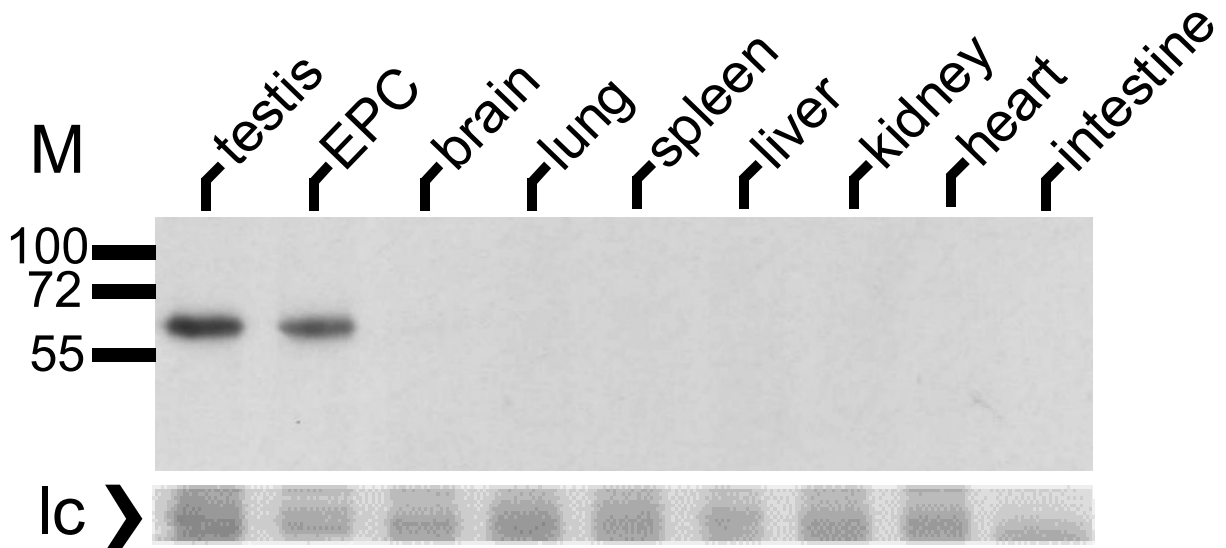


**Fig. 9.** Western blot showing the expression of wdr16 or lack thereof in the indicated rat tissues and in ependymal primary culture (EPC). Thirty micrograms of protein from each tissue sample were separated by SDS PAGE and transferred to a nitrocellulose membrane by electroblotting. The membrane was probed with guinea pig Wdr16 antiserum diluted 1:10,000 and donkey-anti guinea pig IgG-peroxidase conjugate diluted 1:120,000. The incubation time for each individual antibody was 1 h. Detection was performed by the enhanced chemiluminescence system. Replica gels were stained with Coomassie Brilliant Blue R250 to verify equal loading of the individual gel pockets. Ic, loading control; M, relative molecular mass  $\times 10^{-3}$ .

## 2.5. Analysis of tissue-specific Wdr16 protein expression by Western blotting

### 2.5.1. Rat tissues and cell cultures

The monospecific Wdr16 antiserum was then used to probe the expression profile of the wdr16 gene in several adult rat tissues. The Western blot analysis depicted in Fig. 9 shows the presence of Wdr16 in a 13 day-old EPC and in testis, while no signal is visible in brain, lung, spleen, liver, kidney, heart or small intestine.

### 2.5.2. Wdr16 in developing rat testis, ependymal primary culture and astroglial primary culture

The presence of Wdr16 immunoreactivity in a 13 day-old EPC and in adult rat testis raised the question about the temporal onset of Wdr16 expression in the respective biological systems.

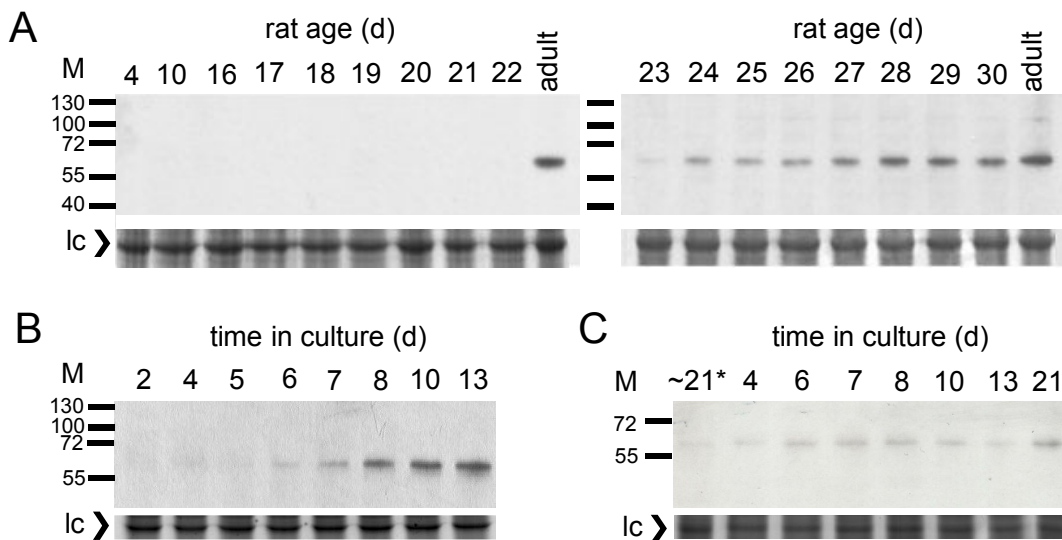


**Fig. 10.** Western blots depicting the expression of wdr16 in **A**, rat testis at different ages of the animal; **B**, ependymal primary cultures; and **C**, astroglial primary cultures over time. Thirty micrograms of protein from samples obtained at individual time points were separated by SDS PAGE and transferred to a nitrocellulose membrane by electroblotting. The membrane was probed with guinea pig Wdr16 antiserum (1:10,000) and donkey anti-guinea pig IgG-peroxidase conjugate (1:120,000). The incubation time for each individual antibody was 1 h. Detection was performed by an enhanced chemiluminescence system. Replica gels were stained with Coomassie Brilliant Blue R250 to verify equal loading of the individual gel pockets. Ic, loading control; \* indicates a nearly homogeneous astroglia culture; M, relative molecular mass  $\times 10^{-3}$ .

According to a Western blot study (Fig. 10 A) following the time course of testis development from postnatal day 4 up to adulthood, Wdr16 levels begin to rise at approximately 24 days of age and persist until adulthood. In EPC, where the occurrence of the Wdr16 protein was monitored over time from day 2 up to day 13, immunoreactivity appears approximately from day 7 onward (Fig. 10 B). In APC, the Wdr16 signal increases with culture age, but the expression levels are much lower compared to EPC and testis. In an almost homogeneous, virtually ependymocyte-free astroglia culture, no Wdr16 immunoreactivity is detectable (Fig. 10 C).

### 2.5.3. Bull sperm

The Wdr16 antiserum was expected to also recognise the orthologous bovine protein, because the rat sequence against which the peptide was raised differs from the bovine sequence in only one amino acid. Specifically, the neutral asparagine residue at position 55 of the rat protein is substituted by a neutral glutamine residue in the protein from *Bos taurus*. This cross-reactivity was taken advantage of by analysing bull semen constituents for the presence of Wdr16 by Western blotting.

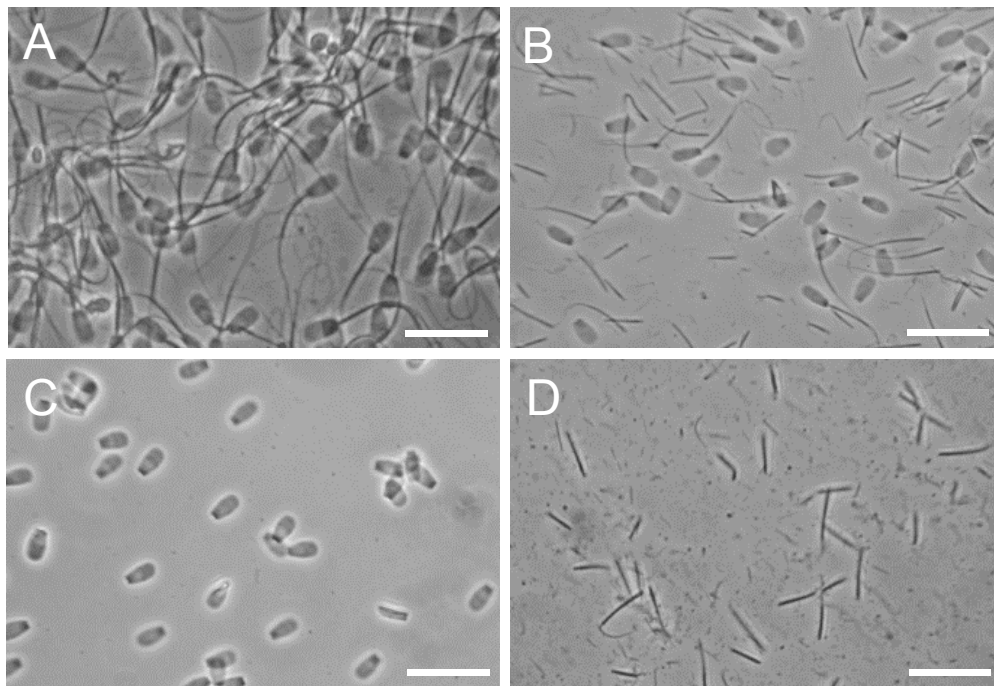


**Fig. 11.** Separation of bull sperm into head and tail fractions. Bull sperm (A) was fractured by sonification (B). Pure head (C) and tail fractions (D) were enriched by centrifugation of the fractured sperm through a sucrose cushion. Scale bars: 50  $\mu$ m.

Bull sperm was fractured into heads and tails by ultrasonic irradiation, followed by the separation of the fragments via centrifugation in a sucrose buffer. The successful separation is documented in Fig. 11, demonstrating both a sperm head fraction devoid of either contaminating tails or unseparated sperm, and a pure tail fraction.

The Western blot depicted in Fig. 12 confirms the cross-reactivity of the Wdr16 antiserum with the bovine Wdr16 ortholog. While Wdr16 immunoreactivity is not present in the seminal plasma and is only hardly detectable in the sperm head fraction, high protein levels are seen in unseparated bovine sperm, fractured sperm and in the sperm tail fraction (Fig. 12).

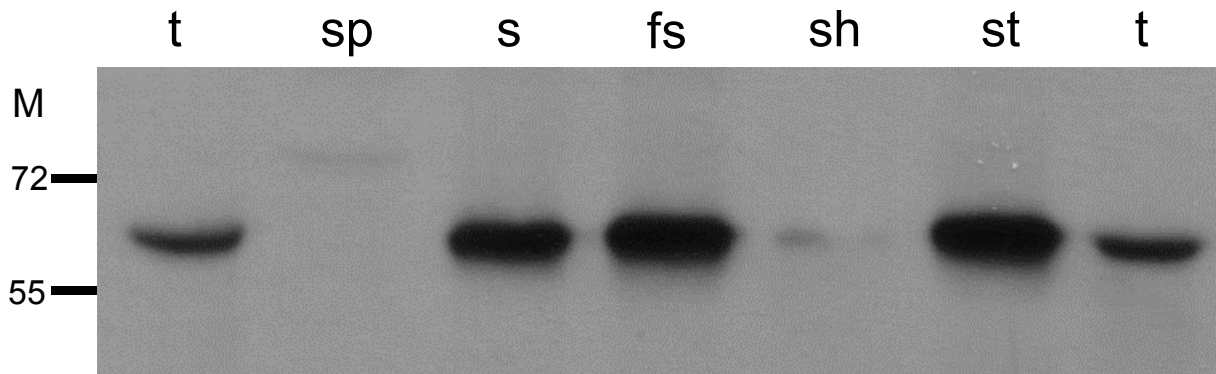


**Fig. 12.** Western blot revealing the expression of wdr16 in bull semen constituents. Thirty micrograms of protein obtained from testis (t), seminal plasma (sp), sperm (s), fractured sperm (fs), sperm heads (sh) and sperm tails (st) were separated by SDS PAGE and transferred to a nitrocellulose membrane by electroblotting. The membrane was probed with guinea pig Wdr16 antiserum diluted 1:10,000 and donkey anti-guinea pig IgG-peroxidase conjugate diluted 1:120,000. The incubation time for each individual antibody was 1 h. Detection was performed by an enhanced chemiluminescence system. M, relative molecular mass  $\times 10^{-3}$ .

#### 2.5.4. HepG2 cell line

The human Wdr16 ortholog has been shown to be present in the hepatocellular carcinoma cell line HepG2 by Silva et al. (2005). Since an antibody was not available to these authors, their work was restricted to the level of mRNA. Due to the cross-reactivity of Wdr16 antiserum not only with the bovine, but also with the human protein, the expression of wdr16 in HepG2 cells could indeed be confirmed by Western blot analysis (Fig. 13).

## Results

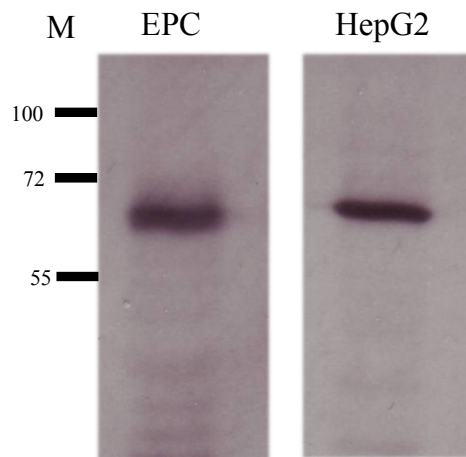


**Fig. 13.** Western blot reflecting the expression of wdr16 in the hepatocellular carcinoma cell line HepG2. Proteins were separated by SDS PAGE and transferred to a nitrocellulose membrane by electroblotting. Thirty micrograms of protein were obtained from an ependymal primary culture (EPC) and from HepG2 cells (passage number 2), respectively. Proteins were separated by SDS PAGE and transferred to a nitrocellulose membrane by electroblotting. The membrane was probed with guinea pig Wdr16 antiserum (1:10,000) and donkey anti-guinea pig IgG-peroxidase conjugate (1:120,000). The incubation time for each individual antibody was 1 h. Detection was performed by an enhanced chemiluminescence system. M, relative molecular mass  $\times 10^{-3}$ .

## 2.6. Analysis of mammary gland for wdr16 expression

### 2.6.1. Real-time RT-PCR

Subjecting the Wdr16 mRNA sequence to further bioinformatic analysis via the bioinformatic “harvester” at the web page of the European Molecular Biology Laboratory (<http://harvester.embl.de>) yielded cDNA microchip array data demonstrating the wdr16 gene to be highly transcribed not only in testis, but also in the lactating mammary gland. The “harvester” is a search engine for the human, mouse and rat genomes that combines gene and protein information for target sequences resulting from searches of major databases and prediction servers (Liebel et al., 2005). Rat lactating mammary gland was analysed for presence of Wdr16 message by real-time RT-PCR. No efficiency for Wdr16 amplification could be determined and Wdr16 mRNA has to be considered to be absent from lactating mammary gland (Fig. 14). Thus the bioinformatic data are apparently misleading.



## Results

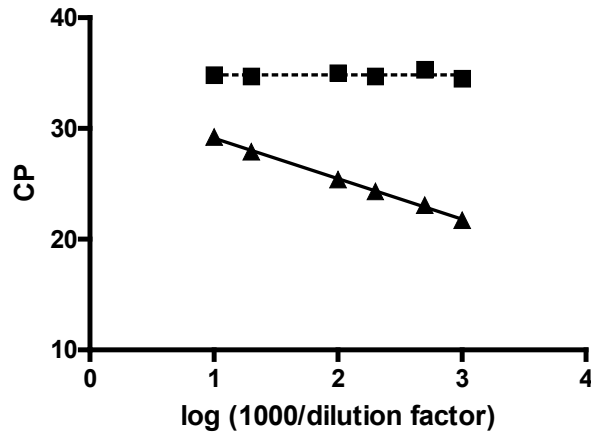


**Fig. 14.** Real-time PCR analysis demonstrating the absence of Wdr16 mRNA from lactating mammary gland. A dilution series of lactating mammary gland cDNA was generated in duplicate and each dilution was analysed by real-time PCR using Wdr16- (■) and cyclophilin-specific primers (▲), respectively. The housekeeping gene cyclophilin encodes a peptidyl-prolyl isomerase that is transcribed constitutively and independently from the analysed tissue and can therefore be used as a positive control to demonstrate the integrity of the employed cDNA. Recorded crossing points were plotted against  $\log(1000/\text{dilution factor})$  and subjected to a linear regression. Solid line, linear regression line with a goodness of fit ( $R^2 \geq 0.98$ ), indicating that an RT-PCR efficiency could be determined and the target message was present. Dotted line, linear regression line with  $R^2 < 0.98$  indicating that no RT-PCR efficiency was determinable and the target message was absent. CP, crossing point.

### 2.6.2. Western blot

The lack of Wdr16 immunoreactivity in homogenates from lactating mammary gland further exposes the reported presence of Wdr16 message in the tissue as database artefact (Fig. 15).

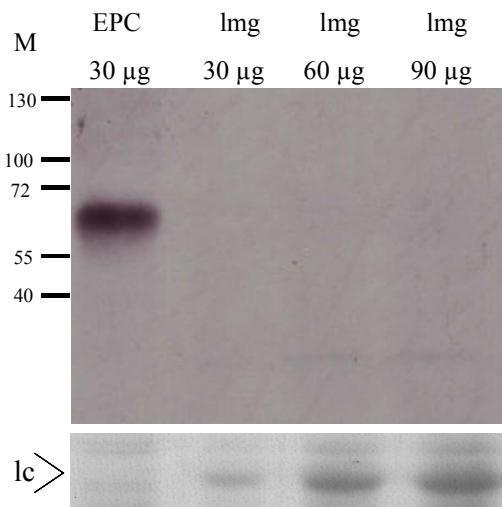


**Fig. 15.** Western blot demonstrating the absence of Wdr16 from lactating rat mammary gland. The indicated amounts of protein from lactating mammary gland (1mg) and from ependymal primary culture (EPC) homogenate, respectively, were separated by SDS PAGE and transferred to a nitrocellulose membrane by electroblotting. The membrane was probed with guinea pig Wdr16 antiserum (1:10,000) and donkey anti-guinea pig IgG-peroxidase conjugate (1:120,000). The incubation time for each individual antibody was 1 h. Detection was performed by an enhanced chemiluminescence system. Replica gels were stained with Coomassie Brilliant Blue R250 to verify equal loading of the individual gel pockets. lc, loading control; M, relative molecular mass  $\times 10^{-3}$ .

## 2.7. Comparison of transcription kinetics between wdr16, sperm-associated antigen 6, hydin and polaris

The temporal course of wdr16 transcript levels in the developing rat testis and in differentiating EPCs was not only analysed by Western blotting, but also by real-time RT-PCR. In testis the level of Wdr16 mRNA reaches half-maximal value at an animal age of 25 days, as determined from the regression curve connecting the individual datapoints (Fig. 16 A). In the case of EPC, this occurs after 7.7 days in culture (Fig. 16 E). In order to determine the relationship between Wdr16 and the presence of kinocilia, the temporal pattern of wdr16 transcription was compared to the ones of the genes for Spag6, a protein limited to the axoneme of kinocilia (Sapiro et al., 2000), for hydin, a protein exclusively expressed in kinocilia-containing tissues (Davy and Robinson, 2003), and for *Tg737<sup>orpk</sup>* (polaris), a component of the IFT apparatus (Haycraft et al., 2001). The efficiencies for the PCR amplification of the respective targets are listed in Table 4.

**Table 4.** Goodness of fit ( $R^2$ ) and efficiencies (E) of the respective real-time PCR analyses of spag6, hydin and polaris mRNA.  $R^2$  values indicate the goodness of fit of a linear regression line connecting the crossing points of a cDNA dilution series from each tissue, whereby  $R^2 \geq 0.98$  is considered to demonstrate linearity and therefore the generation of the PCR product. Efficiencies are calculated from the slope of the respective regression line via the equation  $E = 10^{(-1/\text{slope})}$ .

Tissue	$R^2$ of regression line (Spag6)	Efficiency Spag6	$R^2$ of regression line (hydin)	Efficiency hydin	$R^2$ of regression line (polaris)	Efficiency polaris
EPC	0.99	1.68	0.99	1.89	0.99	1.96
testis	0.98	1.66	0.99	1.95	0.99	1.98

In testis as well as in EPC, the levels of Wdr16 mRNA increase at approximately the same time points and with practically identical time courses as the transcripts of spag6 and hydin (Fig. 16 A-H). The polaris transcript, however, behaves differently. In testis, polaris mRNA levels increase five days prior to the levels of the messages for Wdr16, spag6 and hydin, i.e. on day 19 (Fig. 16 K). In EPC, the polaris mRNA level is found to be substantially lower and no remarkable elevation is detectable over time (not shown).

## Results

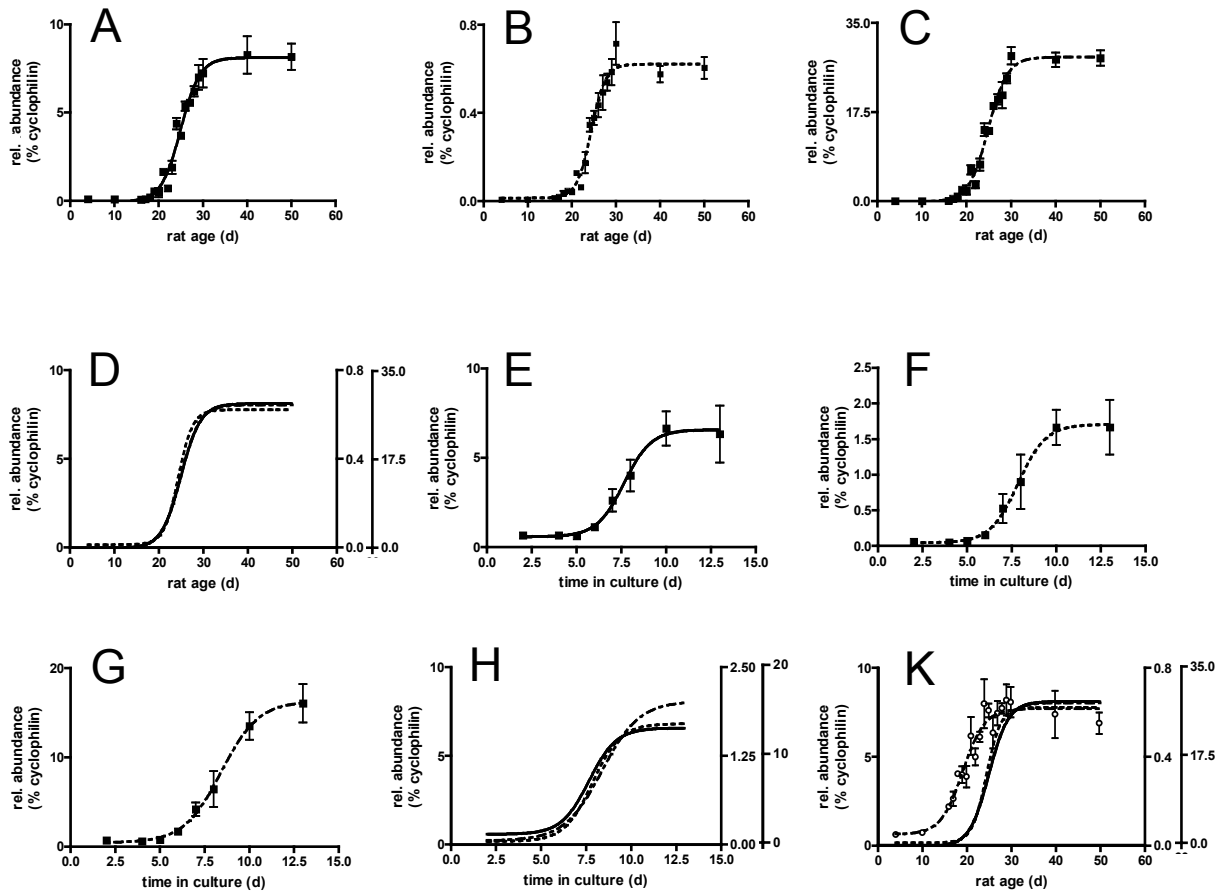


**Fig. 16.** Real-time PCR analysis of time-dependent change in mRNA levels for Wdr16 (A,E), hydin (B,F) and Spag6 (C,G) compared to cyclophilin mRNA in rat testis (A-D) and in ependymal primary culture (EPC; E-H), respectively. The housekeeping gene cyclophilin encodes a peptidyl-prolyl isomerase that is transcribed constitutively and independently from the developmental stage and can therefore be used as a standard to which the Wdr16 mRNA levels can be referred to. One microgram of total RNA was reverse-transcribed and subjected to the PCR in a LightCycler® instrument over 45 cycles using the FastStart DNA Master SYBR Green I system (for details see 4.2.10.). Each data point indicates the mean  $\pm$  standard error of the mean of the relative amount of target mRNA measured in three independent rat testes and four ependymal primary cultures, respectively, at the indicated age. The individual data points are connected by a line obtained by computer-fitting the parameters of the function  $A = B + (P - B)(1 + e^{-(t - t_{50})/s})^{-1}$  to them by the method of least squares. A, relative abundance; B, basal level; P, plateau value;  $t_{50}$ , time at half-maximal level; t, time; s, slope. Overlay of the curves for Wdr16, hydin and Spag6 are depicted in D and H, respectively (data points omitted). Ordinates refer, from left to right, to Wdr16, hydin, and Spag6, respectively. The calculated  $t_{50}$  values are (in order testis, ependymal primary culture): Wdr16,  $25.0 \pm 0.3$  and  $7.7 \pm 0.4$ ; hydin,  $24.4 \pm 0.3$  and  $7.9 \pm 0.4$ ; Spag6,  $24.9 \pm 0.3$  and  $8.4 \pm 0.4$  days. The  $R^2$  values represent the accuracy of the curve fit (in order testis, EPC): Wdr16, 0.944 and 0.758; hydin, 0.925 and 0.740; Spag6, 0.964 and 0.880. Panel K represents figure D supplemented by the data points for tg737<sup>orpK</sup> (polaris/IFT88). The ordinate for polaris is the middle one.  $t_{50}$  for polaris is  $19.2 \pm 0.7$ , while  $R^2$  is 0.808.

## 2.8. Antigen affinity and specificity of Wdr16 antiserum in immunostainings

In order to analyse wdr16 expression on the cellular level, antigen affinity and specificity of the guinea pig Wdr16 antiserum had to be demonstrated prior to its application in immunocyto- and immunohistochemical labellings.

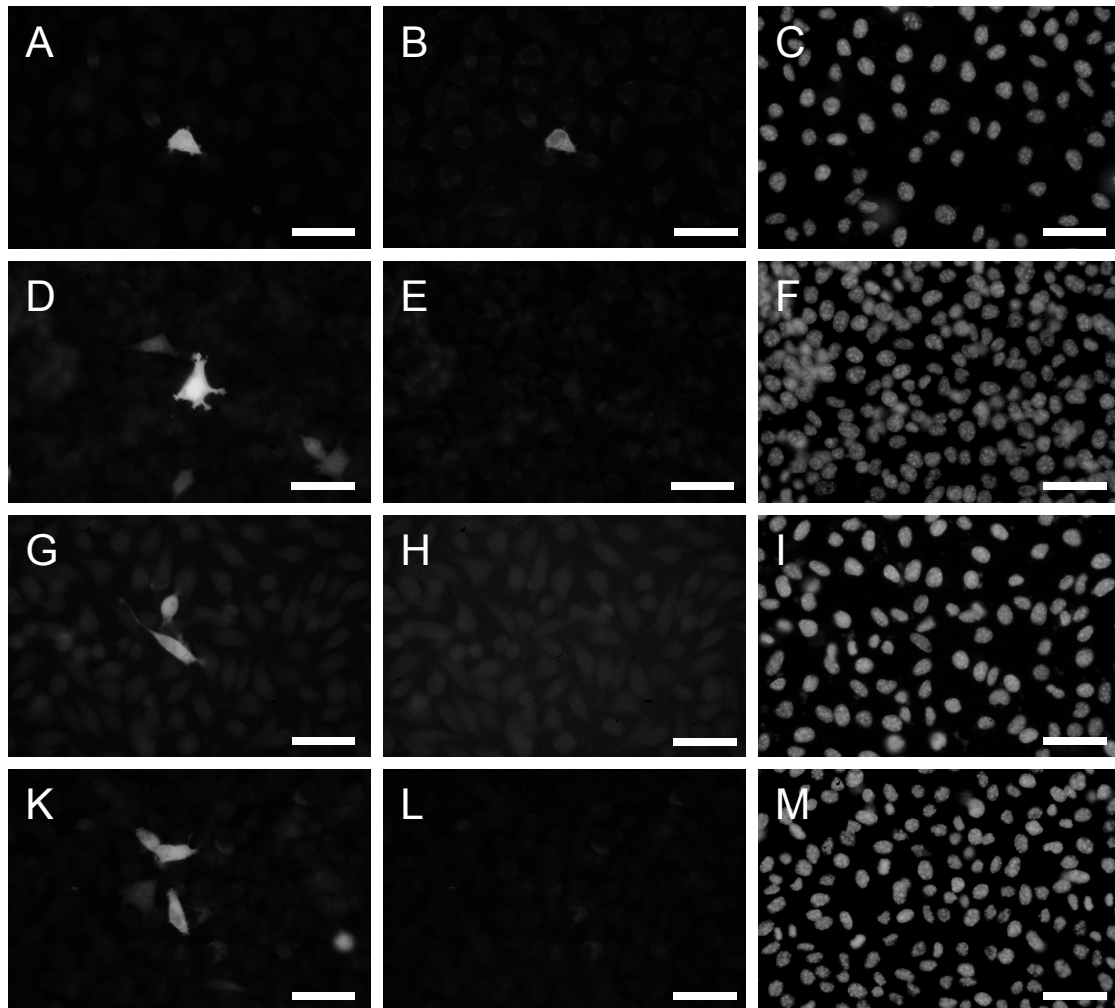


**Fig. 17.** Immunocytochemical stainings demonstrating the antigen affinity and specificity of the guinea pig Wdr16 antiserum. A9 fibroblasts (passage number 42), grown on coverslips, were transfected with 2  $\mu$ g of either pEGFP-N1 vector in which the Wdr16 cDNA is fused to the N-terminus of the coding sequence of enhanced green fluorescent protein (rows **A - C**, **G - I** and **K - M**) or with the pEGFP-N1-vector only (row **D - F**). Transfected cells were immunostained with Wdr16 antiserum diluted 1:1,000 (rows **A - C**, **D - F**), preimmune serum (row **G - I**) or Wdr16 antiserum preabsorbed with the peptide against which the antiserum was raised (row **K - M**). The incubation time was 2 h. Goat anti-guinea pig IgG-Alexa 546 conjugate was used as the secondary antibody in a dilution of 1:4,000 and applied for 1 h. Nuclei counterstained with 4',6-diamidino-2-phenylindole are shown in column **C - M**. Scale bars: 50  $\mu$ m.

In preparation for a first experiment to demonstrate the reactivity and specificity of the Wdr16 antiserum in immunolabellings, the rat Wdr16 cDNA was cloned into the MCS of the pEGFP-N1 vector, facilitating its expression fused to the N-terminus of enhanced green fluorescent protein (EGFP). This fusion construct and the pEGFP-N1 vector lacking an insert, respectively, were transfected into A9 fibroblasts (Littlefield, 1966). The A9 fibroblast cell line was chosen since it was readily available and it is known to be transfectable with commercial transfection reagents. Successful transfection of the cells is indicated by fluorescence due to EGFP expression (Fig. 17 photomicrographs A, D, G, K). A9 fibroblasts transfected with the wdr16-egfp-fusion construct are stained by the Wdr16 antiserum (Fig. 17, row A - C), but neither by the corresponding preimmune serum (Fig. 17, row G - I), nor by the antiserum preabsorbed with the antigenic peptide against which it was raised (Fig. 17, row K - M). The absence of staining in fibroblasts transfected with the pEGFP-N1 vector lacking an insert (Fig. 17, row D - F) demonstrates that the antiserum does not react with the expressed EGFP tag, but specifically recognises the expressed Wdr16 protein in immunolabelling experiments.

## **2.9. Affinity purification of Wdr16 antibody**

### **2.9.1. ELISA**

The Wdr16 antiserum was not readily suitable for staining of EPCs due to weak signal intensity and high unspecific background (not shown). Thus, the guinea pig Wdr16 antiserum was purified using the immunogenic peptide coupled to agarose as an affinity matrix. After elution from the matrix, the purified antibody was subjected to an ELISA in order to assess its immunoreactivity towards Wdr16 and to compare its titer to the one of the unpurified guinea pig Wdr16 antiserum. According to this analysis, the purified antibody preparation maintained its titer (Fig. 18).

## Results

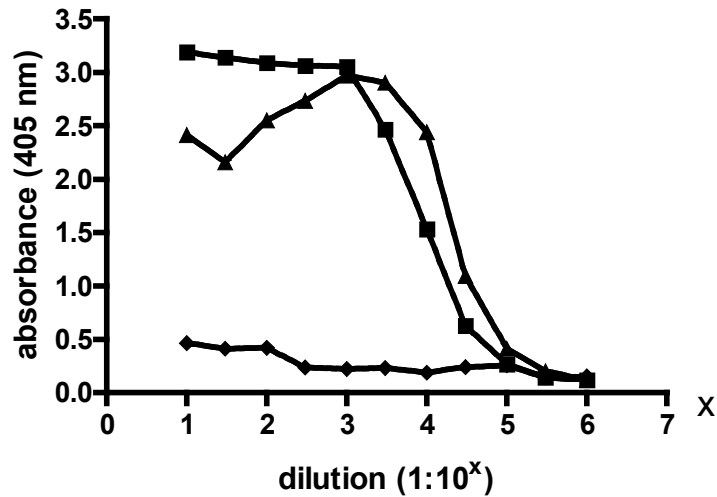


**Fig. 18.** ELISA demonstrating antigen recognition by the affinity-purified Wdr16 antibody. A 96 well plate was coated with 250 ng BSA-conjugated antigenic peptide. Affinity-purified Wdr16 antibody eluted from the affinity column (■), unpurified guinea pig Wdr16 antiserum (▲) and the preimmune serum (◆), respectively, were applied in a dilution series from 1:10 up to 1:10<sup>6</sup>. The incubation time was 2 h. Goat anti-guinea pig IgG-alkaline phosphatase conjugate (1:1,000) was applied as secondary antibody for 1 h. The product of enzymatic cleavage of p-nitrophenylphosphate was measured at a wavelength of 405 nm in an ELISA reader.

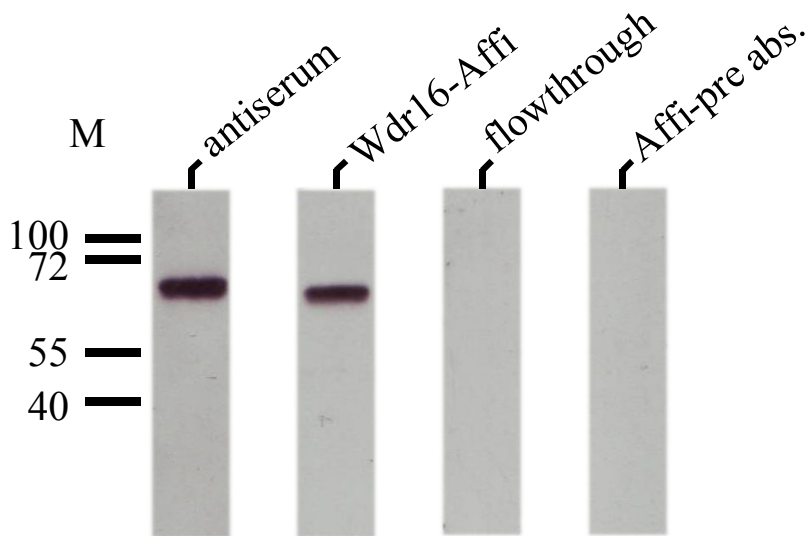


**Fig. 19.** Western blot displaying the immunoreactivity of the affinity-purified Wdr16 antibody. The proteins were separated by SDS PAGE and transferred to a nitrocellulose membrane by electroblotting. Each lane of a 10 % denaturing polyacrylamide gel was loaded with 30  $\mu$ g of protein from an ependymal primary culture homogenate. The membrane was then probed for 1 h with unpurified guinea pig Wdr16 antiserum (antiserum), affinity-purified Wdr16 antibody (Wdr16-Affi), the flowthrough of the column used in the affinity purification (flowthrough) and the affinity-purified Wdr16 antibody preabsorbed with the antigenic peptide (Affi-pre abs.), respectively. The dilution was 1:10,000 with respect to the original serum in each case. The secondary antibody used was donkey-anti guinea pig IgG-peroxidase conjugate, diluted 1:120,000. Secondary antibody incubation time was 1 h. Detection was performed with an enhanced chemiluminescence system. M, relative molecular mass  $\times 10^{-3}$ .

## 2.9.2. Western Blot

Furthermore, the purified Wdr16 antibody was used in Western blotting experiments with EPC homogenate to verify its maintained antigen affinity (Fig. 19). Like the guinea pig Wdr16 antiserum, application of the affinity-purified Wdr16 antibody also resulted in a band corresponding to the relative molecular mass of Wdr16 (approximately 68,000). The affinity column flow-through, however, did not show any immunoreactivity (Fig. 19).

## 2.10. Immunostaining of cell cultures

### 2.10.1. Immunostaining of ependymal primary culture for Wdr16

The purified Wdr16 antibody was employed to analyse the expression of wdr16 in 13 day-old EPCs by indirect immunofluorescent labelling (Fig. 20).

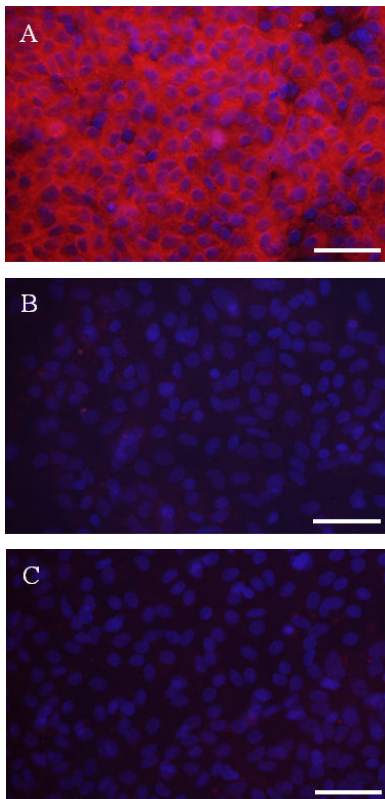


**Fig. 20.** Immunocytochemical stainings to demonstrate reactivity and specificity of the affinity-purified Wdr16 antibody in rat ependymal primary culture. Paraformaldehyde-fixed cells on a coverslip were treated with purified Wdr16 antibody diluted 1:200 (**A**), preimmune serum (**B**) and purified Wdr16 antibody preabsorbed with the peptide against which the antibody was raised (**C**), respectively. Incubation time was 30 min. The secondary antibody, donkey anti-guinea pig IgG-Cy3 conjugate, was diluted 1:1,000 and applied for 50 min. The Wdr16 immunoreactivity is indicated by red fluorescence; nuclei appear blue due to staining with 4',6-diamidino-2-phenylindole. Scale bars: 50  $\mu$ m.

A signal due to Wdr16 immunoreactivity was seen in the cytosol of cells of an EPC after application of the antiserum, while it remained absent when either the preimmune serum or the antiserum preabsorbed with antigenic peptide was employed. It can be concluded that the affinity purification yielded a reactive and specific Wdr16 antibody which may serve as a tool for studying the spatial and temporal expression of wdr16 on the cellular level.

### **2.10.2. Immunocytochemical double stainings of ependymal primary cultures and astroglial primary cultures for Wdr16 and $\alpha$ -tubulin**

To clarify whether the Wdr16-positive cell clusters observed in EPC are indeed ependymal cells, immunofluorescent double stainings were performed using the Wdr16 antibody in combination with a monoclonal antibody directed against  $\alpha$ -tubulin. Since  $\alpha$ -tubulin is abundantly present in the ciliary axoneme, it can be used as a ciliary marker (Prothmann et al., 2001). The localisation of Wdr16 in the cytosol of kinocilia-bearing cells within an EPC is depicted in Fig. 21 A. This finding indicates that the Wdr16 signal stems from ependymal cells, since all other cell types possibly present as contaminants in EPCs are devoid of kinocilia. Thus, while unciliated cells and cells bearing a solitary, primary-like cilium do not show any Wdr16 immunoreactivity, polyciliated, kinocilia-bearing cells express the Wdr16 protein (Fig. 21 A - B).

APCs are known to be contaminated with ependymal cells. When such APCs were subjected to immunofluorescent double labelling using the purified Wdr16 antibody and a monoclonal anti- $\alpha$ -tubulin antibody for counterstaining of cilia, solely ciliated ependymal islands were found to express wdr16. The signal was absent from all other non-ciliated cells surrounding the scattered immunopositive cell clusters (Fig. 21 C).



### 2.10.3. Immunocytochemical double stainings of primary cultures for Wdr16 and the brain isoform of glycogen phosphorylase

In ependymal cells, kinocilia are known to be colocalised with the brain isoform of glycogen phosphorylase (GP BB; Verleysdonk et al., 2005). GP BB is therefore expected to be colocalised with Wdr16 in view of the results listed above. This is indeed the case (Fig. 21 D).

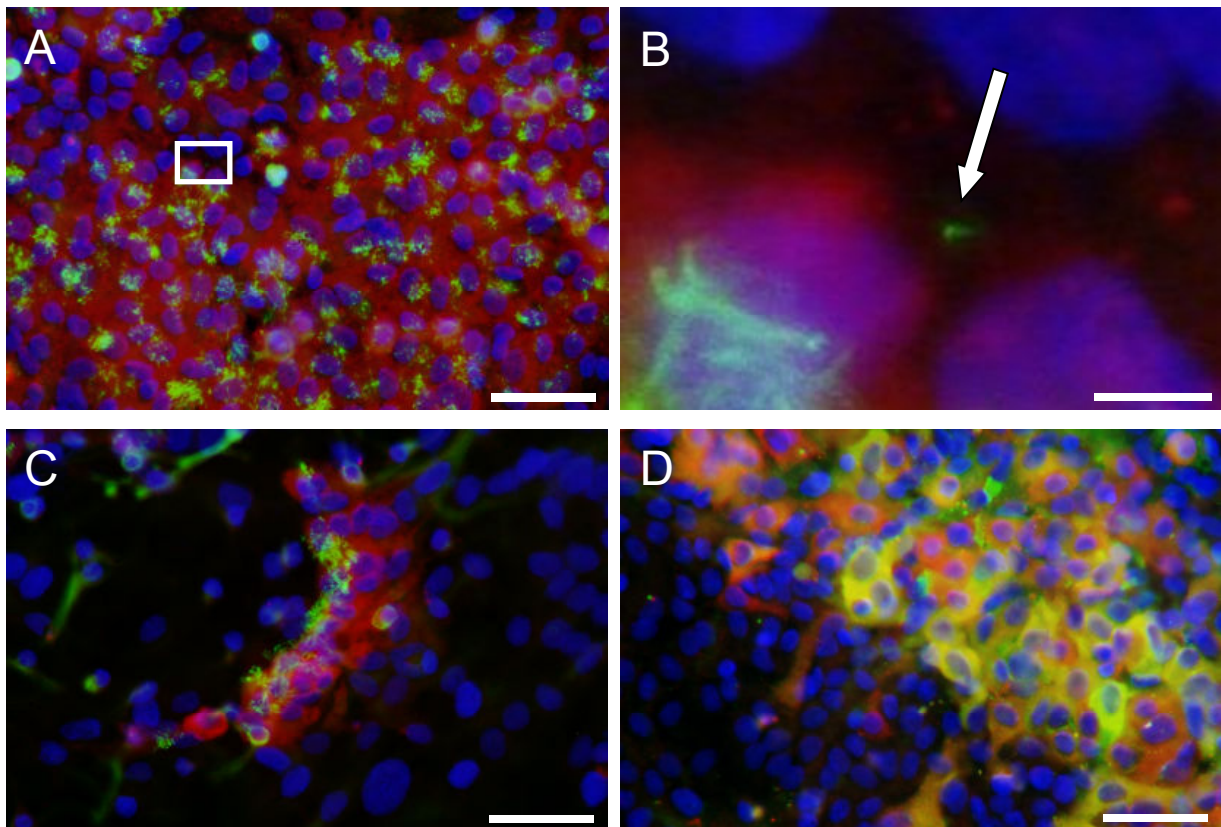


**Fig. 21.** Immunocytochemical double stainings for Wdr16 and  $\alpha$ -tubulin (**A-C**) or brain isoform of glycogen phosphorylase (GP BB; **D**) in rat brain primary cultures. Paraformaldehyde-fixed cells on a coverslip were stained with Wdr16 antibody (1:200) and donkey anti-guinea pig IgG-carbocyanin 3 conjugate (1:1,000) to indicate the presence of Wdr16 (red). For double labellings, two consecutive stainings with in-between fixation were performed. The antibodies used for counterstaining of cilia (green) were mouse monoclonal anti- $\alpha$ -tubulin antibody (1:1,000) and rabbit anti-mouse IgG-fluorescein isothiocyanate conjugate (1:2,000). The counterstaining for GP BB (green) was performed with rabbit anti-glycogen phosphorylase antiserum (1:1,000) in combination with goat anti-rabbit IgG-Alexa 488 conjugate (1:1,000). Incubation times were 30 min each for the first antibodies, and 50 min each for the secondary antibodies. Nuclei were counterstained with 4',6-diamidino-2-phenylindole (blue). **A**, 13 d old ependymal primary culture stained for Wdr16 (red) and  $\alpha$ -tubulin (green). The area enclosed by the frame is depicted in **B** with higher magnification. The arrow in **B** points to a primary cilium. **C**, 13 d old astroglial primary culture stained for Wdr16 (red) and  $\alpha$ -tubulin (green). **D**, 13 d old astroglial primary culture stained for Wdr16 (red) and GP BB (green). Colocalisation is indicated by yellow colour resulting from superposition of red and green images. Scale bars: A, C, D 50  $\mu$ m; B 10  $\mu$ m. Note that the plane of focus is the same in A, B and C and differs from that in D.

## **2.11. Immunohistochemistry**

In the next step, the Wdr16 antibody was used to investigate the expression of wdr16 in rat testis and rat brain by indirect immunofluorescent staining. Since paraffin-embedded sections failed to yield a clear signal (not shown), cryosections with a thickness of 10  $\mu\text{m}$  were used.

### **2.11.1. Staining of rat testis for Wdr16 at different animal age**

In the developing rat testis, the Wdr16 signal is absent from testicular tubules of 17 day-old animals (Fig. 22 A). At 23 days of age, Wdr16 immunofluorescence begins to appear in the cytosol of early spermatocytes (Fig. 22 B). A strong wdr16 expression is maintained in the cytosol of early spermatocytes from day 25 to day 30, whilst the cytosolic signal intensity is weak in putative early spermatids at this age (Fig. 22 C, D). In the adult rat testis, a strong Wdr16 signal localises to pachytene spermatocytes, while the region of excess spermatid cytoplasm exhibits an ambiguous signal (Fig. 22 E). No staining can be observed in the lumen of the testicular tubules where the sperm flagella are located (Fig. 22 E). When the anti-Wdr16 antibody is replaced by preimmune serum (Fig. 22 G) or is preabsorbed with the antigenic peptide (Fig. 22 H), the fluorescence signal disappears, demonstrating the specificity of the Wdr16 antibody also in immunofluorescent staining of rat testis cryosections.

### **2.11.2. Staining of adult rat brain for Wdr16**

When the Wdr16 antibody preparation was applied to 10  $\mu\text{m}$  cryosections of adult rat brain, the total ependymal layer exhibited immunoreactivity, while the brain parenchyma was devoid of the signal (Fig. 23). When preimmune serum was used or when the antibody was preabsorbed with the antigenic peptide, no specific fluorescence signal was detectable in the ventricular epithelium lining the ventricles or elsewhere.

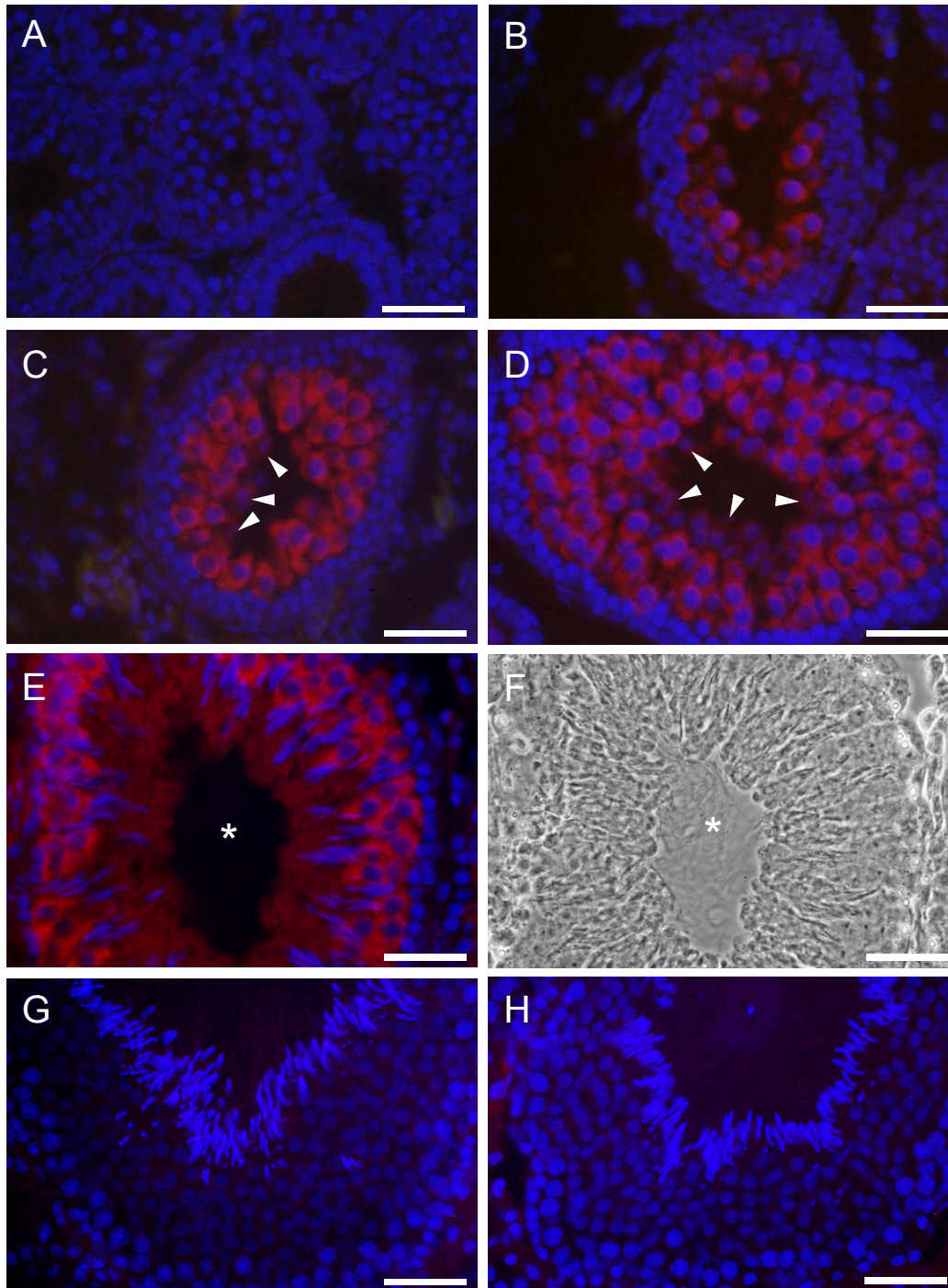


**Fig. 22.** Immunohistochemical stainings showing the expression of wdr16 in the developing rat testis. Ten micrometers thin paraformaldehyde-fixed cryosections were incubated with Wdr16 antibody (diluted 1:200) for 30 min. The secondary antibody, donkey anti-guinea pig IgG-carbocyanin 3 conjugate, was diluted 1:1,000 and applied for 50 min. The presence of Wdr16 is indicated by red fluorescence. The nuclei, counterstained with 4',6-diamidino-2-phenylindole, appear blue. **A**, testis from 17 d old rat; **B**, testis from 23 d old rat; **C**, testis from 25 d old rat; **D**, testis from 30 d old rat; **E**, testis from adult rat; **F**, phase contrast view of E. **G**, Substitution of the antibody by preimmune serum; **H**, The Wdr16 antibody was preabsorbed with the antigenic peptide. Arrowheads point to early spermatids. Asterisks mark the lumen of the seminiferous tubule. Scale bars: 50  $\mu$ m.

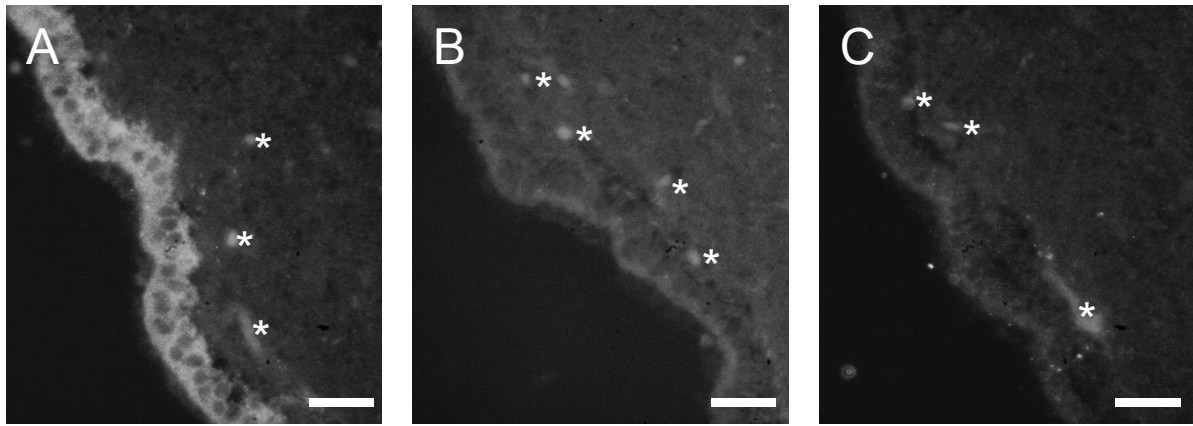


**Fig. 23.** Immunohistochemical stainings demonstrating reactivity and specificity for the Wdr16 antibody in the rat brain. Ten micrometers thin paraformaldehyd-fixed cryosections of an adult rat brain from the area of the third ventricle were treated with Wdr16 antibody diluted 1:200 (**A**), Wdr16 antibody preabsorbed with the peptide against which the antibody was raised (**B**), and preimmune serum (**C**), respectively. Incubation time was 30 min. The secondary antibody, donkey anti-guinea pig IgG-carbocyanin 3 conjugate, was diluted 1:1,000 and applied for 50 min. Asterisks mark blood-filled capillaries in the parenchyma exhibiting fluorescence unrelated to Wdr16. Scale bars: 50  $\mu$ m.

### 2.11.3. Double immunostaining of developing rat brain

For immunofluorescent double stainings of developing rat brain, two consecutive staining protocols with in-between fixation had to be performed to avoid the loss of the Wdr16 signal.

#### 2.11.3.1. Wdr16 and $\alpha$ -tubulin stainings of embryonic rat brain at day 19 of gestation

In the embryonic rat brain at day 19 of gestation, the ependyma still lacks kinocilia, as demonstrated here for the dorsal third ventricle immediately below the choroid plexus (Fig. 24 A) and for the dorsal lateral ventricle (Fig. 24 B). The presence of kinocilia can be taken as a differentiation marker, and the ependyma is therefore not yet mature in a 19 day-old rat embryo. Rather, the ventricle-lining cells are still in the process of proliferation, as indicated by the presence of mitotic nuclei (Fig. 24 B, inset). In the already further developed nasopharyngeal epithelium, however, wdr16 is expressed in the cytosol of kinocilia-bearing epithelial cells, while it is absent from kinocilia-free cells (Fig. 24 C, D).



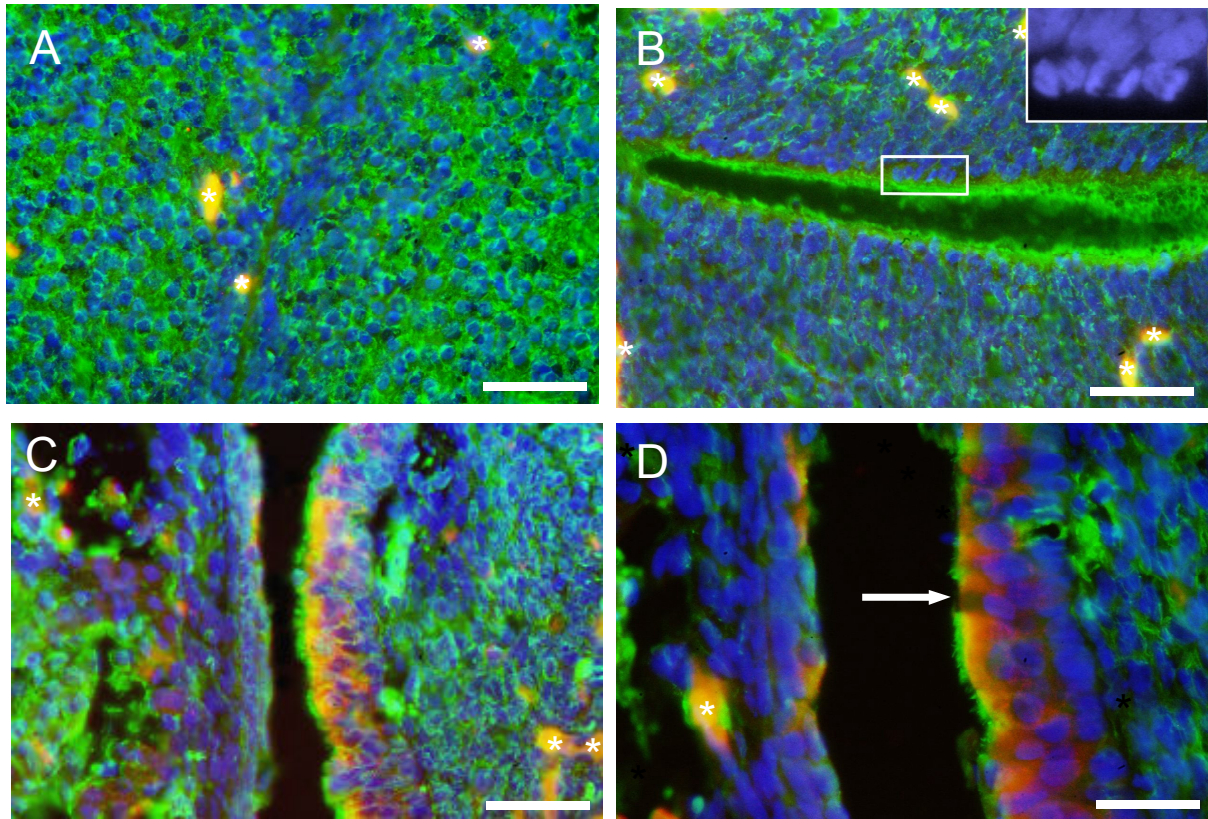


**Fig. 24.** Immunofluorescent double stainings of Wdr16 and  $\alpha$ -tubulin in the head of embryonal rats at day 19 of gestation. Ten micrometers thin paraformaldehyde-fixed cryosections were incubated with Wdr16 antibody (1:200) and donkey anti-guinea pig IgG-carbocyanin 3 conjugate (1:1,000) to indicate the presence of Wdr16 (red). After an additional fixation, cilia (green) were counterstained with monoclonal mouse anti- $\alpha$ -tubulin antibody (1:1,000) in combination with goat anti-mouse IgG-Alexa 488 conjugate (1:1,000). Incubation times were 30 min each for the first antibodies, and 50 min each for the secondary antibodies. Nuclei were counterstained with 4',6-diamidino-2-phenylindole and appear blue. **A**, dorsal third ventricle, immediately below the choroid plexus; **B**, dorsal lateral ventricle with mitotic nuclei (inset); **C**, **D**, nasal respiratory epithelium. The arrow in **D** points to a non-ciliated and Wdr16-negative cell, surrounded by neighbouring kinocilia-bearing, Wdr16-positive cells. Asterisks mark blood-filled capillaries in the parenchyma exhibiting fluorescence unrelated to Wdr16 (autofluorescence). Scale bars: A, B, C 50  $\mu$ m; D 25  $\mu$ m.

### 2.11.3.2. Staining of brain from newborn rat for Wdr16 and $\alpha$ -tubulin

In the brain of newborn rats, wdr16 expression can be observed in the ventral (Fig. 25 A) and in the dorsal cerebral aqueduct (Fig. 25 B), where ependymal differentiation is evident from kinocilia projecting into the ventricles. The cerebral aqueduct is the region from where ependymal differentiation starts its progression through the ventricles in newborn animals (Banizs et al., 2005). At that developmental stage, the undifferentiated cells lining the ventricles are either unciliated or equipped with a single primary cilium, and they are also devoid of Wdr16

immunoreactivity (Fig. 25 C, D, E). Single cells further advanced in the differentiation process possess kinocilia and show a cytosolic localisation of Wdr16 (Fig. 25 F).

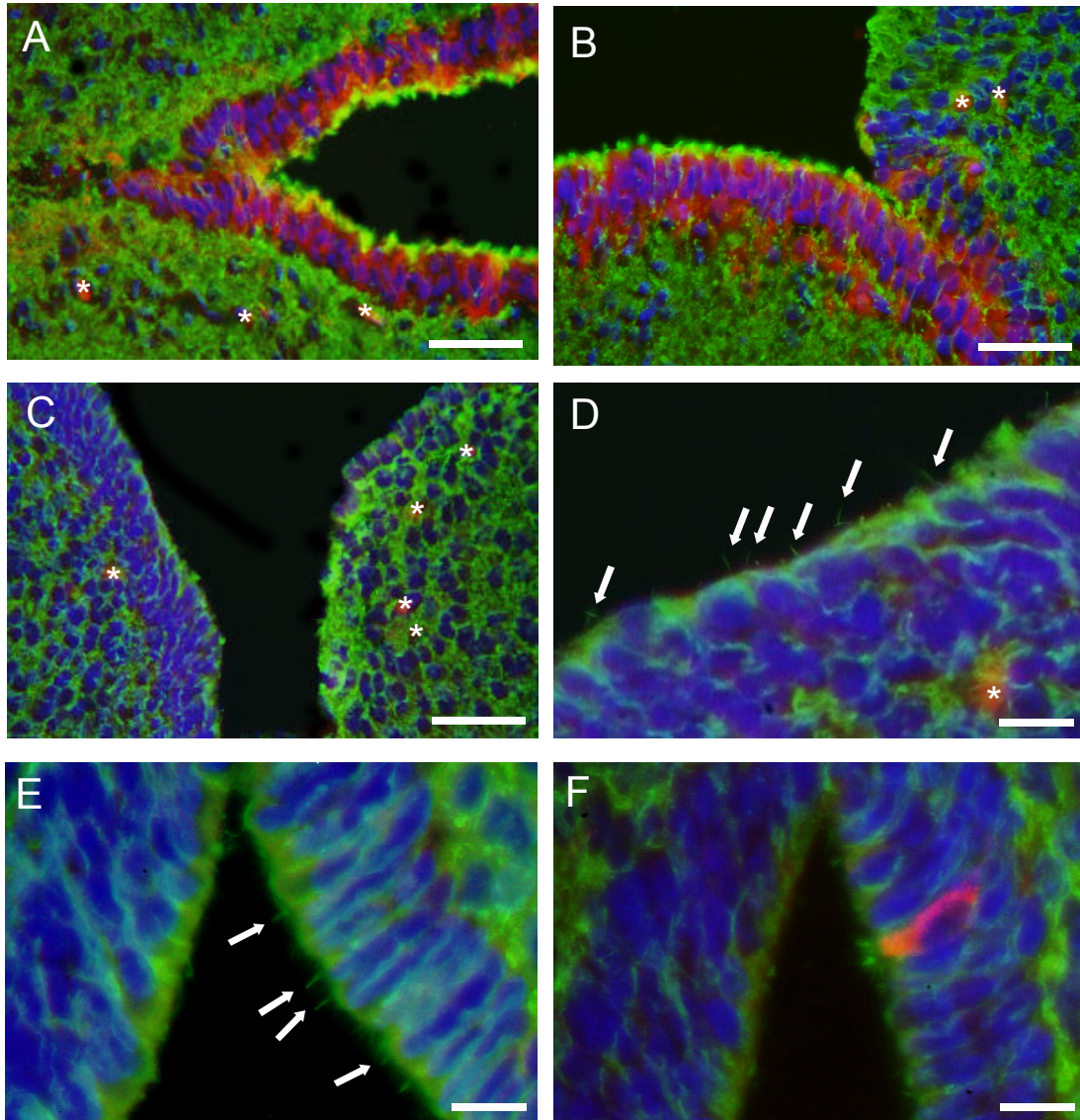


**Fig. 25.** Immunofluorescent double stainings of Wdr16 and  $\alpha$ -tubulin in the brain of newborn rat. Ten micrometers thin paraformaldehyde-fixed cryosections were incubated with Wdr16 antibody (1:200) and donkey anti-guinea pig IgG-carbocyanin 3 conjugate (1:1,000) to indicate the presence of Wdr16 (red). After an additional fixation, cilia (green) were counterstained with monoclonal mouse anti- $\alpha$ -tubulin-antibody (1:1,000) in combination with rabbit anti-mouse IgG-fluorescein isothiocyanate conjugate (1:2,000). Incubation times were 30 min each for the first antibodies, and 50 min each for the secondary antibodies. Nuclei were counterstained with 4',6-diamidino-2-phenylindole and appear blue. **A**, ventral cerebral aqueduct; **B**, dorsal cerebral aqueduct; **C**, fourth ventricle; **D**, detail of C with primary cilia (arrows). Images A-D are from one and the same brain slice. **E**, third ventricle with Wdr16-negative cells bearing primary cilia (arrows); **F**, third ventricle with a single Wdr16-positive, kinocilia-bearing cell. Blood-filled capillaries in the parenchyma give bright fluorescence signals unrelated to Wdr16 (autofluorescence) and are marked by asterisks. Scale bars: A, B, C 50  $\mu$ m; D, E, F 10  $\mu$ m.



### 2.11.3.3. Costaining of Wdr16 and either $\alpha$ -tubulin or the brain isoform of glycogen phosphorylase in the brain of two day-old rat

In the brain of two day-old rat, ependymal differentiation has reached the ventricles. While neither Wdr16 nor kinocilia are apparent in the ventral floor of the third ventricle (Fig. 26 A), the polyciliated dorsal area of the third ventricle exhibits strong Wdr16 immunoreactivity (Fig. 26 C). The middle region of the third ventricle shows the transition from kinocilia-bearing to kinocilia-free ependymal cells (Fig. 26 B), which is accompanied by a gradient of wdr16 expression.

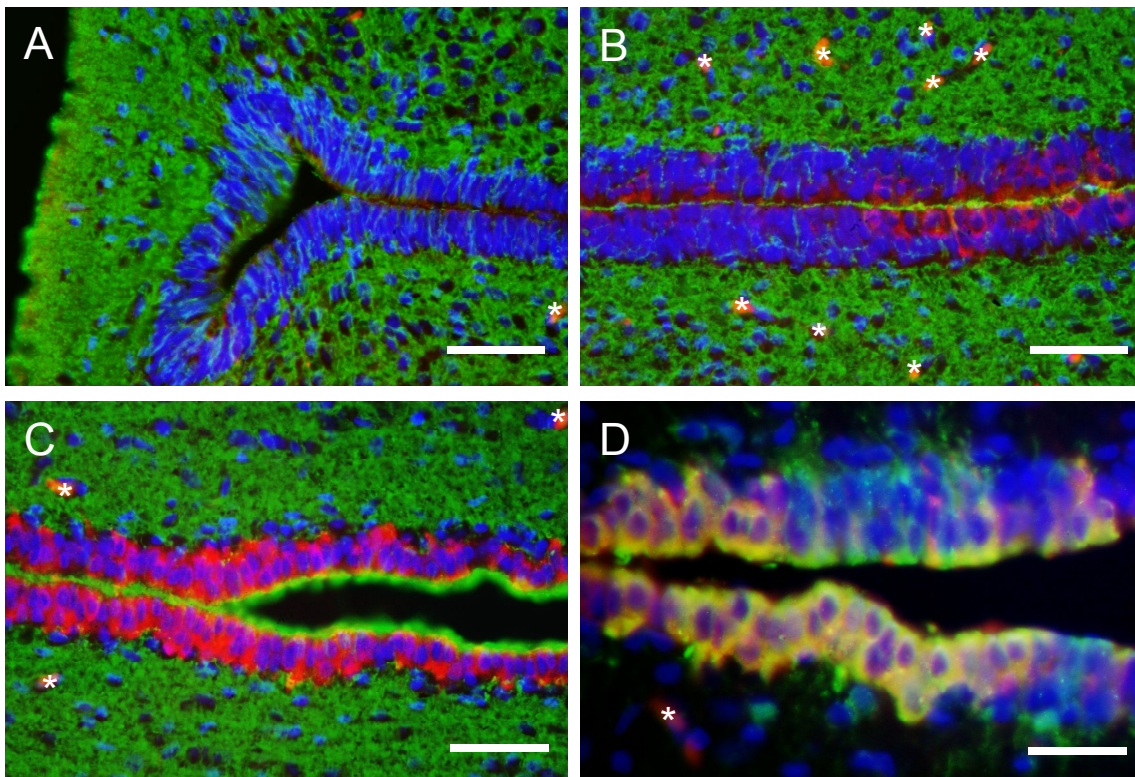


**Fig. 26.** Immunofluorescent double stainings of Wdr16 and  $\alpha$ -tubulin (**A-C**) or the brain isoform of glycogen phosphorylase (GP BB; **D**) in the brain of 2 day-old rat. Ten micrometers thin paraformaldehyde-fixed cryosections were incubated with Wdr16 antibody (1:200) and donkey anti-guinea pig IgG-carbocyanin 3 conjugate (1:1,000) to indicate the presence of Wdr16 (red). After an additional fixation, cilia (green) were counterstained with monoclonal mouse anti- $\alpha$ -tubulin-antibody (1:1,000) in combination with rabbit anti mouse IgG-fluorescein isothiocyanate conjugate (1:2,000). The counterstaining for GP BB (green) was performed with rabbit anti-glycogen phosphorylase antiserum (1:1,000) in combination with goat anti-rabbit IgG-Alexa 488 conjugate (1:1,000). Incubation times were 30 min each for the first antibodies, and 50 min each for the secondary antibodies. Nuclei were counterstained with 4',6-diamidino-2-phenylindole and appear blue. **A**, ventral floor of third ventricle; **B**, middle area of third ventricle; **C**, dorsal third ventricle. Figs. A-C were photographed from one and the same slide. **D**, colocalisation (yellow) of Wdr16 and GP BB in the area of the dorsal third ventricle. Blood-filled capillaries in the parenchyma give bright autofluorescence signals unrelated to Wdr16 and are marked by asterisks. Scale bars: A, B, C 50  $\mu$ m; D 25  $\mu$ m.

The colocalisation of Wdr16 and GP BB shown in this work in the primary culture system also holds true for the rat brain ependyma (Fig. 26 D).

## **2.12. Zebrafish embryo as a suitable model organism for investigating possible Wdr16 functions**

A knockdown of the *wdr 16* gene has the potential to identify the role of this protein in health and disease. A suitable model organism to study the effect of a gene knockdown is the zebrafish (*Danio rerio*). The embryos are transparent and are readily available due to the high number of offspring and the short generation time of *Danio rerio*, enabling a quick and easy identification of knockdown-associated phenotypes. An appropriate tool to generate a transient gene knockdown in zebrafish are the so-called 'morpholinos'. These antisense oligomers have a morpholine backbone connected by phosphorodiamidates instead of phosphate-interconnected ribose residues (Summerton and Weller, 1997) An antisense morpholino was designed to hybridise to the region around the translation initiation site on the mRNA of the zebrafish *wdr16* ortholog, preventing translation. All experiments described in the following were conducted in the laboratory of Hans-Martin Pogoda at the Max Planck Institute of Immunobiology in Freiburg, Germany.

### **2.12.1. Analysis of the presence of Wdr16 mRNA in zebrafish embryo by in-situ hybridisation**

Prior to the knockdown experiments, the tissue-specific occurrence of *Wdr16* mRNA in the zebrafish was investigated by in-situ hybridisation with DIG-labelled antisense RNA probe in whole-mount embryos. Representative results are depicted in Fig. 27. In the 10 somite embryo, *Wdr16* mRNA is present in the neural tube (Fig. 27 A, B), the otical placodes (Fig. 27 A) and in the pronephric mesoderm (Fig. 27 B). One day-old embryos exhibit the signal in the canal of the spinal cord, the pronephric ducts (Fig. 27 C), the olfactory placode, the SCO (Fig. 27 D) and in the region of the aqueduct between the midbrain and hindbrain (Fig. 27 C, D, E, arrow). A two day-old



embryo retains the *Wdr16* message in the nose, the SCO (Fig. 27 F) and in the midbrain ventricle (Fig. 27 F, arrow).

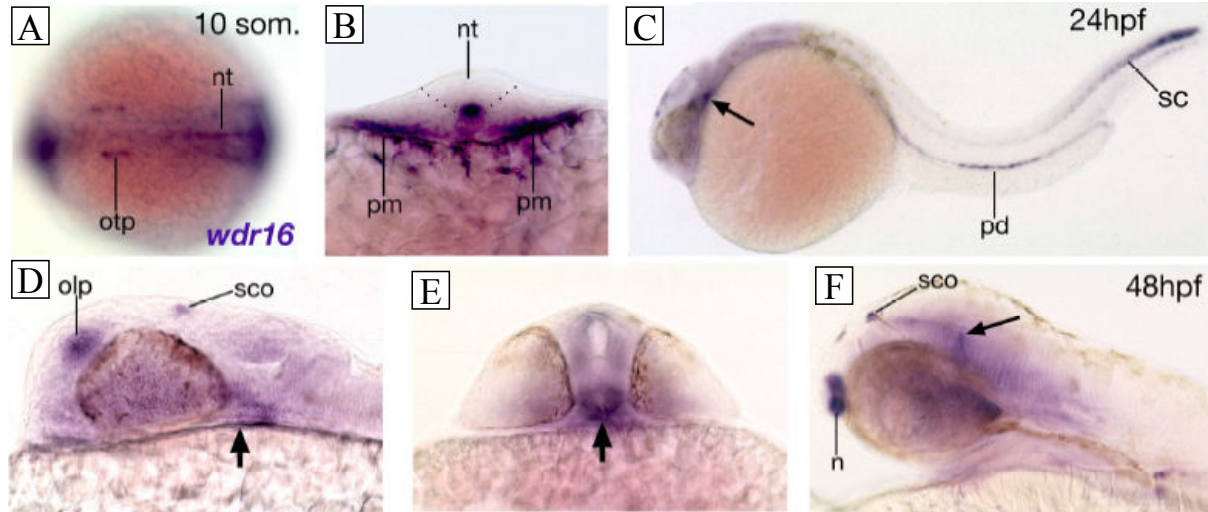


**Fig. 27.** In-situ hybridisation demonstrating the presence of *Wdr16* mRNA in zebrafish. In-situ hybridisation in the whole mount embryo was conducted with a digoxigenin-labelled antisense RNA probe against *Wdr16* mRNA.

**A**, 10 somite stage embryo, exhibiting *Wdr16* mRNA signals in the neural tube (nt) and otical placode (otp); **B**, Optical cross-section of a 10 somite stage embryo revealing a signal for *Wdr16* message in the pronephric mesoderm (pm) and in the floor of the neural tube (nt); **C**, 1 d old embryo showing *Wdr16* mRNA in the canal of the spinal cord (sc), the pronephric duct (pd) and in the area of the aqueduct (arrow) between the midbrain and the hindbrain ventricles; **D**, 1 d old embryo exhibiting the *Wdr16* message in the olfactory placode (olp), the subcommissural organ (sco) and the aqueduct (arrow); **E**, Cross-section of a 1 d old embryo displaying a pronounced signal in the aqueduct (arrow); **F**, *Wdr16* mRNA is present in the nose (n), the subcommissural organ (sco) and in the midbrain ventricle (arrow) of a 2 d old embryo. som., somite; hpf, hours post fertilisation.

### 2.12.2. Efficiency and specificity of the *Wdr16* antisense morpholino

The knockdown efficiency and specificity of the *Wdr16* antisense morpholino had to be validated by a control experiment. For that purpose, RNA was isolated from a 1 day-old zebrafish embryo, reverse-transcribed and subjected to a PCR reaction with suitable primers for the amplification of cDNA containing the part of the mRNA sequence against which the antisense morpholino was directed. The PCR product was then cloned into the MCS of the XLT.GFP<sub>TL</sub>-CS2 vector, resulting in a fusion construct between a part of *Wdr16* and the green fluorescent protein (GFP) ORF. This fusion construct was coinjected into embryos at the single cell stage together with either the antisense morpholino (*wdr16*MO; Fig. 28, row C, D) or the control

morpholino (*wdr16CoMo*; Fig. 28, row A, B). In case of the negative control, green fluorescence is visible in the injected embryos at the mid gastrulation stage (Fig. 28 B), while the signal is abrogated in animals treated with *wdr16MO* (Fig. 28 D). The absence of GFP expression from the embryos treated with *wdr16MO*, but not from embryos treated with *wdr16CoMo*, demonstrates the knockdown effectiveness and specificity of the antisense *wdr16* morpholino employed.

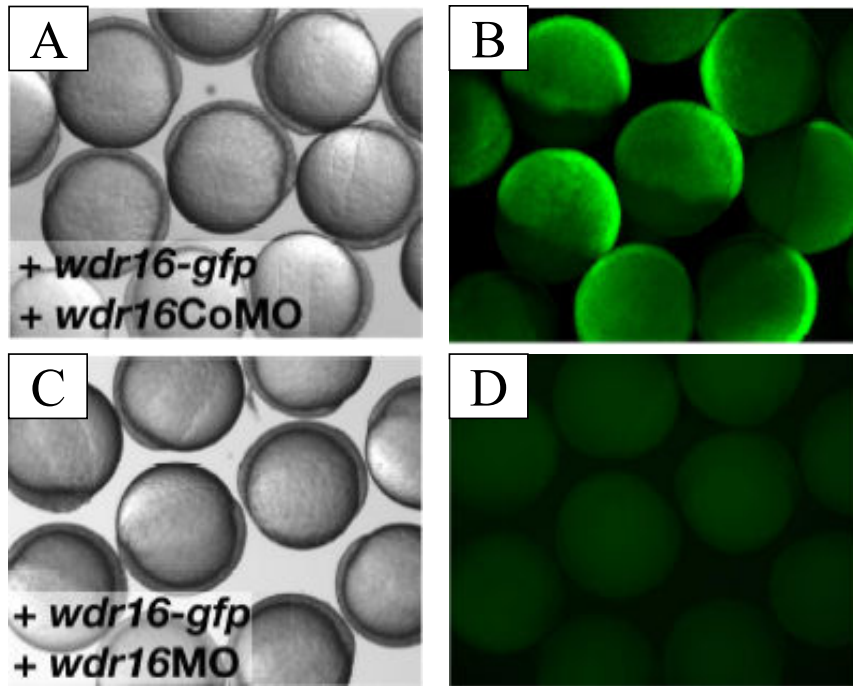


**Fig. 28.** Transfection control experiment demonstrating specific inhibition of *Wdr16* mRNA translation by a *Wdr16*-directed antisense morpholino. Zebrafish embryos at the one cell stage were coinjected with a construct in which a part of the *Danio Wdr16* antisense morpholino target sequence is fused to the ORF of green fluorescent protein (GFP; +*wdr16-gfp*) and either (A) the control morpholino (+*wdr16CoMO*) or (C) the antisense morpholino directed against the *Wdr16* sequence (+*wdr16MO*). Whilst embryos treated with the control morpholino exhibit green fluorescence (B), the signal is absent from fish injected with the antisense morpholino (D).

### 2.12.3. Consequences of *Wdr16* knockdown in zebrafish embryos

Embryos at the one cell stage were injected with either *wdr16MO* or with the inactive inverse sequence *wdr16CoMo*. The phenotype was inspected after 48 h post fertilisation (hpf). Representative examples are depicted in Fig. 29. Of 102 surviving embryos injected with the *wdr16MO*, 73 animals developed pronounced hydrocephalus (Fig. 29 A) and a further 19 exhibited less severe but still clear

hydrocephalus, while only 10 fish remained indistinguishable from the wild type. When *wdr16CoMo* was injected, 58 out of 67 embryos did not differ in their phenotype from the uninjected control (Fig. 29 B), while 9 fish displayed unspecific mild retardation in development. Among the uninjected wild type controls, 35 out of 39 embryos developed normally (Fig. 29 C). The dilatation of the ventricles remained the only visible phenotype in *Wdr16* knockdown zebrafish 48 hpf.

The ependymal epithelium of the hydrocephalic zebrafish brains did not show any untypical morphology or disorganisation in comparison to control animals. Additionally, the beating of the ependymal kinocilia was unaltered compared to the controls as measured by high speed videography (Hirschner et al., 2007).

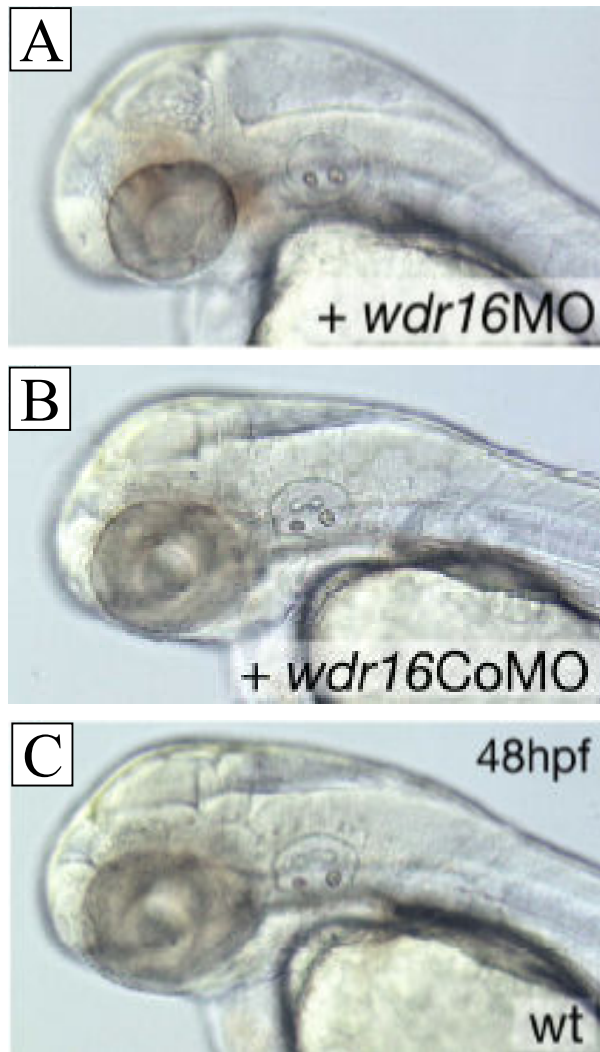


**Fig. 29.** Phenotypes of 48 h-old zebrafish embryos after *Wdr16* knockdown. Zebrafish embryos injected at the one cell stage with the *Wdr16* antisense morpholino (+*wdr16MO*) display severe hydrocephalus (**A**), whilst this phenotype is not visible in animals injected with a control morpholino (+ *wdr16CoMO*, **B**) or in the wildtype (wt, **C**). hpf, hours post fertilisation.

## 2.13. Yeast-Two Hybrid Screen

WD-repeat proteins are known to mediate protein-protein interactions (Smith et al., 1999). Therefore, a Yeast-Two Hybrid Screen was performed to find interaction partners of Wdr16. Since wdr16 is highly expressed in testis, the full-length Wdr16 sequence was used as bait to screen a human testis cDNA library using the “Matchmaker Gal4 Two-Hybrid System 3” (purchased from Clontech), in close collaboration with D. Scheible, IFIB, University of Tübingen. The only identified candidate clone to come into question to represent a Wdr16 interaction partner corresponded to KIAA0179 mRNA (accession number NM\_015056), the corresponding protein of which belongs to the Npp protein family. These proteins are localised in the nucleolus where they are involved in the generation of rRNA (<http://harvester.embl.de>). However, the capability of this clone to grow on selective medium disappeared after replating, and an ORF matching the sequence of the KIAA protein could not be identified. Therefore, the identified sequence turned out to be an artefact, which coincides with the observation that nuclear proteins are frequently obtained as false positives in a Yeast-Two Hybrid screen (K. Nau, F. Madeo, personal communication).

## **3. Discussion**

### **3.1. Potential of subtractive ependymal cDNA libraries**

Screening of the subtracted ependymal and SCO cDNA libraries yielded, among others, clones encoding Wdr16 and Spag6, indicating ependyma-specific transcription of these genes in the CNS. In total, 139 of the clones identified in the laboratory were sequenced, among which the wdr16 transcript was represented by 6 sequences, while 10 cDNA fragments represented parts of the spag6 transcript. Spag6 is a constituent of the ciliary central apparatus (Sapiro et al., 2000) and can therefore be regarded as a marker for kinocilia. Since in the brain ependymal cells are the only cell type bearing kinocilia, the frequent finding of Spag6 confirms the high quality of the subtracted libraries and suggests them as effective tools for finding genes that are expressed in ependymal cells, but not elsewhere in the brain parenchyma.

### **3.2. Comparison of Wdr16 with other WD40-repeat proteins**

The predicted three-dimensional structure of the Wdr16 protein resembles the X-ray structure of actin-interacting protein 1 (AIP 1; Voegtli et al., 2003), a WD repeat protein that had been predicted by bioinformatic analysis to contain at least 10 repeats (Ono, 2001). The architecture of AIP 1 with its two covalently linked 7-bladed  $\beta$ -propellers supports the assumption that the formation of two smaller  $\beta$ -propellers instead of only one huge propeller containing a larger number of blades seems to be the preferred option for proteins with more than 7 WD repeats (Voegtli et al., 2003). The protein involved in apoptosis, apoptotic protease activating factor-1 (Apaf-1) with its 12 or 13 WD repeats (Shi, 2002), also obeys this rule (Acehan et al., 2002).

Therefore, the predicted fold of Wdr16 into two 7-bladed  $\beta$ -propellers appears very likely.

Despite the common motif, members of the WD-repeat protein family show a high degree of functional diversity, which makes it impossible to derive the physiological relevance of Wdr16 from its structure alone. The most prominent WD protein the crystal structure of which has been resolved is the  $\beta$ -subunit of the heterotrimeric G-protein transducin (Wall et al., 1995; Sondek et al., 1996). Another member of the WD protein family that is involved in signal transduction is the receptor for activated C-kinase 1 (Croze et al., 2000). Other identified functions of WD repeat proteins aside from participation in signal transduction are reviewed in Li and Roberts (2001), e.g. cell cycle control (CDC20), transcriptional regulation (several TATA box-binding protein-associated factors), chromatin assembly (chromatin assembly factor 1), apoptosis (Apaf-1), motor protein complex assembly (intermediate chain 78 of Chlamydomonas outer dynein arm) and vesicular trafficking ( $\alpha$ - and  $\beta$ -coatamer protein).

Despite its yet unknown physiological function, Wdr16 has to be assumed to be engaged in protein-protein interactions, as known from other WD proteins (Smith et al., 1999).

### **3.3. Congruence between Wdr16 and the expression of kinocilia**

Bioinformatic studies revealed Wdr16 orthologs to be restricted to organisms in possession of kinocilia. High evolutionary conservation of Wdr16, the occurrence in unicellular flagellated, as well as in kinocilia-possessing metazoic, but absence from flagella-lacking organisms suggests a fundamental role in cellular function connected to kinocilia-bearing cells.

The correlation between the presence of Wdr16 and kinocilia also holds true for rat organs and tissues. The apparent absence of Wdr16 from lung shown by the Western blot experiment depicted in Fig. 9 is most readily explained by a protein level below the detection limit in view of the low amount of Wdr16 mRNA in lung compared

to EPC and testis (Table 3). Since RT-PCR also demonstrated the existence of exon 2, wherein the antigenic sequence is located against which the antibody was raised, a lack of the antibody recognition site due to the occurrence of a splice variant cannot be the reason for the missing immunoreactivity. An attempt during the present study to stain rat lung and trachea with the Wdr16 antibody was unsuccessful due to an overwhelming background signal, probably because of the mucus contained in these tissues. However, wdr16 expression was demonstrated in the nasopharyngeal region, which is part of the upper airway epithelium. An analogous case has been described in Zhang et al. (2002), in which the murine ortholog of the axonemal protein Pf20 was detectable by immunoblotting in testis but not in the lung, although both tissues definitely contain kinocilia and therefore the protein.

Another indication, beside bioinformatic analysis, that Wdr16 upregulation is tied to the presence of kinocilia or flagella is the appearance of the protein in rat testis at animal age of 24 days, which is also the time when the primary spermatocyte number per unit area of the seminiferous tubule peaks and the production of spermatids starts (Zhengwei et al., 1990). In the process of mammalian sperm assembly, the round spermatids are described to be the differentiation state, in which the formation of the axoneme commences (Irons and Clermont, 1982).

In differentiating EPCs, the occurrence of Wdr16 protein at approximately day 7 coincides with the beginning of kinocilia formation (S. Verleysdonk, unpublished data). The increase of Wdr16 protein synthesis in ageing APCs reflects an increase in the number of contaminating ependymal cells, a phenomenon that has already been observed by B. Hamprecht (personal communication, unpublished data). In the maturing zebrafish embryo, the message for the ortholog Wdr16 is exclusively present in tissues that have reached a developmental stage in which kinocilia are present. Kinocilia-bearing cells occur in the olfactory and otic placodes (Byrd et al., 1996; Sumanas et al., 2003) and also in the kidney, where they are of the 9 + 2 axonemal structure, in contrast to mammalian primary cilia in this organ (Kramer-Zucker et al., 2005). Thus, the temporal expression pattern of Wdr16 protein in rat testis and in primary cell cultures, together with the observed distribution of Wdr16 mRNA in the zebrafish, strongly implies Wdr16 as a differentiation marker for kinocilia-bearing cells.

Immunostainings localised Wdr16 to the cytosol of sperm precursor cells and to the cytosol of ependymal cells, while sperm tails and ependymal cilia were found to be free from immunofluorescence. On the other hand, Wdr16 immunoreactivity has been found in the tail fraction - but not in the head fraction - of fractured bull sperm by Western blot experiments. This allows for the possibility that the apparent lack of Wdr16 immunofluorescence in the immunostaining experiments on cells and tissues might be due to an incapacity of the Wdr16 antibody to recognise the antigen in the densely packed environment of the sperm axoneme. Considering that Wdr16 is a WD-repeat protein mediating protein-protein interactions (see above), the antigenic peptide stretch is very likely to be masked by an interaction partner. In view of the presence of a Wdr16-specific signal in the Western blot analysis of bull sperm tails, combined with the lack of an immunofluorescence signal in spermatozoa treated with the Wdr16 antiserum, it may be concluded that the peptide antibody is able to detect Wdr16 reliably under denaturing blot conditions, but not always in the more native environment present during immunostainings. This assumption is corroborated by the analogous absence of an  $\alpha$ -tubulin signal in sperm tails after immunostaining with a monoclonal anti  $\alpha$ -tubulin antibody (D. Scheible, personal communication). The presence of Wdr16 in the tail fraction does not necessarily mean that the protein is also present in ependymal kinocilia. The sperm tail fraction, namely, does not only contain the axonemal structure, but also mitochondria (Fawcett, 1975). Although Wdr16 was found to be predominantly cytosolic, it cannot be ruled out to be also present in mitochondria and it may persist in the middle section of sperm due to mitochondrial binding as it has been described for other cytosolic proteins like hexokinase (Wilson 1997). Thus, the immunoreactive signal in the Western blot originating from the sperm tail fraction gives no independent information about the subcellular localisation of Wdr16.

Immunostainings not only indicate the presence of Wdr16 in kinocilia-bearing cells, but also its absence from non-ciliated and monociliated cells. This observation confirms on the cellular level what is already indicated by the correlation of wdr16 transcription with the transcription kinetics of the kinocilia markers Spag6 and hydin on the one hand, but not with the general ciliary marker, polaris, on the other hand (Haycraft et al., 2001). Since primary cilia are known to already occur in the kinocilia-free embryonic testis (Ward et al., 2003), the above-zero baseline of polaris mRNA in



this tissue (Fig. 16 K) reflects their presence in very early stages of development. The strong increase in testicular polaris mRNA after postnatal day 10 is based on the augmented demand for IFT proteins that are required for the assembly of sperm flagella. Therefore, the absence of Wdr16 in monociliated cells but its presence in polyciliated ones demonstrates that the wdr16 gene is not expressed prior to differentiation of the kinocilia-bearing cells in these tissues.

In summary, Wdr16 can be considered as a marker protein for differentiated kinocilia-bearing ependymal cells and thus can be used for their identification in primary cultures and in the brain.

### **3.4. Expression of the wdr16 gene in the hepatocellular carcinoma cell line HepG2**

In a study published by Silva et al. (2005), Wdr16 mRNA is shown to be present in hepatocellular carcinomas and in hepatoma cell lines, but not in normal liver tissue. In the present study, Western blot analysis confirms the expression of Wdr16 in the hepatocellular tumor cell line HepG2, as well as the lack of Wdr16 in noncancerous liver. However, the role of Wdr16 in cell proliferation postulated by Silva et al. (2005) appears highly unlikely, since dividing ependymal cells are definitely devoid of Wdr16 immunoreactivity and, beyond that, its occurrence is tied to differentiated but not to undifferentiated tissues. Therefore, it has to be noted that the functional pattern of proteins in highly dedifferentiated cancer cells does not necessarily reflect their functions under physiological conditions.

### **3.5. Colocalisation of Wdr16 and the brain isoform of glycogen phosphorylase**

Wdr16 is shown to colocalise with GP BB. The glycogen present in ependymal cells (Cataldo and Broadwell, 1986; Prothmann et al., 2001) is thought to serve as an internal energy store that is degraded by GP BB in response to an increased cellular energy demand. For example, the neurotransmitters serotonin and noradrenaline

cause an increase in ependymal ciliary beat frequency and simultaneously in glycogenolysis (Nguyen et al., 2001; Prothmann et al., 2001; Verleysdonk et al., 2005). Beyond that, ependymal cells seem to be involved in water homeostasis of the brain, a process that requires active, ATP-driven ion transport (see Introduction and Brown et al., 2004). These active ion transport processes, putatively elicited by NPs that are known to evoke a response in ependymal cells (Wellard et al., 2003; 2006) might be another cause for glycogen-fueled energy consumption.

### **3.6. Comparison of Wdr16 knockdown-associated hydrocephalus with other animal models of hydrocephalus**

The knockdown of Wdr16 in zebrafish results in the formation of severe hydrocephalus, while ciliary motility and ependymal morphology are unaltered with respect to the control animals and the wild type.

This is in contrast to several animal models linking the formation of hydrocephalus to defunct cilia. For example, mice with a mutated gene encoding dynein heavy chain Mdnah5 are characterised by a reduced number of outer dynein arms in the axoneme of ependymal cilia, which leads to impaired ciliary beating. This in turn abrogates the directed CSF flow through the aqueduct of Sylvius resulting in aqueductal stenosis with dilated lateral and third ventricles (Ibanez-Tallon et al., 2002; 2004). While Mdnah5<sup>-/-</sup> mice always suffer from enlarged ventricles, human beings bearing mutations in the orthologous gene dnah5 incur only an 80 times higher risk of developing aqueductal stenosis compared to the average of the population (Ibanez-Tallon et al., 2004). The clinical symptoms of primary ciliary dyskinesia (PCD; OMIM 244400) are a 50 % chance of situs inversus (randomisation of body left-right axis), chronic respiratory infections and immotile sperm due to defunct cilia and flagella. Hydrocephalus, however, is not commonly associated with this disease (Afzelius and Mossberg, 1995). Therefore, ciliary immotility need not necessarily result in the formation of ventriculomegaly, as evident from mice deficient in Spag6, a protein that localises to the central apparatus of the axoneme (Sapiro et al., 2000; 2002). While Spag6<sup>-/-</sup> mice show ultrastructural defects in and impaired

motility of the sperm axoneme, only 50 % of these animals are affected by hydrocephalus (Sapiro et al., 2002). The fact that defects in ciliary motility alone are not the decisive factor for the development of hydrocephalus is further evident from mice harbouring a defect in the gene *tg737*. This gene encodes *polaris*, a constituent of the IFT machinery (Haycraft et al., 2001). The IFT complex is required for the assembly and the maintenance of cilia (Rosenbaum and Witman, 2002). *Tg737<sup>orpk</sup>* mice, in fact, have disorganised ependymal cilia and display impaired ciliary beating in combination with reduced fluid flow along the ependymal cell surface, but the onset of hydrocephalus in these animals has been reported to precede cilia formation (Banizs et al., 2005). These authors postulated that hydrocephalus in *tg737<sup>orpk</sup>* mutants forms because of altered ion fluxes. A disturbance in brain water homeostasis and osmoregulation has also been suggested for mutant *hy3* mice which, besides hydrocephalus, also develop brain edema (McLone et al., 1971; 1973). The transcription profile of the underlying *hyd* gene is similar to the one established for *wdr16* in the present study. The eventual loss of cilia and disruption of the ependymal layer seen in *hy3* mice with full-blown hydrocephalus is regarded as a secondary effect (Bannister and Chapman, 1980). The hydrocephaly with hop gait (*hyh*) mouse strain bears a defect in the gene encoding  $\alpha$ -SNAP (Hong et al., 2004), a protein with a crucial role in membrane trafficking. The consequence of  $\alpha$ -SNAP malfunction is a mislocalisation of apical proteins like E-cadherin,  $\beta$ -catenin, atypical protein kinase C and the soluble NSF attachment protein receptor (SNARE) *Vamp7* (Bajjalieh, 2004; Chae et al., 2004). These observations in the *hyh* mouse strain clearly link cell polarity defects to hydrocephalus. Furthermore, the lack of the transmembrane domain of the cellular adhesion molecule L1CAM, resulting from a frameshift mutation, prevents its proper localisation and causes hereditary X-linked hydrocephalus (Takahashi et al., 1997). A defect in cell polarity might also be the cause for the ventriculomegaly observed in *Wdr16*-deficient zebrafish embryos, as discussed in 3.8.

The denudation of the ependyma and the malformation of cilia have been described as consequences or secondary effects, rather than causes, of hydrocephalus. Since the zebrafish *Wdr16* knockdown phenotype occurs in a very early developmental stage, namely embryonal day two, it can not be excluded that such secondary effects would manifest in older animals. The period of time, however, during which zebrafish

morphant phenotypes can be characterised is limited to early stages. The amount of antisense morpholino per cell is halved with each cell division. In consequence its gene-silencing effect and the associated phenotype will disappear during adolescence, a period of massive cell proliferation.

### **3.7. Impact of cilia on the generation of cell polarity and intracellular signalling**

As apparent from the animal models mentioned above, one important primary mechanism of pathogenesis for hydrocephalus seems to involve the perturbation of cell polarity. Epithelial cells, and by this token also ependymal cells, possess an apical and a basolateral region. Moreover, they can be polarised within the plane perpendicular to the apical-basal cell axis (Drubin and Nelson, 1996; Shulman and St. Johnston, 2000). This phenomenon, described as planar cell polarity (PCP), is orchestrated by the Wnt/PCP pathway, also known as noncanonical Wnt pathway (Katoh, 2005). In contrast to the canonical (classical) Wnt signalling pathway involving glycogen synthase kinase  $3\beta$  and  $\beta$ -catenin, the PCP pathway results in the activation of RhoA, c-Jun N-terminal kinase (JNK) and NF-kappaB essential modulator-like kinase (Katoh, 2005). A core signalling molecule of the PCP pathway in *Drosophila* is van Gogh/strabismus, a four-pass transmembrane protein that plays a key role in organising wing hair and ommatidium polarity (Taylor et al., 1998; Wolff and Rubin, 1998). On the molecular level, van Gogh/strabismus is discussed to repress the canonical Wnt/ $\beta$ -catenin pathway and to activate JNK (Park and Moon, 2002). Defects in the van Gogh/strabismus mammalian ortholog *vangl2* lead to mispolarised hair cells in the inner ear (Montcouquiol et al., 2003). Loop tail mice (Strong and Hollander, 1949) bearing mutations in *vangl2* (also termed *Ltap*) suffer from an open neural tube, a defect termed craniorachischisis (Kibar et al., 2001; Murdoch et al., 2001). Ross et al. (2005) described these phenotypes also for mice bearing mutations in genes that are associated with the inheritable disease known as Bardet-Biedl syndrome (BBS; OMIM 209900). Eleven BBS genes have been identified to date (Blacque and Leroux, 2006) and their corresponding proteins are localised to ciliary structures like the axoneme and the basal body (Beales, 2005). Thus, BBS is linked to defects affecting the assembly or function of cilia and basal

bodies (Ansley et al., 2003; Li et al., 2004). BBS genes are known to genetically interact with the PCP gene *vangl2* in mice and zebrafish (Ross et al., 2005). Since the *vangl2* protein is localised to the basal body and along the axoneme (Ross et al., 2005), its expression is reminiscent of that of the BBS proteins. This indicates that cilia are intrinsically involved in PCP processes, demonstrating a function for these organelles independent from generating motility and fluid flow. Similar to van Gogh/strabismus, the protein inversin that is located to cilia and basal bodies has been shown to turn off the classical Wnt/ $\beta$ -catenin pathway, and it appears to direct signalling towards the noncanonical route (Simons et al., 2005). These considerations allow for a connection to be made between (kino)cilia and cell polarity, offering an explanation for the involvement of cilia in the pathogenesis of hydrocephalus independent from their motility. Defects in cell polarity might conceivably lead to mislocalisation of proteins critical for water homeostasis and osmoregulation (see 3.8).

### **3.8. Putative function of Wdr16**

While sensing, signalling, as well as the generation and maintenance of cell polarity have been linked to primary immotile cilia with a 9+0 architecture rather than to motile 9+2 kinocilia, this sharp distinction appears to be unjustified.

The embryonal node, a triangular indentation in developing mammals, protrudes cilia with the 9+0 architecture that are endowed with dynein arms (Takeda et al., 1999) and propel a leftward fluid flow required for the left-right patterning of the body axis (Nonaka et al., 1998). On the other hand, dynein arm-lacking olfactory cilia, which are equipped with receptors for perceiving odours show a 9+2 axonemal structure (Afzelius, 2004), making them an example for 9+2 cilia involved in environment sensing and transmitting signals. Apart from that, sensory 9+2 cilia exist on vestibular hair cells (Ibanez-Tallon et al., 2003), and they have been shown to be motile (Flock et al., 1977). However, sensory 9+2 kinocilia must be regarded as the exception and not as the standard.

All extant flagella and cilia, regardless of their axonemal organisation, are evolutionary derived from a precursor featuring the 9+2 axonemal architecture (Mitchell, 2004). During evolution from flagellated, free-living genera to kinocilia-bearing cells within highly organised metazoan organisms, the function of the organelle presumably has changed substantially. The role in generating locomotive force has apparently become uncoupled from the ciliary capability to organise the cell and to generate its polarity. This hypothesis might explain why hydin knockdown morphants of bloodstream trypanosoma show motility defects (Broadhead et al., 2006), while no impaired ependymal cilia beating has been described for hydin mutant mice (Davy and Robinson, 2003). A presumed decoupling of ciliary locomotive and cell-organising functions is likely to have two evolutionary consequences. The first one is the loss of motility-generating constituents in stationary metazoan cells, resulting in central apparatus- and outer dynein arm-deficient primary cilia (Afzelius, 2004). Secondly, there may be a functional and/or spatial rearrangement of former motility-associated ciliary proteins. For instance, an ion channel previously required for  $\text{Ca}^{2+}$  entry into the ciliary compartment in connection with axonemal movement (Machemer and Ogura, 1979) might have evolved into a sensor involved in cellular signalling. It is also plausible that such channels became localised to the plasma membrane during the process of restructuring the axoneme, where they evolved into ion channels or transporters that now play a crucial role in secretion, osmoregulation and fluid homeostasis. In both cases, the channels or transporters have to reach their proper target, and proteins like Hydin and Wdr16 may be hypothesised to be involved in directing them to the correct cellular domain. During evolution, former Hydin and Wdr16 interaction partners may have changed function and/or subcellular location, but could still depend on Hydin and Wdr16 to guarantee their proper cellular targeting and therefore the polarisation of the cells. This situation resembles the one reported for the vesicular trafficking protein  $\alpha$ -SNAP, which is required for targeting various proteins in the cell (Bajjalieh, 2004; Chae et al., 2004).

In summary, the most likely function of Wdr16 is that of an adapter protein contributing to the proper polarisation of the cell by targeting ion channels and transporters to their correct destination.

### 3.9. Outlook and perspectives

The present work has shown *Wdr16* to be tied to the formation of kinocilia, and a gene knockdown by antisense morpholinos resulted in the formation of severe hydrocephalus in the zebrafish without altered ependymal morphology or ciliary beat. These knockdown effects should be further validated by additional morpholinos that, for instance, block the correct splicing of *Wdr16* pre-mRNA. A rescue experiment in which the full length *Wdr16* mRNA coinjected with *wdr16*MO should restore the wild type phenotype would be another desirable experiment to confirm the reliability of the *wdr16* knockdown phenotype.

*Wdr16* knockdown studies by the RNAi technique with EPCs as the model would be an effective instrument to analyse the late effects of *Wdr16* silencing that could not be accessed in the zebrafish model.

In order to gain a deeper insight into the molecular function of *Wdr16*, it would be desirable to identify its interaction partners. Since a Yeast-Two Hybrid screen using *Wdr16* as a bait failed, coimmunoprecipitation or tandem affinity purification should be tried.

Additionally, *Wdr16* knockout mice would be a powerful system to study further the pathological defects associated with *Wdr16* malfunction.

## 4. Materials and methods

### 4.1. Materials

#### 4.1.1. Devices

Autoclave	Type 669, Aigner, München
Cameras	Coolpix 995, Nikon, Düsseldorf Canon EOS 350D, Canon, Krefeld Lumenera Lu 170 high-speed, Lumenera, via Framos, München
Cell incubator	Type B 5060 EC CO <sub>2</sub> , Heraeus, Hanau
Centrifuge	Heraeus/Christ Varifuge K, Heraeus, Hanau
Containment hood	Lamin Air HLB 2448, TL 2448, Heraeus, Hanau
Cryostat	HM 505 E, Microm, Volketswil, Switzerland
Cryosystem	Chronos 80 and N <sub>2</sub> -tank Jupiter, Siegtal Cryotherm, Siegen
Drying furnace	Typ U-30, Memmert, Schwabach
Electroblotting chamber	Bio-Rad, München
Electrophoresis chamber	for agarose gels: Model B1 (110x90mm), Owl separation systems, USA for polyacrylamide gels: Bio-Rad, München
ELISA reader	Titertec Plus MS 212, Friedrich S. Bartolomey Labortechnik, Alfter; connected to a personal computer (PC), running EIA3 software by ICN, Meckenheim
Gel documentation system	Mitsubishi, Japan
Heating block	Grant QBT, CLF Laborgeräte, Emersacker
Hybridisation oven	Biometra, Göttingen
LightCycler <sup>®</sup>	Roche, Mannheim
Magnetic stirrer	IKAMAG RCT, Bachofer, Reutlingen
Microscopes	Model IM 35 and Axiovision 2, Zeiss, Oberkochen
Microwave oven	Micro-Chef FM 3915 Q, Moulinex, Kaufland, Tübingen



## Materials and methods

---

Osmometer	Osmometer Automatic, Knauer, Eppenheim
PCR Thermocycler	Primus 96 plus, MWG AG Biotech, Ebersberg
pH-meter	PHM 92, Radiometer, Copenhagen, Denmark
Pipettors	Finn pipettors (5-40 µl, 40-200 µl, 200-1000 µl), Labsystems, Finland  Eppendorf pipettors (0.5-10 µl, 10-100 µl, 200-1000 µl), Eppendorf, Hamburg  Multichannel pipettor Titerman, Eppendorf, Hamburg
Power supply	Consort E 132, BioBlock Scientific, Illkirch, France  2301 Macrodrive 1, LKB Bromma, Vienna, Austria  Power Supply Model 200, Bethesda Research Laboratories, Life Technologies, Inc., USA  Computer Controlled Electrophoresis Power Supply Model 3000 X, Bio Rad, München
Scales	Typ 1403, L2205 and 1712, Sartorius, Göttingen
SDS PAGE device	Ready Gel Cell, Bio-Rad, München
Shaker	Vortex Genie, Bender & Hobein, München
Shaking platform	Horizontal-Schüttelplattform KL2, Bühler, Tübingen  Inkubator, Wilhelm Störk, Klingenberg
Sonifier	Branson B-30 with microtip, Heinemann, Schwäbisch Gmünd
Spectrophotometers	Shimadzu UV-120-01, Kyoto, Japan  Uvikon 860 with Plotter 800, Kontron, Eching
Table top centrifuge	Centrifuge 5415 C, Eppendorf, Hamburg
Tissue homogeniser	Potter-Elvehjem homogeniser, Braun, Melsungen
Vacuum filter device	Sterilfiltrationsapparatur, Millipore, Eschborn
Water bath	Julabo Standard, Julabo PC Thermostat, Labora, Mannheim
Water conditioning unit	USF Elga (0.22 µm-filter), Purelabs, USA
Welding apparatus	Super Poly 281, Audion Elektron, Kleve
X-ray film developing machine	Röntgenfilm-Entwicklungsmaschine SRX-101, Konica Europe, Hohenbrunn
X-ray film exposure cassette	Hypercassette, Amersham Buchler, Braunschweig

### 4.1.2. General material

Coverslips (24 mm x 60 mm)	Roth, Karlsruhe
Coverslips (18 mm x 18 mm)	Roth, Karlsruhe
Cryotubes 5 ml, sterile	Greiner, Frickenhausen
Culture dishes (35 mm x 10 mm), sterile	Becton Dickinson, Heidelberg
Culture flasks 80 cm <sup>2</sup> , sterile	Nunc, Wiesbaden
Filter paper (Whatman 3MM)	Whatman, Göttingen
Filtration units (Millex units), sterile	Millipore, Eschborn
Glass pipettes 1 ml, 5 ml, 10 ml	Hirschmann, Eberstadt
Glassware	Schott, Mainz; Brand, Wertheim
Hybridisation container	Fisher Scientific, Schwerte
Microscope slides (26 mm x 76 mm x 1 mm)	Menzel, via Roth, Karlsruhe
Microscope slides "Superfrost" (26 mm x 76 mm x 1 mm)	Menzel, via Roth, Karlsruhe
Microtiter plates (Immunoplate F96)	Nunc, Wiesbaden
Nitrocellulose membrane (Trans-Blot, 0.45 µm)	Bio-Rad, München
Nylon cloth (132, 210 µm mesh size)	Sefar GmbH, Wasserburg/Inn
Nylon membrane, positively charged	QBIOgene, Heidelberg
PCR tubes (0.2 ml), sterile	PeqLab, Erlangen
Petri dishes (AD94/H16 mm), sterile	Roth, Karlsruhe
Pipette tips	Braun, Melsungen
Plastic tubes 14 ml, sterile	Greiner, Frickenhausen
Plastic tubes 50 ml, sterile	Nunc, Wiesbaden
Plastic reaction tubes 1.5 ml	Brand, Wertheim
X-ray film	Amersham, Freiburg

### 4.1.3. Chemicals

Ammonium peroxodisulfate (APS)	Fluka, Steinheim
Bradford assay dye reagent	Bio-Rad, München
Bromophenol blue	Fluka, Steinheim
BSA	Sigma-Aldrich, Steinheim

"CDP-Star" chemiluminescence substrate	Roche, Mannheim
Coomassie Brilliant Blue R 250	Sigma-Aldrich, Steinheim
D-Glucose	Fluka, Steinheim
Dimethylsulfoxide (DMSO)	Sigma-Aldrich, Steinheim
EDTA	Roth, Karlsruhe
Glycerol	Roth, Karlsruhe
Glycine	Roth, Karlsruhe
Isopentane	Fluka, Steinheim
JetPEI™ transfection reagent	QBIogene, Heidelberg
Mercaptoethanol	Roth, Karlsruhe
MnCl <sub>2</sub>	Fluka, Steinheim
3-(N-Morpholino) propanesulfonic acid (MOPS)	Fluka, Steinheim
NaCl	Roth, Karlsruhe
NaHCO <sub>3</sub>	Roth, Karlsruhe
Neg 50 cryomedium	Richard-Allan Scientific, Kalamazoo, MI, USA
PageRuler™ prestained protein ladder	MBI Fermentas, St. Leon-Rot
Paraformaldehyde (PFA)	Fluka, Steinheim
p-Nitrophenylphosphate	Roche, Mannheim
Ponceau S	Serva, Heidelberg
RbCl <sub>2</sub>	Sigma-Aldrich, Steinheim
Roti®-Block 10-fold Concentrate	Roth, Karlsruhe
Roti®-ImmunoBlock 10-fold Concentrate	Roth, Karlsruhe
Rotiphorese® Gel 30	Roth, Karlsruhe
SDS	Fluka, Steinheim
Sucrose	Roth, Karlsruhe
N,N,N',N'-Tetramethylethylenediamine (TEMED)	Sigma-Aldrich, Steinheim
Tissue Tek O.C.T compound	Sakkura Finetek, Zoeterwoude, the Netherlands
Trichloroacetic acid	Fluka, Steinheim
Tris(hydroxymethyl)aminomethane (Tris)	Roth, Karlsruhe
Tween® 20	Fluka, Steinheim

Vectashield mounting medium  
with 4',6-diamidino-2-phenylindole  
(DAPI; 1.5 µg/ml)

Vector, via Alexis (Axxora), Grünberg

All other chemicals were purchased from E. Merck, Darmstadt

#### 4.1.4. Kits

Advantage <sup>®</sup> 2 PCR kit	Clontech (now Takara Bio), Heidelberg
Enhanced chemiluminescence (ECL) detection reagent	Amersham, Freiburg
FastStart DNA Master SYBR Green I kit	Roche, Mannheim
High Fidelity PCR Enzyme Mix	MBI Fermentas, St. Leon-Rot
HotStarTaq Master Mix	Qiagen, Hilden
Imject <sup>®</sup> Conjugation kit	Pierce, via PerbioScience, Bonn
Omniscript reverse transcriptase kit	Qiagen, Hilden
PCR digoxigenin (DIG) probe synthesis kit	Roche, Mannheim
PCR Select <sup>™</sup> cDNA subtraction kit	Clontech (now Takara Bio), Heidelberg
PCR-Select differential screening kit	Clontech (now Takara Bio), Heidelberg
QIAGEN PCR Cloning <sup>plus</sup> kit	Qiagen, Hilden
QIAprep spin miniprep kit	Qiagen, Hilden
QIAquick gel extraction kit	Qiagen, Hilden
QIAquick PCR purification kit	Qiagen, Hilden
RNeasy RNA isolation kit	Qiagen, Hilden
SAWADY Pwo DNA Polymerase kit	PeqLab, Erlangen
SMART <sup>™</sup> PCR cDNA synthesis kit	Clontech (now Takara Bio), Heidelberg
SulfoLink <sup>®</sup> Coupling gel	Pierce via PerbioScience, Bonn
T4 ligation kit	MBI Fermentas, St. Leon-Rot

#### 4.1.5. Reagents for molecular biology

Agarose	PeqLab, Erlangen
Anti-DIG-alkaline phosphatase (AP), Fab fragments	Roche, Penzberg
dATP, dCTP, dGTP, dTTP (10 µM each)	Promega, Mannheim
Deoxyribonucleoside triphosphate (dNTP; (10 mM each)	PeqLab, Erlangen
Dithiothreitol (DTT), 0.1 M	Gibco BRL, Karlsruhe
DNA size standards (peqGold 100 bp Plus DNA ladder, 1kb plus DNA ladder)	PeqLab, Erlangen
Ethidium bromide	Fluka, Steinheim
Oligo(dT <sub>15</sub> ) adapter primer	Invitrogen, Karlsruhe
PANScript NH <sub>4</sub> buffer	PAN Biotech, Aidenbach
PCR primers	Invitrogen, Karlsruhe
Phenol/chloroform/isoamyl alcohol (25 : 24 : 1)	Applichem, Darmstadt
Random hexamer primer (500 µg/ml)	Promega, Mannheim
RNAsin ribonuclease inhibitor (40 U/µl)	Promega, Mannheim

#### 4.1.6. Enzymes for molecular biology

Avian myeloblastosis virus (AMV) reverse transcriptase (20 U/µl)	PeqLab, Erlangen
Calf intestine alkaline phosphatase (CIAP; 70 U/µl)	Invitrogen, Karlsruhe
BamHI	New England Biolabs, Frankfurt a.M.
EcoRI	New England Biolabs, Frankfurt a.M.
EcoRV	New England Biolabs, Frankfurt a.M.
HindIII	New England Biolabs, Frankfurt a.M.
PvuII	MBI Fermentas, St. Leon-Rot
XhoI	New England Biolabs, Frankfurt a.M.

#### 4.1.7. Constituents and reagents for bacterial and mammalian cell culture media

Antimycotic	Sigma-Aldrich, Steinheim
Carbenicillin, disodium salt	Roth, Karlsruhe
Dulbecco's modified Eagle's medium (DMEM), powder lacking pyruvate and NaHCO <sub>3</sub>	GibcoBRL, Karlsruhe
Fetal calf serum (FCS)	Biochrome, Berlin
Hank's balanced salt solution (HBSS)	GibcoBRL, Karlsruhe
Insulin	Sigma-Aldrich, Steinheim
Kanamycin	Applichem, Darmstadt
LB (lysogeny broth) agar powder	Fluka, Steinheim
LB powder	Fluka, Steinheim
Minimal Essential Medium (MEM) powder	GibcoBRL, Karlsruhe
Penicillin G, potassium salt	Serva, Heidelberg
Super optimal broth, catabolite repression (SOC) medium	Novagen, Schwalbach/Ts.
Streptomycin sulfate	Serva, Heidelberg
Thrombin (human)	provided by M. Rapp, ZLB Behring, Marburg
Transferrin	Roche, Mannheim
Trypsin	ICN, Eschwege

#### 4.1.8. Antigenic peptide

CQAINTEQNFLHGHGN	synthesized by K.-H. Wiesmüller, Interfaculty Institute for Biochemistry (IFIB), University of Tübingen
------------------	---

## 4.1.9. Antibodies

### 4.1.9.1. Primary antibodies

Monoclonal anti- $\alpha$ -tubulin ascites fluid	Sigma-Aldrich, Steinheim
Rabbit antiserum against GP BB	gift from B. Pfeiffer-Guglielmi, IFIB, University of Tübingen

### 4.1.9.2. Secondary antibodies

Donkey anti-guinea pig IgG-carbocyanin 3 (Cy3) conjugate	Jackson, via Dianova, Hamburg
Donkey anti-guinea pig IgG-peroxidase conjugate	Jackson, via Dianova, Hamburg
Goat anti-guinea pig IgG-Alexa 546 conjugate	Molecular Probes, via Invitrogen, Karlsruhe
Goat anti-mouse IgG-Alexa 488 conjugate	Molecular Probes, via Invitrogen, Karlsruhe
Goat anti-guinea pig IgG-AP conjugate	Jackson, via Dianova, Hamburg
Goat anti-rabbit IgG-Alexa 488 conjugate	Molecular Probes, via Invitrogen, Karlsruhe
Rabbit anti-mouse IgG-fluorescein isothiocyanate (FITC) conjugate	Jackson, via Dianova, Hamburg

## 4.1.10. Bacterial strains

DH5 $\alpha$ E. coli cells	gift from F. Madeo, IFIB, University of Tübingen
NovaBlue Singles <sup>TM</sup> competent cells	Novagen, Schwalbach/Ts.
Qiagen EZ competent cells	Qiagen, Hilden

### 4.1.11. Mammalian cells

A9 fibroblasts (mouse)

provided by B. Hamprecht,  
IFIB, University of Tübingen

HepG2 cells

American Type Culture Collection (ATCC;  
catalog number HB-8065), via Promochem,  
Wesel

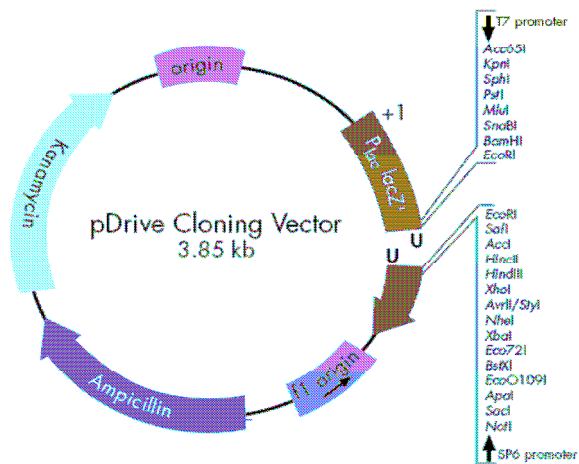
### 4.1.12. Animals

Wistar rats

purchased from Charles River, Kisslegg,  
bred in the animal facility of the institute

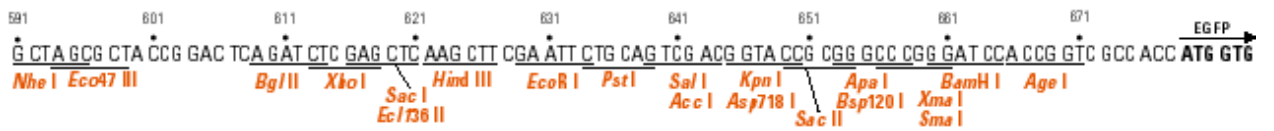
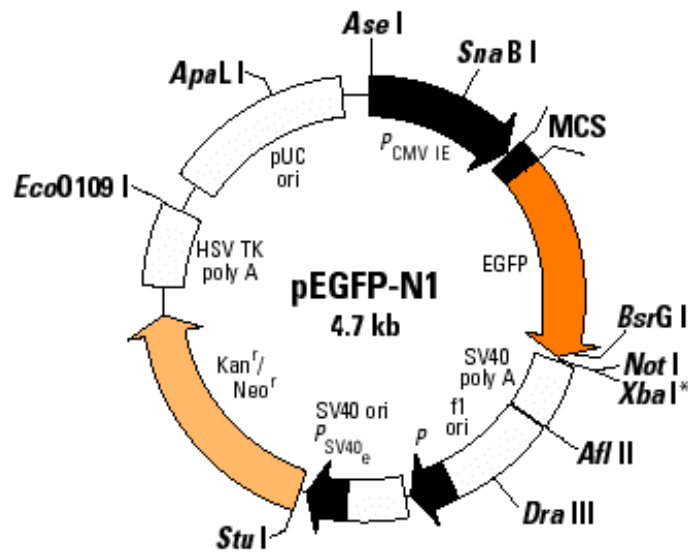
### 4.1.13. Vectors

pDrive cloning vector, Qiagen, Hilden

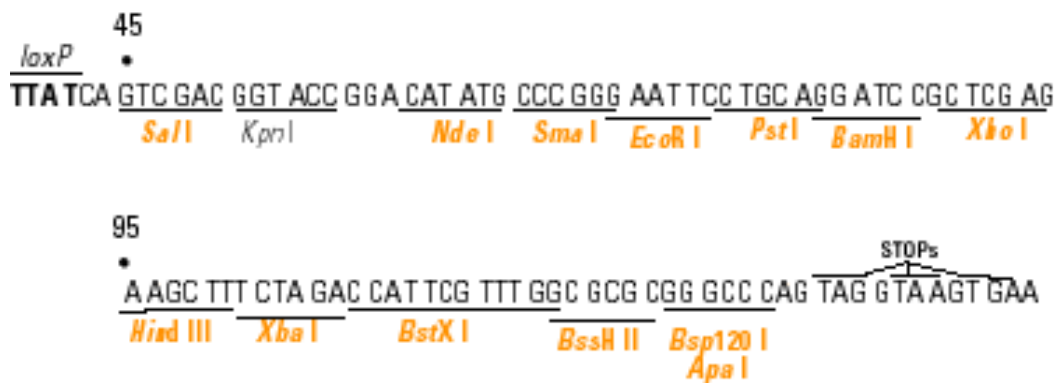
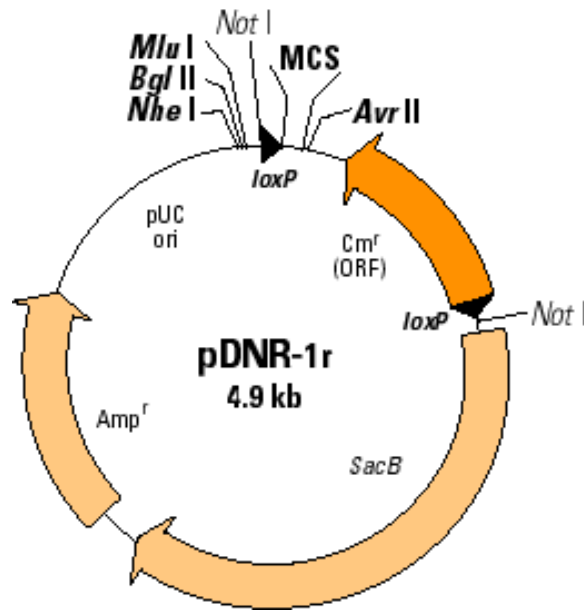




pEGFP-N1 vector, Clontech (now Takara Bio), Heidelberg



pDNR-1r vector, Clontech (now Takara Bio), Heidelberg



## 4.2. Methods

### 4.2.1. Cell culture techniques

#### 4.2.1.1. Media and solutions for cell cultivation

##### Penicillin/streptomycin (PS) stock solution

651 mg penicillin G potassium salt (1536 U/mg) and 1 g streptomycin sulfate (750 U/mg) dissolved in 50 ml ddH<sub>2</sub>O

**Puck's D1 solution**

137 mM NaCl, 5.4 mM KCl, 0.22 mM KH<sub>2</sub>PO<sub>4</sub>, 0.17 mM Na<sub>2</sub>HPO<sub>4</sub>; pH 7.4

**Puck's D1 / Gluc / Suc solution**

5 mM D-glucose, 58.4 mM sucrose in Puck's D1 solution

**Trypsin solution 0.05 % (w/v)**

Puck's D1 / Gluc / Suc solution supplemented with 0.2 % (v/v) phenol red and 0.05 % (w/v) trypsin

**MEM<sub>wash</sub>**

9.65 g MEM powder and 2.2 g NaHCO<sub>3</sub>, dissolved in 1 L ddH<sub>2</sub>O. The medium was gassed with CO<sub>2</sub> until the colour became orange.

**MEM<sub>C</sub>**

MEM<sub>wash</sub> medium supplemented with 0.5 g/L BSA, 5 mg/L insulin, 10 mg/L transferrin and 1 mL PS stock solution per liter of medium

**MEM<sub>CT</sub>**

MEM<sub>C</sub> supplemented with 500 U/L thrombin

**DMEM**

133.75 g DMEM powder lacking pyruvate and NaHCO<sub>3</sub>, 2.2 g sodium pyruvate and 74 g NaHCO<sub>3</sub> were dissolved in 20 L ddH<sub>2</sub>O. The medium was gassed with CO<sub>2</sub> until the colour became orange. The osmolarity was 320-340 mOsmol/L.

**90 % DMEM / 10 % FCS**

900 mL DMEM plus 100 mL FCS

**90 % DMEM / 10 % FCS / PS**

1 mL PS stock solution was added to 1 L 90 % DMEM / 10 % FCS

**90 % DMEM / 10 % FCS / antimycotic**

1 mL 1000-fold concentrated antimycotic stock solution was added to 1 L 90 % DMEM / 10 % FCS

#### **4.2.1.2.Ependymal primary cultures**

EPCs were prepared from brains of newborn Wistar rats not older than 24 h according to the method of Weibel et al. (1990) as modified by Prothmann et al. (2001).

##### **Coating of culture dishes with fibronectin**

Fibronectin was isolated according to Miekka et al. (1982) with modifications described by Prothmann (1995).

Culture dishes 35 mm in diameter were incubated with 0.7 mL of sterile-filtered fibronectin solution (200 µg/mL) at 37°C for 2 h. Afterwards, fibronectin was sucked off and replaced by 2 mL MEM<sub>wash</sub>. Coated culture dishes were stored in a cell incubator at 37°C in an atmosphere of 95 % air and 5 % CO<sub>2</sub> until cells were seeded.

##### **Preparation of rat brains**

Newborn rats were decapitated with a pair of scissors. The brains were squeezed through the foramen magnum by application of pressure to the skull roof and transferred to a Petri dish containing 10 mL ice-cold Puck's D1 / Gluc / Suc solution.

##### **Dissociation into single cells**

Prior to the procedure, nylon cloth (132 µm and 210 µm mesh size) was sealed with a welding apparatus to obtain nylon gauze bags. The brains were packed into a 210 µm mesh size nylon gauze bag and dissociated by massaging them through the mesh with sterile forceps. The suspension was collected in a Petri dish filled with 10 mL ice cold Puck's D1 / Gluc / Suc solution, where it was triturated to apparent homogeneity with a 10 mL glass pipette. For removal of remaining large aggregates, the cell suspension was filtered through a 132 µm mesh size gauze bag into a 50 mL plastic tube. After 5 min of centrifugation in a Heraeus/Christ Varifuge K at 1500 revolutions per minute (rpm) and 4°C, the supernatant was sucked off and the pellet was resuspended in 10 mL of MEM<sub>C</sub>. The suspension was passed through a 132 µm mesh size gauze bag into an appropriate volume of MEM<sub>C</sub> to yield the seeding suspension. For each dissociated brain, 30 mL of MEM<sub>C</sub> were used.

### **Seeding of dissociated brain cells**

MEM<sub>wash</sub> was removed from fibronectin-coated dishes and replaced by 2 mL cell suspension in MEM<sub>C</sub>. Seeded cells were cultivated at 37°C in an atmosphere of 95 % air and 5 % CO<sub>2</sub>. After 2 days, MEM<sub>C</sub> was replaced by MEM<sub>CT</sub>. The culture medium was renewed every 2 or 3 days until the cultures were used for experiments. The state of the cultures was permanently monitored under a microscope.

### **4.2.1.3. Astroglial primary cultures**

APCs were prepared from the brains of newborn Wistar rats following the procedure of Hamprecht and Löffler (1985) with the modifications described below. The animals were used at a maximal age of 36 h.

#### **Dissociation into single cells**

This procedure was conducted as described in 4.2.1.2. with the following modifications:

After centrifugation, the pellet was resuspended in 90 % DMEM / 10 % FCS / PS. For each brain, 50 mL of medium were used.

#### **Seeding of the cells**

The cell suspension was transferred to culture dishes 35 mm in diameter. Seeded cells were cultivated at 37°C in an atmosphere of 90 % air and 10 % CO<sub>2</sub>. The medium was routinely renewed on culture day 7 and from thereon each seventh day. The state of the cultures was regularly monitored under a microscope.

Nearly homogeneous astroglial cultures (provided by R. Schmid, IFIB, University of Tübingen) were derived from APCs by replacing the standard medium with 90 % DMEM / 10 % FCS lacking all amino acids except serine, glutamine and glycine at culture day 5 (Verleysdonk, 1994).

#### **4.2.1.4. Cultures of the mouse fibroblast cell line A9**

##### **Starting of the culture**

The A9 fibroblast cell line (Littlefield, 1966) was provided by B. Hamprecht as a cryostock at passage number 36. The cryostock was thawed rapidly at 37°C. Afterwards, the cell suspension was transferred to an 80 cm<sup>2</sup> culture flask containing 20 mL 90 % DMEM / 10 % FCS / PS which was subsequently incubated at 37°C in an atmosphere containing 10 % CO<sub>2</sub> (in air) for 4 h. After that time the cells were attached to the culture dish and the medium was renewed by fresh 90 % DMEM / 10 % FCS / PS.

##### **Maintenance of the cell culture**

The A9 fibroblast cell line was cultured in 80 cm<sup>2</sup> culture dishes using 90 % DMEM / 10 % FCS / PS at 37°C in an atmosphere containing 10 % CO<sub>2</sub> (in air). The medium was renewed every third day. The state of the cultures was regularly monitored under a microscope.

##### **Passaging of the cells**

When the cells became confluent in the 80 cm<sup>2</sup> flask (after approximately 8-10 days), the culture medium was sucked off and the adherent cells were washed with 1 mL trypsin solution (0.05 %, w/v). Subsequently, the washing solution was discarded, replaced by 2 mL trypsin solution (0.05 %, w/v) and the flask was incubated at 37°C in a cell incubator until the cells started to detach (after approximately 5 min). To inhibit trypsin activity, 10 mL of 90 % DMEM / 10 % FCS / PS were added to the detached fibroblasts and the suspension subsequently transferred to a 50 mL plastic tube. After centrifugation (1500 rpm, 4°C, 5 min) in a Heraeus/Christ Varifuge K, the supernatant was discarded and the cell pellet was triturated with 20 mL 90 % DMEM / 10 % FCS / PS. To start a new passage, 500 µL of this cell suspension were added to a new culture flask containing 10 mL 90 % DMEM / 10 % FCS / PS.

##### **Preparation of cryostocks**

For the preparation of cryostocks, a DMSO cell-freezing solution was prepared containing 2.9 mL 90 % DMEM / 10 % FCS / PS and 0.7 mL DMSO per cryosample. The solution was kept on ice until further use. The cells were trypsinised as described above and resuspended in 10 mL culture medium (90 % DMEM / 10 % FCS / PS)

after centrifugation. Two milliliters of the cell suspension were transferred to a 5 mL cryovial followed by the addition of 2.4 mL precooled DMSO cell-freezing solution, resulting in a final DMSO concentration of approximately 10 %. The cryovials were wrapped in paper towels, cooled down in a -80°C freezer and then frozen in liquid nitrogen to be finally stored in a cell bank over liquid nitrogen.

#### **4.2.1.5. Cultures of the human hepatocellular carcinoma cell line HepG2**

##### **Starting of the culture**

Frozen HepG2 cells, purchased from ATCC via LGC Promochem, were thawed at 37°C in a waterbath. The tube content was then transferred to an 80 cm<sup>2</sup> culture flask filled with 30 mL 90 % DMEM / 10 % FCS / antimycotic followed by an incubation at 37°C in an atmosphere containing 10 % CO<sub>2</sub> (in air) for 6 h. After that time the cells were attached to the culture dish and the medium was renewed.

##### **Maintenance of the cell culture**

HepG2 cells were cultured in 80 cm<sup>2</sup> culture flasks using 90 % DMEM / 10 % FCS / antimycotic as the culture medium in an atmosphere containing 10 % CO<sub>2</sub>. The medium was renewed every fourth day.

##### **Passaging of the cells**

The cells were passaged as described for A9 fibroblasts in 4.2.1.4. However, the trypsin solution contained 0.25 % trypsin and 0.53 mM EDTA in phosphate buffered saline (PBS) at pH 7.4.

##### **Preparation of cryostocks**

The cryostocks were prepared as described for A9 fibroblasts in 4.2.1.4. The culture medium used was 90 % DMEM / 10 % FCS / antimycotic.

## **4.2.2. Harvesting of rat organs and cells**

### **4.2.2.1. Harvesting of rat organs for RNA isolation and for preparation of protein homogenates**

Young and adult Wistar rats were anaesthetised with CO<sub>2</sub> in a gas chamber and subsequently decapitated with a pair of scissors or a guillotine, respectively. The desired organs were dissected out and transferred to a precooled plastic tube, frozen in liquid nitrogen and stored at -80°C until further use.

### **4.2.2.2. Harvesting of rat organs for immunohistochemical stainings**

Animals were killed as described above. Subsequently, tissues were incubated in 4 % PFA / PBS at 4°C for 24 h, soaked with 30 % sucrose / PBS at 4°C for 20 h, embedded in Neg 50 cryomedium and frozen in isopentane that had been precooled by liquid nitrogen until bleb formation. Samples were stored at -80°C.

### **4.2.2.3. Harvesting of cells from culture dishes 35 mm in diameter**

Dependent on the experimental requirements, 4-20 culture dishes 35 mm in diameter were used. After removal of the culture medium, the cells were washed 3 times with 2 mL ice-cold PBS. Subsequently, 1 mL ice-cold PBS was pipetted into the first dish and the cells were scraped off with a rubber policeman. The resulting suspension was sequentially transferred to a second, third, etc. culture dish from which the medium had been removed and that had been washed with PBS, and the cells were again scraped off after each transferral. The suspension coming from the last dish was finally pipetted into a 1.5 mL reaction tube and centrifuged at 3000 rpm and 4°C for 5 min in a table top centrifuge. The supernatant was discarded and the pellet was stored at -20°C until experiments were conducted.



#### **4.2.2.4. Collecting of cells grown in 80 cm<sup>2</sup> culture flasks**

Cells were trypsinised as described in 4.2.1.4. After centrifugation the pellet was resuspended in 1 mL HBSS. After an additional centrifugation at 5000 rpm and 4°C for 5 min in a table top centrifuge, the supernatant was discarded and the pellet was stored at -80°C.

#### **4.2.3. Preparation of homogenates**

Homogenisation buffer: 50 mM Tris/HCl, 1mM EDTA; pH 7.4

##### **4.2.3.1. Preparation of homogenates from rat organs**

Frozen rat organs (obtained as described in 4.2.2.1.) were weighed and transferred to ice-cold homogenisation buffer (50 µL buffer per 10 mg tissue). Subsequently, the organs were homogenised by a Branson sonifier (output control 2, duty cycle 50 %, approximately 100 pulses). During sonication the samples were permanently kept on ice. Lysates were cleared by two sequential centrifugations (13000 rpm, 4°C, 15 min) in a table top centrifuge. The pellet was discarded and the protein-containing supernatant was frozen at -20°C until further use.

##### **4.2.3.2. Preparation of homogenates from cultured cells**

Cells harvested as described in 4.2.2.3. and 4.2.2.4., respectively, were resuspended in homogenisation buffer in a 1.5 mL reaction tube. A pellet of approximately 1 mm thickness was suspended in 150 µL homogenisation buffer. From thereon, the procedure was identical to the one described in 4.2.3.1.

#### **4.2.4. Preparation of cryosections from rat tissues**

Tissues were obtained as described in 4.2.2.2. Frozen tissues were cut into 10  $\mu\text{m}$  thin sections in a cryostat at  $-25^{\circ}\text{C}$  and transferred to “Superfrost” microscopic slides. After air drying, sections were stored at  $-80^{\circ}\text{C}$  until further use.

#### **4.2.5. Subtracted ependymal cDNA libraries**

##### **4.2.5.1. Generation of a subtracted ventricular ependymal cDNA library and a subtracted bovine subcommissural cDNA library**

All kits employed for library construction were used according to the respective manufacturer’s instructions.

Freshly slaughtered cows were decapitated in the local abattoir. The skulls were skinned and opened by cutting off the occipital part under a hydraulic guillotine. Care was taken not to crush the brains in the process. The brains were removed through the opening, and the lateral ventricles were carefully opened by cutting with a scalpel. The ependymal layer was scraped off the ventricular walls with a curve-bladed scalpel and stored in ice-cold HBSS. Additionally, the SCOs were dissected out and also stored in ice-cold HBSS until further use (within 6 h of the deaths of the animals). PolyA RNA was obtained from the prepared tissue with “RNeasy” RNA isolation kits. A RT reaction, using the SMART<sup>TM</sup> PCR cDNA synthesis kit, and a subsequent cDNA amplification by the Advantage<sup>®</sup> 2 PCR system were performed to obtain “tester” cDNA. “Driver” cDNA was generated from ependyma-free bovine brain tissue of the cortical region by the same method. The further procedure was performed with the PCR Select<sup>TM</sup> cDNA subtraction kit according to the principle of suppression subtractive hybridization described by Diatchenko et al. (1996). The subtracted SCO cDNA library was constructed by the same procedure with “tester” cDNA generated from SCO RNA.

#### **4.2.5.2. Screening of subtracted ependymal cDNA libraries**

Subtracted libraries were screened with a dot blot array, following the protocol supplied with the PCR-Select differential screening kit. Putative differentially expressed sequences were sent to SeqLab Laboratories, Göttingen, for commercial sequencing.

#### **4.2.6. Other molecular biology techniques**

##### **4.2.6.1. Preparation of medium for bacterial liquid cultures**

LB powder (20 g) was dissolved in 1 L ddH<sub>2</sub>O with the aid of a magnetic stirrer and subsequently autoclaved at 121°C for 15 min. After the liquid had cooled down to approximately 50°C, 1 mL of a 1000-fold concentrated antibiotic stock solution was added to the medium. LB medium was stored at 4°C.

1000-fold concentrated carbenicillin stock solution: 50 mg/mL

1000-fold concentrated kanamycin stock solution: 50 mg/mL

##### **4.2.6.2. Preparation of agar plates**

Preparation of selection plates was performed according to 4.2.6.1., but 30 g LB agar were used instead of LB. After autoclaving and addition of the antibiotic stock solution, the liquid was distributed among Petri dishes under sterile conditions. When the agar had hardened, the plates were stored at 4°C.

##### **4.2.6.3. Bacterial liquid cultures**

In order to amplify bacterial clones for plasmid isolation, bacterial liquid cultures were prepared. For this, bacteria from a streakout were transferred to 5 mL of antibiotic-containing LB medium via a sterile toothpick. Subsequently, liquid bacterial cultures were incubated overnight at 37°C on a shaker platform.

#### **4.2.6.4. “Mini” scale preparation of plasmid DNA from bacterial liquid cultures**

Bacterial liquid overnight cultures (4.2.6.3.) were centrifuged in a Heraeus/Christ Varifuge K (3000 rpm, 4°C, 15 min). The supernatant was discarded and plasmid DNA was isolated from the bacterial pellet with the QIAprep Spin miniprep kit according to the manufacturer’s instructions. The amount of isolated DNA was measured photometrically as described in 4.2.6.6.

#### **4.2.6.5. Preparation of bacterial glycerol stocks**

For preparing bacterial glycerol stocks, 0.5 mL of a bacterial overnight culture and 0.5 mL glycerol were mixed; the resulting suspension was then frozen in liquid nitrogen and stored at -80°C.

#### **4.2.6.6. Photometric determination of nucleic acid concentration**

The concentration of DNA or RNA solution was determined photometrically. For this, the absorbance (OD) was measured at a wavelength of 260 nm. The solvent in which the sample was diluted was used as a reference (blank). An OD<sub>260</sub> value of 1 corresponded to a concentration of 50 µg/mL for double stranded DNA, and to 40 µg/mL for RNA. The dilutions were prepared in such a way that the absorbance fell into the range from 0.1 to 1, assuring linear correlation between nucleic acid concentration and absorbance. The sample volume was 10 µL. To estimate purity of samples, the OD<sub>260</sub>/OD<sub>280</sub> ratio was calculated. A protein-free nucleic acid solution was assumed to display a ratio of 1.8 up to 2.0.

#### **4.2.6.7. Cloning of the Wdr16 PCR product into the pDNR-1r vector**

Total cellular RNA was isolated from EPCs with the RNeasy RNA isolation kit according to the manufacturer’s protocol. One microgram of total RNA was mixed

with 1  $\mu\text{L}$  RNasin (40 U/ $\mu\text{L}$ ) and 1  $\mu\text{L}$  oligo(dT<sub>15</sub>) adapter primer (500  $\mu\text{g}/\text{mL}$ ). The reaction volume was filled up to 12  $\mu\text{L}$  with ddH<sub>2</sub>O and incubated at 70°C for 10 min. After brief chilling on ice, the following components were added: 1  $\mu\text{L}$  RNasin (40 U/ $\mu\text{L}$ ), 2  $\mu\text{L}$  10-fold concentrated Omniscript buffer RT, 2  $\mu\text{L}$  DTT (0.1 M), 1  $\mu\text{L}$  dNTP (10 mM each) and 1  $\mu\text{L}$  ddH<sub>2</sub>O. The tube content was incubated at 42°C for 2 min. After addition of 1  $\mu\text{L}$  Omniscript RT (4 U/ $\mu\text{L}$ ), the reaction was further incubated at 42°C for 50 min to facilitate reverse transcription. The enzyme was heat-inactivated at 95°C for 5 min, the reaction tube briefly chilled on ice, and the cDNA was stored at -80°C until further use.

For amplification of Wdr16 cDNA, the High Fidelity PCR Enzyme Mix was used. For this, 1  $\mu\text{L}$  of cDNA was mixed with 5  $\mu\text{L}$  10-fold concentrated High Fidelity PCR buffer, 2  $\mu\text{L}$  primer mix (10  $\mu\text{M}$  each), 5  $\mu\text{L}$  dNTPs (2 mM each) and 0.25  $\mu\text{L}$  High Fidelity enzyme mix (5 U/ $\mu\text{L}$ ). The reaction volume was brought to 50  $\mu\text{L}$  with ddH<sub>2</sub>O. The PCR primers bore restriction sites for BamHI and HindIII, respectively, and had the sequences 5'-GCATACGGATCCGCATGGAAGAACAATTTTACCCGAGACC-3' and 5'-GCATACAAGCTTAGCAAATGGGTATTTCCACCTCAAGAT-3'. The cycling parameters used were: 94°C, 30 s; 59.3°C, 30 s; 72°C, 2 min 10 s (30 times); final elongation (72°C, 10 min). Before thermal cycling, the samples were heated to 95°C for 2 min. The PCR product was then purified with the QIAquick PCR purification kit according to the manufacturer's instructions.

The purified Wdr16 PCR product was digested with Hind III (4.2.6.9.) followed by a phenol / chloroform / isoamyl alcohol extraction with subsequent ethanol precipitation (4.2.6.10.) and was finally cut with BamHI (4.2.6.9.). The pDNR-1r vector DNA was digested under identical conditions with HindIII / BamHI and dephosphorylated with CIAP (4.2.6.11.) in order to prevent vector self-ligation in the subsequent ligation reaction.

The digested Wdr16 PCR product as well as the pDNR-1r vector DNA were purified by preparative agarose gel electrophoresis (4.2.6.12.). The desired bands were cut out from the agarose gel (4.2.6.13.), and DNA was isolated with the QIAquick gel extraction kit according to the manufacturer's instructions.

pDNR-1r vector DNA and the amplified Wdr16 PCR product were ligated using T4 ligase (4.2.6.14.), transferred into NovaBlue Singles<sup>TM</sup> competent cells (4.2.6.16.) and transformed cells were selected on carbenicillin-containing agar plates. The streak-outs of these colonies were used as a source to start bacterial liquid cultures, from which the recombinant plasmid DNA was isolated with the QIAprep Spin miniprep kit according to the manufacturer's protocol. The isolated recombinant plasmid DNA was subjected to two individual restriction digestions with EcoRI and EcoRV, respectively, and analysed on an analytical 1.2 % agarose gel. The plasmids showing the expected restriction pattern were commercially sequenced by SeqLab Laboratories, Göttingen, Germany. One of the bacterial clones bearing the mutation-free recombinant plasmid was used to prepare a bacterial glycerol stock that was stored frozen at -80°C.

#### **4.2.6.8. Cloning of the Wdr16 PCR product into the pEGFP-N1 vector**

For amplification of the Wdr16 insert, the pDNR-1r/Wdr16 recombinant vector was used as a template instead of cDNA. This allowed for a lower number of cycles in the PCR reaction, which in turn reduced the likelihood of point mutations in the amplification process.

For amplification of the Wdr16 insert, the SAWADY Pwo-DNA-Polymerase kit was used. For the PCR reaction, two master mixes were prepared. Master mix I contained 5 ng pDNR-1r/Wdr16 recombinant vector DNA, 2 µL dNTPs (10 mM each) and 6 µL primer mix (10 µM each). It was filled up with ddH<sub>2</sub>O to a total volume of 50 µL. Master mix II contained 10 µL 10-fold concentrated complete reaction buffer, 2.5 µL Pwo polymerase (1 U/µL) and 37.5 µL ddH<sub>2</sub>O. The cloning primers bore restriction sites for BamHI and XhoI, respectively, and had the sequences 5'-GCATACCTCGAGATGGAAGAACAAATTTTACCCGAGACC-3' and 5'-GCATACGGATCCCGAGCAAATGGGTATTTCCACCTCAAGAT-3'. Both master mixes were heated to 94°C for 2 min separately from each other, before they were combined to commence amplification. The cycle parameters used were: 94°C, 30 s; 55°C, 30 s; 72°C 2 min 10 s (13 times); final elongation (72°C, 7 min).

The further cloning procedure followed the protocol described in 4.2.6.7. with the following modifications: pEGFP-N1 vector and the Wdr16 PCR product were both digested in a double digestion reaction with BamHI and XhoI. After ligation, DH5 $\alpha$  competent cells were transformed with the recombinant pEGFP-N1/Wdr16 vector DNA and streaked out for selection on kanamycin-containing agar plates. In order to verify the cloned vector, bacterial clones were multiplied in kanamycin-containing bacterial liquid medium, and an analytical digestion was performed with PvuII.

### **4.2.6.9. Cutting of DNA with restriction endonucleases**

#### **Preparative digestion of vector DNA and PCR product**

Three to four milligrams vector DNA or a PCR product that had previously been purified with the QIAquick PCR purification kit according to the manufacturer's instructions (eluted with 44  $\mu$ L H<sub>2</sub>O), respectively, were digested with 10 U of the corresponding restriction enzymes in the appropriate buffers for 4 h. The total reaction volume was 50  $\mu$ L.

#### **Analytical digestion of recombinant DNA**

Five hundred micrograms of the recombinant plasmid DNA were digested with 10 U of the corresponding restriction enzymes in the appropriate buffers for 2 - 4 h at 37°C according to the advice of the manufacturer. The total reaction volume was 50  $\mu$ L.

If a sequential digestion was necessary, a phenol / chloroform / isoamyl alcohol extraction with subsequent ethanol precipitation (4.2.6.10.) was performed after digestion with the first restriction enzyme. The extracted and precipitated DNA was subsequently subjected to the digestion with the second restriction enzyme.

#### **4.2.6.10. Phenol/Chloroform/Isoamyl alcohol extraction of DNA with subsequent ethanol precipitation**

DNA solution was mixed with 1 volume phenol / chloroform / isoamyl alcohol (25 : 24 : 1, v / v), vortexed and centrifuged (13000 rpm, RT, 5 min) in a table top centrifuge. The upper, aqueous, DNA-containing phase was transferred to a new 1.5 mL reaction tube and combined with 3 volumes of pure ethanol. The DNA was allowed to precipitate for 2 h at -20°C. After centrifugation (13000 rpm, 10 min), the pellet was washed with 80 % ethanol, dried briefly and dissolved in 44 µL ddH<sub>2</sub>O, before it was finally subjected to a further restriction digestion with another enzyme.

#### **4.2.6.11. Dephosphorylation of vector DNA**

Dephosphorylation buffer: 500 mM Tris/HCl, 1 mM EDTA; pH 8.0

##### Experimental procedure

Five microliters dephosphorylation buffer and 0.5 µL CIAP (70,000 U/ml) were added to 50 µL of the restriction digestion reaction, followed by an incubation at 37°C for 1h. Subsequently, the enzyme was heat-denatured at 80°C for 10 min.

#### **4.2.6.12. Agarose gel electrophoresis**

##### Solutions

50-fold concentrated TAE: 2 M Tris, 0.1 M EDTA, Na salt; pH 8.5 (pH was adjusted with glacial acetic acid)

5-fold concentrated DNA loading buffer: 40 % (w/v) sucrose, 0.25 % (w/v) bromophenol blue

##### Experimental procedure

Agarose gel electrophoresis was used for analytical purpose as well as for preparative DNA purification. Agarose concentrations varied between 1.0 % and 1.2 %, depending on the expected size of the DNA fragments. Agarose was dissolved in 50 mL of TAE by heating the mixture in a microwave oven. After cooling down to approximately 50°C the solution was poured into a gel slide (110 x 90 mm).



A gel comb was then placed into the tray to generate gel pockets. The samples were mixed (5 : 1) with 5-fold concentrated DNA loading buffer. The samples were heated to 65°C for 5 min, chilled on ice and briefly centrifuged in a table top centrifuge to collect the condensate. Electrophoresis was conducted at 100 V in TAE buffer (550 ml) for approximately 1.5 h. “PeqGold 100 bp Plus DNA ladder” or “1 kb plus DNA ladder” were used as size standards. To visualise nucleic acids, the gels were incubated in 0.005 % (v/v) ethidium bromide / TAE for 10 min and then inspected on a UV transilluminator. Photographs were taken with a digital camera. For preparative purpose, gels were processed as described in 4.2.6.13.

#### **4.2.6.13. DNA extraction from preparative agarose gels**

DNA from one sample was loaded into two adjacent lanes of an agarose gel. The lane placed next to a DNA standard, named the analytical lane, contained a lower volume than the preparative lane from which the DNA was to be extracted later on. After gel electrophoresis (4.2.6.12.), the part of the gel containing the marker lane together with the analytical lane was cut off with a scalpel and stained with 0.005 % ethidium bromide / TAE for 10 min. The desired band in the analytical lane was marked by cutting it out under UV illumination. Afterwards, the analytical lane was again aligned precisely to the preparative lane of the gel in order to facilitate the cutting out of the desired band from the preparative lane. Isolation of DNA from the agarose fragment was accomplished by the QIAquick gel extraction kit according to the manufacturer’s protocol. The amount of isolated DNA was measured photometrically as described in 4.2.6.6.

#### **4.2.6.14. Ligation of PCR fragments into vector DNA**

Based on 25 ng vector DNA, a 5-fold molecular excess of insert DNA was used for the ligation reaction. The corresponding amount of insert was calculated with the equation:

$$\text{Amount}_{\text{Insert}} = 125 \text{ ng Vector} \times \text{length}_{\text{Insert}} (\text{bp}) / \text{length}_{\text{Vector}} (\text{bp}).$$

Twenty five nanograms vector DNA and the corresponding amount of insert DNA were supplemented with 1  $\mu$ L 10-fold concentrated MBI ligation buffer and 1  $\mu$ L T<sub>4</sub>-ligase (5 U/ $\mu$ L). The reaction mixture was then filled up to a total volume of 10  $\mu$ L with ddH<sub>2</sub>O. The ligation reaction was incubated overnight at 16°C. The next day, the enzyme was inactivated at 65°C for 10 min.

#### **4.2.6.15. Preparation of E. coli DH5 $\alpha$ competent cells**

##### Solutions

TFB I buffer: 30 mM potassium acetate / 100 mM RbCl<sub>2</sub> / 10 mM CaCl<sub>2</sub> / 50 mM MnCl<sub>2</sub> / 15 % (v/v) glycerol; pH 5.8

TFB II buffer: 10 mM MOPS / 10 mM RbCl<sub>2</sub> / 75 mM CaCl<sub>2</sub> / 15 % (v/v) glycerol; pH 7.0

##### Experimental procedure

E. coli DH5 $\alpha$  cells were kindly provided by F. Madeo as an agar plate streakout. Starting from the streakout, a 5 mL bacteria liquid overnight culture was started in antibiotic-free LB medium. For preparation of competent cells, 500 mL antibiotic-free LB medium were inoculated with 1 mL of the overnight culture and incubated on a shaking platform at 37°C until the bacteria suspension reached an OD of 0.5 at a wavelength of 595 nm. Afterwards, the cells were spun down in a Heraeus/Christ Varifuge K (3000 rpm, 4°C, 15 min). The resulting pellet was resuspended in 150 mL TFB I buffer, incubated 15 min on ice and centrifuged again under the aforementioned conditions. Subsequently the pellet was dissolved in 20 mL TFB II buffer. Finally, 100  $\mu$ L aliquots of DH5 $\alpha$  competent cells were frozen in liquid nitrogen and stored at -80°C until further use.

#### **4.2.6.16. Transformation of competent bacterial cells with plasmid DNA**

##### **Transformation of NovagenBlue Singles™ competent cells**

E. coli NovagenBlue Singles™ competent cells were thawed on ice, mixed carefully with 1.5  $\mu$ L of the ligation solution (4.2.6.14.) and incubated on ice for 5 min.

Subsequently the cells were heat-shocked at 42°C for 30 s. After incubation on ice for 2 min, the cells were mixed with 250 µL SOC medium (provided with the cells) and incubated at 37°C for 1 h on a shaking platform. Volumes of 50 - 120 µL were streaked out on antibiotic-containing agar plates, and the plates were incubated overnight at 37°C. On the next day, the plates were checked for the presence of colonies.

### **Transformation of DH5α cells made competent according to 4.2.6.15**

*E. coli* DH5α competent cells were thawed on ice, carefully mixed with 10 µL of the ligation solution (4.2.6.14.) and kept on ice for 10 min. The heat-shock was conducted at 42°C for 2 min. Afterwards, 900 µL antibiotic-free LB medium were added, and the suspension was incubated at 37°C for 1 h on a shaking platform. The process was continued as described for the transformation of NovagenBlue Singles™ competent cells .

### **4.2.7. Bioinformatic tools**

Sequences were compared to the sequence databases at <http://www.ncbi.nlm.nih.gov/> by BLASTN and TBLASTN. Protein motif scan was carried out at <http://smart.embl-heidelberg.de/> and <http://www.ebi.ac.uk/InterProScan/>. Tertiary structure prediction was performed at <http://www.sbg.bio.ic.ac.uk/~phyre/>. Gene reports were compiled at <http://harvester.embl.de>. Protein characterisation was performed at <http://genome-www.stanford.edu/source>. Phylogenetic and molecular evolutionary analyses were conducted using the MEGA software version 3.1 (Kumar et al. 2004). Default parameters were used for bioinformatic analyses, unless indicated otherwise.

### **4.2.8. Reverse transcriptase reaction**

Total RNA was isolated with the RNeasy RNA isolation kit according to the manufacturer's advice. The reaction mixture for RT of RNA contained 5 mM MgCl<sub>2</sub>, 10 mM each of dATP, dGTP, dCTP and dTTP, 25 U AMV RT, 0.625 µg oligo(dT<sub>15</sub>)

adapter primer, 0.625 µg random hexamer primer and 1 µg total RNA in 50 µL of PAN Script NH<sub>4</sub> buffer. After pipetting on ice, the mixture was heated to 42°C, incubated for 1h, inactivated by heating to 95°C for 5 min, diluted 1 : 2 with H<sub>2</sub>O and stored frozen at -80°C. For control purposes, the process was repeated without addition of RT.

## 4.2.9. Conventional RT-PCR

### RT-PCR for analysis of the wdr16 transcription profile

One microliter of cDNA (obtained as described in 4.2.8.) was mixed with 12.5 µL HotStarTaq master mix, 1 µL primer mix (10 µM each) and 10.5 µL H<sub>2</sub>O to give a total volume of 25 µL. The sequences of the PCR primers used were

target	sequence
Wdr16	5'-CCAGGTGCCGAGATGAGATGTTTGTC-3' 5'-TCCTCGGAGCGTGATAGAAGTGATGC-3'
β-actin	5'-GGGTCAGAAGGACTCCTACG-3' 5'-GGTCTCAAACATGATCTGGG-3'

The cycling parameters used were 94°C, 30 s; 58°C, 30 s; 72°C, 1 min (30 times); final elongation (72°C, 5 min). Before thermal cycling, the polymerase was activated by heating the samples to 95°C for 15 min.

### RT-PCR for analysis of Wdr16 splice variants

Two microliters of cDNA (obtained as described in 4.2.8.) were mixed with 12.5 µL HotStarTaq master mix, 4 µL primer mix (10 µM each) and 6.5 µL H<sub>2</sub>O to give a total volume of 25 µL. The sequences of the PCR primers spanning intron 2 of Wdr16 were 5'-TAACGACTAGGAGACGCT-3' and 5'-CAGCTCCCTCTTCTTAAA-3'. The cycle parameters used were 94°C, 30 s; 55°C, 30 s; 72°C, 20s (30 times); final elongation (72°C, 10 min). Before thermal cycling, the polymerase was activated by heating the samples to 95°C for 15 min.

#### 4.2.10. Real-time PCR

Real-time PCR was performed with the FastStart DNA Master SYBR Green I kit according to the manufacturer's instructions. The reaction mixture contained 3 mM MgCl<sub>2</sub>, 0.2 μM of each primer and 2 μL of cDNA (obtained as described in 4.2.8.). PCR was carried out in the LightCycler® instrument over 45 cycles under the following conditions: denaturation at 95°C for 10 s, step-down annealing (67°-57°C; 1°/cycle) over 10 cycles and constant annealing temperature of 57°C thereafter for 10 s, elongation at 72°C for 12 s. The primer sequences were

target	sequence
Wdr16	5'-TGGAATGGCCGACGATGACAGC-3' 5'-CCTCGGAGCGTGATAGAAGTGATG-3'
Spag 6	5'-TGTACCTACCTACCAGCCCTCGAGC-3' 5'-CCTGGCTCTGCTTTTATCTCCTGGA-3'
hydin	5'-AACCTGTCCACTTCCAGACCGTTCTT-3' 5'-CCACGCTGACTTCAGTGCCACC-3'
polaris	5'-GTGAAGAGTGCGAGCTGCGACCAA-3' 5'-GGGCCTCTTTATAGAACTCAGCTGCCT-3'
cyclophilin	5'-GGGGAGAAAGGATTTGGCTA-3' 5'-ACATGCTTGCCATCCAGCC-3'

The specificity of the PCR reaction was verified by melting point analysis and agarose gel electrophoresis. To monitor inter-run variability, a standard with a known invariant CP was included with each run. To generate the standard, RNA from 3 different testes and 3 different EPC was reverse transcribed as described in 4.2.8. and finally combined, resulting in a total volume of 300 μL as invariant standard.

In order to determine the efficiencies of RT-PCR amplification for different primer pairs and RNA sources, a dilution series was prepared from each RNA preparation and subjected to real-time PCR analysis. The CPs obtained from these experiments were plotted against the logarithms of the respective concentrations (undiluted sample set to 1000 arbitrary units) in one diagram per RNA source, and a straight line was obtained from these plots by linear regression analysis. The PCR amplification efficiencies (E) were then calculated from the slopes of the regression lines according to the equation  $E = 10^{(-1/\text{slope})}$ . In those cases in which the Wdr16-specific PCR product could not be obtained from the majority of the diluted solutions, the squared linear correlation coefficient ( $R^2$ ) remained below 0.98, indicating that no

PCR efficiency was obtainable for the RNA source and that the target Wdr16 mRNA had to be assumed to be absent from it. PCR efficiencies derived from regression lines with  $R^2 \geq 0.98$  were used to calculate the amounts of Wdr16 mRNA relative to that of the mRNA for cyclophilin as the standard according to the formula  $A_t/A_c$ .  $A_t = E_{\text{target}}^{-\text{CP}(+)} - E_{\text{target}}^{-\text{CP}(-)}$ ;  $A_c = E_{\text{cyclophilin}}^{-\text{CP}(+)} - E_{\text{cyclophilin}}^{-\text{CP}(-)}$  ( +, presence of RT; -, absence of RT).

#### 4.2.11. Generation of the Wdr16 peptide antibody

For generating a peptide antibody, the peptide with the sequence CQAINTEQNFLHGHGN, corresponding to rat Wdr16 (position 50 - 65), was coupled to sulfosuccinimidyl 4-[N-maleimidomethyl]cyclohexane-1-carboxylate-activated KLH or likewise-activated BSA with the Imject Maleimide Activated Immunogen Conjugation kit according to the manufacturer's advice. The N-terminal cysteine of the peptide is not contained in the Wdr16 sequence, but was added as a linker amino acid necessary to ensure coupling to the carrier. Immunisation of guinea pigs was carried out commercially by Charles River Laboratories, Kisslegg. For the initial immunisation and the subsequent boosts (additional injections of the antigenic peptide) at day 28 and day 56, 0.1 mg of the KLH-conjugated peptide were injected, and final bleeding was carried out at day 70. The BSA-conjugate was stored at  $-20^\circ\text{C}$  until it was used in ELISA experiments.

#### 4.2.12. Affinity purification of the Wdr16 antibody

##### Solutions

Elution buffer: 100 mM glycine; pH 3.0 (adjusted with HCl)

Neutralisation buffer: 1 M Tris/HCl; pH 7.5

##### Experimental procedure

Four milliliters of the SulfoLink<sup>®</sup> Coupling gel slurry were used to charge a gravity-flow column resulting in a gel bed volume of 2 mL. Two milligrams of the antigenic peptide with the sequence CQAINTEQNFLHGHGN were dissolved in 1 mL

Coupling buffer (provided with the kit), loaded onto the column and coupled to the gel matrix via its sulfhydryl groups in a batch procedure. Afterwards, 1.5 mL of the Wdr16 antiserum (4.2.11.) were applied to the peptide-coupled column and the Wdr16 antibody bound to the immobilised peptide was eluted with 8 mL elution buffer. The eluate was collected in 1 mL fractions that were neutralised with 100  $\mu$ L neutralisation buffer. For details refer to the instructions manual provided with the SulfoLink<sup>®</sup> Coupling gel kit.

### 4.2.13. ELISA to determine antibody titer

#### Solutions

Borate buffer:	100 mM boric acid, 25 mM borax, 75 mM NaCl, 0.01 % NaN <sub>3</sub> ; pH 8.4
Blocking solution:	1 % BSA in borate buffer
Washing buffer:	0.2 % Tween 20 in borate buffer
Substrate buffer:	100 mM glycine/NaOH, 1 mM MgCl <sub>2</sub> , 1 mM ZnCl <sub>2</sub> ; pH 10.4
Substrate solution:	1 mg/mL p-nitrophenylphosphate in substrate buffer

#### Experimental procedure

The ELISA was performed in 96 well microtiter plates with round floors. All amounts listed below refer to an individual well.

The wells of the microtiter plate were incubated overnight with 250 ng antigen dissolved in 100  $\mu$ L borate buffer at 4°C. After removal of the antigen solution from the plate by “beating out”, free binding sites were blocked with 200  $\mu$ L blocking solution at 37°C for 1 h. In the meantime, a dilution series of the corresponding antiserum was prepared by diluting in borate-buffer as follows: 1:10, 1: 30, 1:100, 1:300, 1: 10<sup>3</sup>, 1: 10<sup>3.5</sup>, 1:10<sup>4</sup>, 1: 10<sup>4.5</sup>, 1: 10<sup>5</sup>, 1: 10<sup>5.5</sup>, 1: 10<sup>6</sup>. After the microtiter plate had been washed four times with 200  $\mu$ L washing buffer, the rinsed wells were incubated with 100  $\mu$ L of the diluted antiserum at 37°C for 2 h, washed four times with 200  $\mu$ L washing buffer and subsequently incubated at 37°C for 1 h with 100  $\mu$ L of the secondary antibody (goat anti-guinea pig IgG-AP conjugate, diluted 1 : 1,000 in borate buffer). After washing four times with 200  $\mu$ L washing buffer, 100  $\mu$ L of

substrate solution were added to the vials, followed by an incubation at 37°C for 10 min. Finally, the product of the enzymatic reaction was measured in an ELISA reader at a wavelength of 405 nm.

#### **4.2.14. Protein assay (Bradford assay)**

The assay was performed according to Bradford (1976) using the commercially available Bio-Rad dye reagent concentrate. 990 µL of the diluted (1 : 6 with water) reagent were mixed with 10 µL of the sample (prediluted with ddH<sub>2</sub>O if necessary) and incubated at RT for 15 min. Afterwards, 400 µL of the reaction mixture were transferred to a 96 well plate and the absorbance was measured at a wavelength of 595 nm in the ELISA reader. The protein concentrations were calculated from a standard curve prepared with BSA.

#### **4.2.15. Discontinuous SDS PAGE**

SDS PAGE was carried out as described by Laemmli (1970) with the modifications by Garfin (1990).

##### Solutions

Acrylamide solution:	29.2 % (w/v) acrylamide, 0.8 % (w/v) bisacrylamide (Rotiphorese Gel 30)
Running gel buffer:	0.5 M Tris/HCl, pH 8.9
Stacking gel buffer:	1.5 M Tris/HCl, pH 6.8
Electrode buffer:	25 mM Tris, 192 mM glycine, 0.1 % (w/v) SDS; pH 8.5
5-fold concentrated sample buffer:	0.16 M Tris/HCl, 4 % (w/v) SDS, 20 % (w/v) glycerol, 0.38 M mercaptoethanol, 0.008 (w/v) bromophenol blue; pH 6.8



### Preparation of the gels

The gel size was 8 cm x 10 cm x 1 mm. The stacking gels were prepared with 3 % acrylamide at pH 6.8, the running gels with 10 % acrylamide at pH 8.9. The following scheme was used to cast the gels:

Solution	10 % running gel	3 % stacking gel
Acrylamide solution	3.33 mL	0.50 mL
Running gel buffer	2.5 mL	
Stacking gel buffer		1.25 mL
Water	4.05 mL	3.0 mL
	Degassing (2 min)	
10 % (w/v) SDS	100 µL	50 µL
TEMED	20 µL	5 µL
10 % (w/v) APS solution	37.5 µL	200 µL

### Preparation of the samples

Protein solution was mixed with 5-fold concentrated sample buffer and filled up with ddH<sub>2</sub>O to give a final concentration of 1-fold sample buffer in a maximal volume of 18 µL. The mixture was then heated to 95°C for 7 min. After collecting the condensate by brief centrifugation, the samples were applied to the gel.

### Electrophoresis

Electrophoresis was carried out under constant current (35 mA) at RT. When the bromophenol blue front had reached the end of the running gel, the process was stopped. The gels were either stained with Coomassie Brilliant Blue R 250 or used for Western blotting.

## **4.2.16. Coomassie staining of polyacrylamide gels**

### Solutions

Staining solution: 50 % methanol, 40 % H<sub>2</sub>O, 10 % glacial acetic acid, 1 % (w/v) Coomassie Brilliant Blue R 250

Destaining solution: Methanol : H<sub>2</sub>O : glacial acetic acid (3 : 6 : 1)

### Experimental procedure

Polyacrylamide gels were incubated with staining solution at RT for 10 min. Afterwards, gels were briefly rinsed with water and transferred to destaining solution. When the blue background had disappeared and single protein bands became visible, the destaining solution was discarded and the gel was washed with ddH<sub>2</sub>O. Protein bands were documented by a digital camera.

## **4.2.17. Western blot analysis with chemiluminescence detection**

### **Protein Transfer**

#### Solutions

Transfer buffer: 25 mM Tris/ HCl, 192 mM glycine; pH 9.0

Ponceau S solution: 0.2 % (w/v) Ponceau S in 3 % (w/v) trichloroacetic acid

#### Experimental procedure

Thirty micrograms of protein homogenate (4.2.3.) were separated by discontinuous SDS PAGE (4.2.15.). The protein bands were then transferred from the gel to a nitrocellulose membrane using a modification of the protocol described by Burnette (1981).

The nitrocellulose membrane was moistened in transfer buffer. The transfer “sandwich” was packed by piling a plastic lattice, a synthetic fiber mat, a filter paper, the SDS polyacrylamide gel, the nitrocellulose membrane, a filter paper, a synthetic fiber mat and a final plastic lattice. Air bubbles were strictly avoided in the process. The arrangement was inserted into an electroblot chamber filled with transfer buffer. Electrophoretic protein transfer was performed with 140 mA at 4°C for 2 h.

After transfer, the membrane was removed from the transfer chamber and stained by brief immersion in Ponceau S solution. Subsequently the membrane was destained with 0.05 % (v/v) Tween 20 / PBS, washed with PBS and processed as described in the following.

## **Detection of protein bands with enhanced chemiluminescence (ECL) reagent**

### Solutions

Washing buffer: 20 mM Tris/HCl, 150 mM NaCl, 0.02 % (v/v) Tween 20; pH 7.4

Blocking solution: 1-fold concentrated Roti-Block / PBS

Substrate solution: 1 mL ECL solution I + 1 mL ECL solution II

### Experimental procedure

The membrane was incubated overnight with 20 mL blocking solution at RT in order to block unspecific binding sites. It was then washed three times for 5 min with 20 mL washing buffer, and 20 mL of the the guinea pig Wdr16 antiserum (or the corresponding preimmune serum) were added at a dilution of 1:10,000 in washing buffer. The incubation time was 1 h. The membrane was washed three times for 5 min with 20 mL washing buffer before 20 mL of the secondary antibody solution were applied. The secondary antibody was donkey anti-guinea pig IgG conjugated with peroxidase, diluted 1:120,000 in washing buffer. The incubation time was 1 h. The membrane was washed again three times for 5 min with 20 mL washing buffer, rinsed briefly with PBS and then the ECL detection solution (1 ml per membrane) was added to the membrane. After 2 min, the solution was removed, the membrane wrapped in transparent plastic foil and an X-ray film was exposed to it for approximately 5 min in an exposure cassette. The film was developed in an X-ray film developing machine. As a further negative control besides preimmune serum, an excess ( $> 26 \mu\text{M}$ ) of the antigenic peptide against which the antibody had been raised was added to the Wdr16 antiserum solution and incubated at RT for 1 h before it was applied to the membrane.

As loading controls, replica gels were stained with Coomassie Brilliant Blue, as described in 4.2.16.

## **4.2.18. Transfection of A9 fibroblasts**

A9 fibroblasts were trypsinised as described in 4.2.1.4. and seeded in 90 % DMEM / 10 % FCS / PS on 18 mm x 18 mm coverslips that had been placed in culture dishes 35 mm in diameter. After the cells had proliferated to fill approximately 60 % of the

coverslips, the medium was sucked off and replaced by 90 % DMEM / 10 % FCS. The cells were transfected with either 2 µg of pEGFP-N1/Wdr16 recombinant vector DNA or with pEGFP-N1 vector DNA (control). For this purpose, the DNA was combined with 50 µL of 150 µM NaCl solution and was mixed thoroughly with the aid of a vortex mixer. In another reaction tube, 6 µL of “JetPEI”-reagent were combined with 100 µL of 150 µM NaCl solution and mixed thoroughly with the aid of a vortex mixer. Afterwards, the “JetPEI”-containing solution was transferred to the reaction tube with the DNA solution, mixed thoroughly and incubated at RT for 15 min. Subsequently, the transfection solution was added dropwise to the antibiotic-free medium in the culture dishes. After incubation at 37°C for 4 h in an atmosphere consisting of 10 % CO<sub>2</sub> / 90 % air, the medium was exchanged for fresh 90 % DMEM / 10 % FCS / PS. The cells were then incubated under the aforementioned conditions until they had grown to confluency on the next day.

## **4.2.19. Immunofluorescent staining**

### **4.2.19.1. Staining of A9 fibroblasts**

#### Solution

Blocking solution: 10 % goat normal serum / PBS

#### Experimental procedure

For staining, A9 fibroblasts were seeded on coverslips (18 mm x 18 mm) that had been placed in culture dishes 35 mm in diameter. The culture medium was sucked off and the cells on the coverslip were washed three times for 5 min with 2 mL PBS, fixed for 10 min with 2 mL 4 % PFA / PBS, washed again three times for 5 min with 2 mL PBS, incubated for 5 min with 2 mL 0.1 % glycine / PBS and treated with 2 mL 0.15 % glycine / 0.15 % Triton X-100 / PBS for 10 min. Subsequently, the cells were incubated with approximately 100 µL of the guinea pig Wdr16 antiserum or with the corresponding preimmune serum that was directly applied to the coverslip at RT for 2 h. The sera were diluted 1:1,000 in blocking solution. For the peptide competition control, the antigenic peptide was added to the antibody solution to a concentration of 264 µM and incubated at RT for 1 h. After washing three times for 5 min with 2 mL

PBS, approximately 100  $\mu$ L of the secondary antibody solution were applied directly on the cells attached to the coverslip at RT for 1 h. The secondary antibody was a goat anti-guinea pig IgG-Alexa 546 conjugate, diluted 1:4,000 in blocking solution. After washing three times for 5 min with 2 mL PBS, a drop of DAPI-containing Vectashield embedding medium was placed on the coverslip, which was then transferred to a microscope slide for inspection.

#### **4.2.19.2. Staining of rat tissues**

##### Solutions

Blocking solution: 0.9 % (v/v) Triton X-100 in Roti-ImmunoBlock / PBS; pH 7.4

Washing buffer: 0.3 % (v/v) Triton X-100 / PBS; pH 7.4

##### Experimental procedure

Frozen tissue sections (for preparation see 4.2.4.) were brought to room temperature, equilibrated with 60 mL PBS in a glass staining-cuvette for 2 min and fixed with 60 mL 4 % PFA / PBS for 10 min. After washing three times for 5 min with 60 mL PBS, the remaining PFA was inactivated with 60 mL 0.1 % glycine / PBS for 5 min, and the sections were washed again with 60 mL PBS (three times for 5 min), followed by an incubation with 60 mL 0.9 % Triton X-100 / PBS for 10 min. Unspecific binding sites were blocked with approximately 200  $\mu$ L blocking solution in a humid chamber at 37°C for 2.5 h. The blocking solution was applied directly to the tissue sections placed on microscopic slides. Subsequently, the tissue was incubated with approximately 200  $\mu$ L of either the affinity-purified guinea pig anti Wdr16 antibody solution (4.2.12.) at 37°C for 30 min, or the corresponding preimmune serum solution. The dilution of the first antibody was 1:200 in blocking solution. For the preabsorption control, the antigenic peptide was incubated at a concentration of 264  $\mu$ M with a 1:100 dilution of the Wdr16 antibody in PBS at RT for 1 h. It was subsequently centrifuged at high speed in a table top centrifuge, and the supernatant was then employed just like the Wdr16 antibody for which it was to serve as the control. For the further staining, sections were washed three times for 5 min with 60 mL washing buffer in a glass staining-cuvette, followed by an incubation with 200  $\mu$ L of the secondary antibody solution that was applied directly to the tissue sections

placed on microscopic slides at 37°C for 50 min. The secondary antibody was a donkey anti-guinea pig IgG-Cy3 conjugate, diluted 1:1,000 in blocking solution. Finally, sections were washed three times for 5 min in a glass staining-cuvette with 60 mL washing buffer, briefly rinsed in PBS and embedded in a drop of DAPI-containing Vectashield mounting medium under a coverslip.

For double labellings, two consecutive stainings with in-between fixation were performed. Antibodies used for counterstaining of cilia were: monoclonal mouse anti- $\alpha$ -tubulin (diluted 1:1,000) and goat anti-mouse IgG-Alexa 488 conjugate (1:1,000) or rabbit anti-mouse IgG-FITC conjugate (1:2,000). Antibodies used for counterstaining of glycogen phosphorylase were: rabbit antiserum against GP BB (1: 1,000) and goat anti-rabbit IgG-Alexa 488 conjugate (1:1,000).

#### **4.2.19.3. Staining of ependymal primary cultures and astroglial primary cultures**

##### Solutions

Blocking solution: 0.3 % (v/v) Triton X-100 in Roti-ImmunoBlock / PBS; pH 7.4

Washing buffer: 0.1 % (v/v) Triton X-100 / PBS; pH 7.4

##### Experimental procedure

After removal of the culture medium, the cells which had been grown on 18 mm x 18 mm coverslips placed in culture dishes 35 mm in diameter were washed three times for 5 min with 2 mL PBS and fixed with 2 mL 4 % PFA / PBS at RT for 10 min. After washing three times for 5 min with 2 mL PBS, the remaining PFA was inactivated with 2 mL 0.1 % glycine / PBS for 5 min, and the coverslips were washed again with 2 mL PBS (three times for 5 min), followed by an incubation with 2 mL 0.3 % Triton X-100 / PBS for 10 min. Unspecific binding sites were blocked with approximately 100  $\mu$ L blocking solution in a humid chamber at 37°C for 2.5 h. The blocking solution was applied directly to the cells attached to the coverslip. Subsequently, the cells were incubated with approximately 100  $\mu$ L of either the affinity purified guinea pig anti Wdr16 antibody solution (4.2.12.) at 37°C for 30 min, or the corresponding

preimmune serum solution. The dilution of the first antibody was 1:200 in blocking solution. The coverslips in the dish were subsequently washed three times for 5 min with 2 mL washing buffer, followed by an incubation with 100  $\mu$ L of the secondary antibody solution that was applied directly to the cells at 37°C for 50 min. The secondary antibody was a donkey anti-guinea pig IgG-Cy3 conjugate, diluted 1:1,000 in blocking solution. Finally, sections were washed three times for 5 min in the culture dish with 2 mL washing buffer and briefly rinsed in PBS. After the staining procedure, a drop of DAPI-containing Vectashield mounting medium was placed on the coverslip that was finally transferred to a microscope slide for inspection. The peptide competition was performed as described in 4.2.19.2.

For double labellings, two consecutive stainings with in-between fixation were performed using antibody concentrations as described in 4.2.19.2.

### **4.2.20. Separation of bull sperm into head and tail fractions**

The separation of bull sperm into heads and tails was performed according to Hinsch et al. (2003) with the following modifications:

#### Solution

Sucrose solution: 250 mM Sucrose, 1 mM EDTA, 25 mM Tris/HCl; pH 7.2

#### Experimental procedure

Fourteen milliliters of bull-ejaculate/caprogen solution, provided by M. Lautner, were distributed among 14 1.5 mL reaction tubes and centrifuged at 6000 x earth's gravitational acceleration ( $9.81 \text{ m/s}^2$ ; g) at 4°C for 15 min in an Eppendorf table top centrifuge. The resulting supernatant (seminal plasma fraction) was stored at 4°C until the end of the separation process, whereas the sperm-containing pellet was washed three times with sucrose solution. After each washing step, resuspended sperm were spun down again (6000 x g, 4°C, 10 min). The sperm pellet of one reaction tube (total sperm fraction) was resuspended in 200  $\mu$ L PBS and stored at 4°C until the end of the separation process. The remaining aliquots were resuspended in 250  $\mu$ L sucrose solution each and individually exposed to 12

ultrasonic pulses from a Branson sonifier (level 2, output 20 %) to cause separation of sperm heads from tails. Subsequently, fractured sperm from two reaction tubes were spun down (6000 x g, 4°C, 15 min) and the pellet was resuspended in 200 µL PBS (sperm after sonification fraction). The supernatant (supernatant after sonification fraction) was also stored at -20°C. The remaining 11 tubes were centrifuged at 720 x g and 4°C for 40 s. The resulting supernatant mostly contained sperm tails, whereas sperm heads were mainly present in the pellet. The head and tail fractions were further enriched as follows.

The head fractions were washed six times with sucrose solution. Contaminating tails remained in the supernatant after centrifugation (720 x g, 4°C, 40 s). The tail fractions were washed twice with sucrose buffer. Contaminating heads and unfractured sperm were collected in the pellet by centrifugation (720 x g, 4°C, 40 s) and were discarded. After enrichment, the head as well as the tail fractions were pelleted by centrifugation (6000 x g, 4°C, 15 min). The head pellets were suspended in 150 µL PBS (head fraction), and the tail pellets were suspended in 500 µL PBS (tail fraction). After the separation process, the individual fractions were homogenised on ice with 100 sonification pulses using a Branson sonifier (level 2, output 20 %) in the following order: seminal plasma, sperm after sonification, total sperm, tails, heads. The homogenates were cleared by centrifugation at 13600 x g and 4°C for 15 min. The protein content was determined in the resulting supernatant as described in 4.2.14. The protein solution was used in Western blot experiments as described in 4.2.17. Before lysis, a 7 µL aliquot was withdrawn from each individual fraction and transferred to a coverslip, where the separation quality was assessed under a phase contrast microscope. Photomicrographs of each individual fraction were taken with a digital camera.

### **4.2.21. Analysis of Wdr16 in zebrafish embryos**

These experiments were conducted in the laboratory of Hans Martin Pogoda at the Max Planck Institute of Immunobiology in Freiburg.



#### **4.2.21.1. Green fluorescent protein fusion control experiment**

##### Solution

Danieu's buffer: 58 mM NaCl, 0.7 mM KCl, 0.4 mM MgSO<sub>4</sub>, 0.6 mM Ca (NO<sub>3</sub>)<sub>2</sub>, 5 mM HEPES; pH 7.6

##### Experimental procedure

To obtain a wdr16/ gfp fusion protein, a 527 bp fragment of Wdr16 encompassing the antisense morpholino target sequence was amplified from 24 hpf RNA by RT-PCR. Primers were 5'-TCGGATCCCGATTCATAGTCTGAAGCTG-3' and 5'-CGTCTAGAGTTGGTGTACTCTAAGGCGA-3'. The PCR product was cloned via BamHI / XbaI sites into the XLT.GFP<sub>TL</sub>-CS2 vector (gift from the laboratory of R. Moon, Seattle, USA). Capped mRNA of wdr16/gfp was prepared using the Message Machine kit (Ambion) following the manufacturer's instructions after plasmid linearisation with Acc651. wdr16/gfp RNA (25 ng/μL) was coinjected into zebrafish embryos together with wdr16MO (0.66 pmol/nL in Danieu's buffer) and wdr16CoMo in volumes of 1 to 1.5 nL, respectively. Treated embryos were assayed for GFP expression using fluorescence microscopy at mid gastrulation stages.

#### **4.2.21.2. Procedure of Wdr16 knockdown**

##### Solution

Danieu's buffer: 58 mM NaCl, 0.7 mM KCl, 0.4 mM MgSO<sub>4</sub>, 0.6 mM Ca (NO<sub>3</sub>)<sub>2</sub>, 5 mM HEPES; pH 7.6

##### Experimental procedure

The antisense morpholino for Wdr16 (5'-CTTGTGTGTCTTCTGCCATCGTGAT-3') and the corresponding inverse control morpholino (5'-TAGTGCTACCGTCTTCTGTGTGTTC-3') were obtained from Gene Tools Inc. and diluted in Danieu's buffer to a final concentration of 0.066 pmol/nL. Both morpholinos were injected in volumes of 1 to 1.5 nL into zebrafish embryos at the one cell stage as described by Nasevicius and Ekker (2000).

#### **4.2.21.3. Analysis of ciliary beating**

Ciliary beat was observed through an Axiovision 2 microscope (Zeiss, Oberkochen) and recorded by a Lumenera Lu170 highspeed camera connected to a PC. Recorded movies of ciliary beat were played in slow-motion and the beat frequency determined by direct visual counting.

#### **4.2.21.4. In-situ hybridisation**

To generate a DIG-labelled antisense RNA probe for Wdr16, the same fragment used for the GFP fusion construct (4.2.21.1.) was cloned into the pGMTeasy vector (Promega). The orientation of the insert was determined by sequencing, followed by linearisation with BamHI and in vitro transcription using T7 RNA polymerase. Detection of Wdr16 mRNA in whole mount zebrafish embryos by in-situ hybridisation was carried out according to Westerfield (2000).

## 5. References

Acehan D., Jiang X., Morgan D.G., Heuser J.E., Wang X. and Akey C.W. (2002) Three-dimensional structure of the apoptosome: implications for assembly, procaspase-9 binding, and activation. *Mol. Cell* **9**: 423-432.

Afzelius B.A. (2004) Cilia related diseases. *J. Pathol.* **204**: 470-477.

Afzelius B.A. and Mossberg B. (1995) Immotile-cilia syndrome (Primary Ciliary Dyskinesia) including Kartagener Syndrome, in *The Metabolic and Molecular Bases of Inherited Disease*, (Scriver C. R., Beaudet A.L. and Sly W.S., eds) pp. 3943–3954. McGraw-Hill, New York.

Akmayev J.G., Fidelina O.V., Kabolova Z.A., Popov A.P. and Schitkova T.A. (1973) Morphological aspects of the hypothalamo-hypophyseal system. I. Medial basal hypothalamus. An experimental morphological study. *Z. Zellforsch.* **137**: 493-512.

Ansley S.J., Badano J.L., Blacque O.E., Hill J., Hoskins B.E., Leitch C.C., Kim J.C., Ross A.J., Eichers E.R., Teslovich T.M., Mah A.K., Johnsen R.C., Cavender J.C., Lewis R.A., Leroux M.R., Beales P.L. and Katsanis N. (2003) Basal body dysfunction is a likely cause of pleiotropic Bardet-Biedl syndrome. *Nature* **425**: 628-633.

Bajjalieh S. (2004) Trafficking in cell fate. *Nature Genet.* **36**: 216-217.

Banizs B., Pike M.M., Millican C.L., Ferguson W.B., Komlosi P., Sheetz J., Bell P.D., Schwiebert E.M. and Yoder B.K. (2005) Dysfunctional cilia lead to altered ependyma and choroid plexus function, and result in the formation of hydrocephalus. *Development* **132**: 5329-5339.

Bannister C.M. and Chapman S.A. (1980) Ventricular ependyma of normal and hydrocephalic subjects: a scanning electronmicroscopic study. *Dev. Med. Child Neurol.* **22**: 725–735.

## References

---

- Beales P.L. (2005) Lifting the lid on Pandora's box: the Bardet-Biedl syndrome. *Curr. Opin. Genet. Dev.* **15**: 315-323.
- Beisson J. and Wright M. (2003) Basal body/centriole assembly and continuity. *Curr. Opin. Cell Biol.* **15**: 96-104.
- Berger U.V., Tsukaguchi H. and Hediger M.A. (1998) Distribution of mRNA for the facilitated urea transporter UT3 in the rat nervous system. *Anat. Embryol. (Berl)* **197**: 405-414.
- Blacque O.E. and Leroux M.R. (2006) Bardet-Biedl syndrome: an emerging pathomechanism of intracellular transport. *Cell. Mol. Life Sci.* **63**: 2124-216.
- Bradford M.M. (1976) A rapid and sensitive method for quantitation of microgram quantities of protein using the principle of protein-dye binding. *Anal. Biochem.* **72**: 248-254.
- Brightman M.W. and Reese T.S. (1969) Junctions between intimately apposed cell membranes in the vertebrate brain. *J. Cell Biol.* **40**: 648-677.
- Broadhead R., Dawe H.R., Farr H., Griffith S., Hart S.R., Portman N., Shaw M.K., Ginger M.L., Gaskell S.J., McKean P.G. and Gull K. (2006) Flagellar motility is required for the viability of the bloodstream trypanosome. *Nature* **440**: 224-227.
- Brown P.D., Davies S.L., Speake T. and Millar I.D. (2004) Molecular mechanisms of cerebrospinal fluid production. *Neuroscience* **129**: 957-970.
- Bruni J.E. (1998) Ependymal development, proliferation, and functions: A review. *Microsc. Res. Tech.* **41**: 2-13.
- Burnette W.N. (1981) "Western blotting": Electrophoretic transfer of proteins from sodium dodecylsulfate polyacrylamide gels to unmodified nitrocellulose and radiographic detection with antibody and radioiodinated protein A. *Anal. Biochem.* **112**: 195-203.

## References

---

Byrd C.A., Jones J.T., Quattro J.M., Rogers M.E., Brunjes P.C. and Vogt R.G. (1996) Ontogeny of odorant receptor gene expression in zebrafish, *Danio rerio*. *J. Neurobiol.* **29**: 445-458.

Cataldo A.M. and Broadwell R.D. (1986) Cytochemical identification of cerebral glycogen and glucose-6-phosphatase activity under normal and experimental conditions: II. Choroid plexus and ependymal epithelia, endothelia and pericytes. *J. Electron Microsc. Tech.* **15**: 511-524.

Cathcart R.S. and Worthington W.C. (1964) Ciliary movement in the rat cerebral ventricles: Clearing action and direction of currents. *J. Neuropath. Exp. Neurol.* **23**: 609-618.

Chae T.H., Kim S., Marz K.E., Hanson P.I. and Walsh C.A. (2004) The *hyh* mutation uncovers roles for alpha SNAP in apical protein localization and control of neural cell fate. *Nat. Genet.* **36**: 264-270.

Crews L., Wyss-Coray T. and Masliah E. (2004) Insights into the pathogenesis of hydrocephalus from transgenic and experimental animal models. *Brain Pathol.* **14**: 312-316.

Croze E., Usacheva A., Asarnow D., Minshall R.D., Perez H.D. and Colamonici O. (2000) Receptor for activated C-kinase (RACK-1), a WD motif-containing protein, specifically associates with the human type I IFN receptor. *J. Immunol.* **165**: 5127-5132.

Daly L.W. et al. (1957) *Dorland's Illustrated Dictionary*, W.B. Saunders Co., Philadelphia

Davson H. and Segal M.B. (1996) *Physiology of the CSF and Blood-Brain Barriers*. CRC Press, Boca Raton.

## References

---

- Davy B.E. and Robinson M.L. (2003) Congenital hydrocephalus in hy3 mice is caused by a frameshift mutation in Hydin, a large novel gene. *Hum. Mol. Genet.* **12**: 1163-1170.
- Del Bigio M.R. (1995) The ependyma: a protective barrier between brain and cerebrospinal fluid. *Glia* **14**: 1-13.
- Diatchenko L., Lau Y.-F.C., Campbell A.P., Chenchik A., Moqadam F., Huang B., Lukyanov S., Lukyanov K., Gurskaya N., Sverdlov E.D. and Siebert P.D. (1996) Suppression subtractive hybridization: A method for generating differentially regulated or tissue-specific cDNA probes and libraries. *Proc. Natl. Acad. Sci. USA* **93**: 6025-6030.
- Diringer M.N., Kirsch J.R., Ladenson P.W., Borel C. and Hanley D.F. (1990) Cerebrospinal fluid atrial natriuretic factor in intracranial disease. *Stroke* **21**: 1550-1554.
- Doetsch F. and Alvarez-Buylla A. (1996) Network of tangential pathways for neuronal migration in adult mammalian brain. *Proc. Natl. Acad. Sci. USA* **93**: 14895-14900.
- Doetsch F., Caille I., Lim D.A., Garcia-Verdugo J.M. and Alvarez-Buylla A. (1999) Subventricular zone astrocytes are neural stem cells in the adult mammalian brain. *Cell* **97**: 703-716.
- Drubin D.G. and Nelson W.J. (1996) Origins of cell polarity. *Cell* **84**: 335-344.
- El-Sawy M. and Deininger P. (2005) Tandem insertions of Alu elements. *Cytogenet. Genome Res.* **108**: 58-62.
- Fawcett D.W. (1975) The mammalian spermatozoon. Review article. *Dev. Biol.* **44**: 394-436.

## References

---

Fleischhauer K. (1972) Ependyma and subependymal layer, in *The Structure and Function of Nervous Tissue*, sixth edition, (Bourne G.H., ed.) pp. 1-46. Academic Press, New York.

Fishman R.A. (1992) Cerebrospinal Fluid in Diseases of the Nervous System. (Saunders W.B., ed.) pp. 1-42. Philadelphia press.

Flock A., Flock B. and Murray E. (1977) Studies on the sensory hairs of receptor cells in the inner ear. *Acta Otolaryngol.* **83**: 85-91.

Gadsdon D.R., Variend S. and Emery J.L. (1979) Myelination of the corpus callosum. II. The effect of relief of hydrocephalus upon the process of myelination. *Z. Kinderchir. Grenzgeb.* **28**: 314-321.

Garfin D.E. (1990) One-dimensional gel electrophoresis. *Meth. Enzymol.* **182**: 425-441.

Geiger H., Bahner U., Palkovits M., Hugo C., Niklas A. and Heidland A. (1989) Atrial natriuretic peptide in brain preoptic areas: implications for fluid and salt homeostasis. *J. Cardiovasc. Pharmacol.* **13**: 20-23.

Gundlach A.L. and Knobe K.E. (1992) Distribution of preproatrial natriuretic peptide mRNA in rat brain detected by in-situ hybridization of DNA oligonucleotides: enrichment in hypothalamic and limbic regions. *J. Neurochem.* **59**: 758-761.

Hamprecht B. and Löffler F. (1985) Primary glial cultures as a model for studying hormone action. *Methods Enzymol.* **109**: 341-345.

Hamprecht B., Glaser T., Reiser G., Bayer E. and Propst F. (1985) Culture and characteristics of hormone-responsive neuroblastoma glioma x hybrid cells. *Methods Enzymol.* **109**: 316-341.

- Haycraft C.J., Swoboda P., Taulman P.D., Thomas J.H. and Yoder B.K. (2001) The *C. elegans* homolog of the murine cystic kidney disease gene Tg737 functions in a ciliogenic pathway and is disrupted in *osm-5* mutant worms. *Development* **128**: 1493-1505.
- Hinsch E., Boehm J.G., Groeger S., Mueller-Schloesser F. and Hinsch K.-D. (2003) Identification of cytokeratins in bovine sperm outer dense fibre fractions. *Reprod. Dom. Anim.* **38**: 155-160.
- Hirschner W., Pogoda H.-M., Kramer C., Thiess U., Hamprecht B., Wiesmüller K.-H., Lautner M. and Verleysdonk S. (2007) Biosynthesis of Wdr16, a marker protein for kinocilia-bearing cells, starts at the time of kinocilia formation in rat, and *wdr16* gene knockdown causes hydrocephalus in zebrafish. *J. Neurochem.* (in press).
- Hong H.K., Chakravarti A. and Takahashi J.S. (2004) The gene for soluble N-ethylmaleimide sensitive factor attachment protein alpha is mutated in hydrocephaly with hop gait (*hyh*) mice. *Proc. Natl. Acad. Sci. USA* **101**: 1748-1753.
- Ibanez-Tallon I., Gorokhova S. and Heintz N. (2002) Loss of function of axonemal dynein *Mdnah5* causes primary ciliary dyskinesia and hydrocephalus. *Hum. Mol. Genet.* **11**: 715-721.
- Ibanez-Tallon I., Heintz N. and Omran H. (2003) To beat or not to beat: roles of cilia in development and disease. *Hum. Mol. Genet.* **12**: 27-35.
- Ibanez-Tallon I., Pagenstecher A., Fliegauf M., Olbrich H., Kispert A., Ketelsen U.P., North A., Heintz N. and Omran H. (2004) Dysfunction of axonemal dynein heavy chain *Mdnah5* inhibits ependymal flow and reveals a novel mechanism for hydrocephalus formation. *Hum. Mol. Genet.* **13**: 2133-2141.
- Irons M.J. and Clermont Y. (1982) Kinetics of fibrous sheath formation in the rat spermatid. *Am. J. Anat.* **165**: 121-130.



- Jarvis C.R. and Andrew R.D. (1988) Correlated electrophysiology and morphology of the ependyma in rat hypothalamus. *J. Neurosci.* **8**: 3691-3702.
- Johanson C.E. (1999) Choroid plexus, in *Encyclopedia of Neuroscience*, (Adelman G. and Smith B.H., eds.) pp 384-387. Elsevier Science, New York.
- Johansson C.B., Momma S., Clarke D.L., Risling M., Lendahl U. and Frisen J. (1999) Identification of a neural stem cell in the adult mammalian central nervous system. *Cell* **96**: 25-34.
- Junqueira L.C. and Carneiro J. (1996) Histologie. Springer –Verlag, Berlin.
- Kahle W., Leonhardt H. and Platzer W. (1990) Taschenatlas der Anatomie Vol. 3, in *Nervensystem und Sinnesorgane*, 6. Auflage. pp. 262-263. Thieme Verlag, Stuttgart.
- Katoh M. (2005) WNT/PCP signalling pathway and human cancer (Review) *Oncol. Rep.* **14**: 1583-1588.
- Kibar Z., Vogan K.J., Groulx N., Justice M.J., Underhill D.A. and Gros P. (2001) Ltap, a mammalian homolog of *Drosophila* Strabismus/Van Gogh, is altered in the mouse neural tube mutant Loop-tail. *Nature Genet.* **28**: 251-255.
- Korr H. (1980) Proliferation of different cell types in the brain. *Adv. Anat. Embryol. Cell Biol.* **6**: 1-69.
- Kramer-Zucker A.G., Olale F., Haycraft C.J., Yoder B.K., Schier A.F. and Drummond I.A. (2005) Cilia-driven fluid flow in the zebrafish pronephros, brain and Kupffer's vesicle is required for normal organogenesis. *Development* **132**: 1907-1921.
- Kumar S., Tamura K. and Nei M. (2004) MEGA3: Integrated software for molecular evolutionary genetics analysis and sequence alignment. *Brief. Bioinform.* **5**: 150-163.
- Laemmli U.K. (1970) Cleavage of structural proteins during the assembly of the head of bacteriophage T4. *Nature* **227**: 680-685.

Lehmann G.L., Gradilone S.A., Marinelli R.A. (2004) Aquaporin water channels in central nervous system. *Curr. Neurovasc. Res.* **1**: 293-303.

Leonhardt H. (1980) Ependym und circumventriculäre Organe, in *Neuroglia I. Handbuch der mikroskopischen Anatomie des Menschen, Teil IV*, 10. Auflage, (Oksche A. and Vollrath L., eds.) pp 177-655. Springer Verlag, Berlin.

Li D. and Roberts R. (2001) WD-repeat proteins: structure characteristics, biological function, and their involvement in human diseases. *Human genome and diseases: Rev. Cell. Mol. Life Sci.* **58**: 2085-2097.

Li J.B., Gerdes J.M., Haycraft C.J., Fan Y., Teslovich T.M., May-Simera H., Li H., Blacque O.E., Li L., Leitch C.C., Lewis R.A., Green J.S., Parfrey P.S., Leroux M.R., Davidson W.S., Beales P.L., Guay-Woodford L.M., Yoder B.K., Stormo G.D., Katsanis N. and Dutcher S.K. (2004) Comparative genomics identifies a flagellar and basal body proteome that includes the BBS5 human disease gene. *Cell* **117**: 541-552.

Liebel U., Kindler B. and Pepperkok R. (2005) Bioinformatic "Harvester": a search engine for genome-wide human, mouse and rat protein resources. *Methods Enzymol.* **404**: 19-26.

Lindemann C.B. and Kanous K.S. (1997) A model for flagellar motility. *Int. Rev. Cytol.* **173**: 1-72.

Littlefield J.W. (1966) The use of drug-resistant markers to study the hybridization of mouse fibroblasts. *Exp. Cell Res.* **41**: 190-196.

Lois C. and Alvarez-Buylla A. (1994) Long-distance neuronal migration in the adult mammalian brain. *Science* **264**: 1145-1148.

Luskin M.B. (1993) Restricted proliferation and migration of postnatally generated neurons derived from the forebrain subventricular zone. *Neuron* **11**: 173-189.

## References

---

Machemer H. and Ogura A. (1979) Ionic conductances of membranes in ciliated and deciliated paramecium. *J. Physiol. (London)* **296**: 49-60.

Maekawa F., Toyoda Y., Torii N., Miwa I., Thompson R.C., Foster D.L., Tsukahara S., Tsukamura H. and Maeda K. (2000) Localization of glucokinase-like immunoreactivity in the rat lower brain stem: for possible location of brain glucose-sensing mechanisms. *Endocrinology* **141**: 375-384.

Manley G.T., Fujimura M., Ma T., Noshita N., Filiz F., Bollen A.W., Chan P. and Verkman A.S. (2000) Aquaporin-4 deletion in mice reduces brain edema following acute water intoxication and ischemic stroke. *Nat. Med.* **6**: 159-163.

Manthorpe C.M., Wilkin G.P. and Wilson J.E. (1977) Purification of viable ciliated cuboidal ependymal cells from the rat brain. *Brain Res.* **134**: 407-415.

Marumo F., Masuda T. and Ando K. (1987) Presence of the atrial natriuretic peptide in human cerebrospinal fluid. *Biochem. Biophys. Res. Commun.* **143**: 813-818.

McLone D.G., Bondareff W. and Raimondi A.J. (1971) Brain edema in the hydrocephalic hy-3 mouse: submicroscopic morphology. *J. Neuropathol. Exp. Neurol.* **30**: 627-637.

McLone D.G., Bondareff W. and Raimondi A.J. (1973) Hydrocephalus-3, a murine mutant: II. Changes in the brain extracellular space. *Surg. Neurol.* **1**: 233-242.

Menkes J.H. and Sarnat H.B. (2000) Neuroembryology, genetic programming, and malformations, in *Child Neurology*, sixth edition, (Menkes J.H. and Sarnat H.B., eds.) pp. 354 – 377. Lippincott, Williams and Wilkins, Philadelphia.

Miekka S.I., Ingham K.C. and Menache D. (1982) Rapid methods for isolation of human plasma fibronectin. *Thrombosis Res.* **27**: 1-14.

Mitchell D.R. (2004) Speculations on the evolution of 9+2 organelles and the role of central pair microtubules. *Biol. Cell* **96**: 691-696.

## References

---

- Montcouquiol M., Rachel R.A., Lanford P.J., Copeland N.G., Jenkins N.A. and Kelley M.W. (2003) Identification of Vangl2 and Scrb1 as planar polarity genes in mammals. *Nature* **423**: 173-177.
- Murdoch J.N., Doudney K., Paternotte C., Copp A.J. and Stanier P. (2001) Severe neural tube defects in the loop-tail mouse results from mutation of Lpp1, a novel gene involved in floor plate specification. *Hum. Mol. Genet.* **10**: 2593-2601.
- Nasevicius A. and Ekker S.C. (2000). Effective targeted gene 'knockdown' in zebrafish. *Nat. Genet.* **26**: 216-220.
- Neer E.J., Schmidt C.J., Nambudripad R. and Smith T.F. (1994) The ancient regulatory-protein family of WD-repeat proteins. *Nature* **371**: 297-300.
- Nguyen T., Chin W.C., O'Brien J.A., Verdugo P. and Berger A.J. (2001) Intracellular pathways regulating ciliary beating of rat brain ependymal cells. *J. Physiol. (London)* **531**: 131-140.
- Nicholson C. (1999) Signals that go with the flow. *Trends Neurosci.* **22**: 143-144.
- Nonaka S., Tanaka Y., Okada Y., Takada S., Harada A., Kanai Y., Kido M. and Hirokawa N. (1998) Randomization of left-right asymmetry due to loss of nodal cilia generating leftward flow of extraembryonic fluid in mice lacking KIF3B motor protein. *Cell* **95**: 829-837.
- Nualart F., Hein S., Rodriguez E.M. and Oksche A. (1991) Identification and partial characterization of the secretory glycoproteins of the bovine subcommissural organ-Reissner's fiber complex. Evidence for the existence of two precursor forms. *Mol. Brain Res.* **11**: 227-238.
- O'Callaghan C., Sikand K. and Rutman A. (1999) Respiratory and brain ependymal ciliary function. *Pediatr. Res.* **46**: 704-707.

- Ono S. (2001) The *Caenorhabditis elegans* unc-78 gene encodes a homologue of actin-interacting protein 1 required for organized assembly of muscle actin filaments *J. Cell Biol.* **152**: 1313-1319.
- Papadopoulos M.C., Krishna S. and Verkman A.S. (2002) Aquaporin water channels and brain edema. *Mt. Sinai J. Med.* **69**: 242-248.
- Park M. and Moon R.T. (2002) The planar cell-polarity gene *stbm* regulates cell behaviour and cell fate in vertebrate embryos. *Nature Cell Biol.* **4**: 20-25.
- Pattisapu J.V. (2001) Etiology and clinical course of hydrocephalus. *Neurosurg. Clin. North Am.* **12**: 651-659.
- Pfeiffer B., Elmer W., Roggendorf W., Reinhart P.H. and Hamprecht B. (1990) Immunohistochemical demonstration of glycogen phosphorylase in rat brain slices. *Histochemistry* **94**: 73-80.
- Prothmann C. (1995) Charakterisierung ependymaler Zellkulturen und Untersuchungen zu ihrem Glycogenstoffwechsel. Diplomarbeit, Universität Tübingen.
- Prothmann C., Wellard J., Berger J., Hamprecht B. and Verleysdonk S. (2001) Primary cultures as a model for studying ependymal functions: glycogen metabolism in ependymal cells. *Brain Res.* **920**: 74-83.
- Purkinje J.E. (1836) Über Flimmerbewegungen im Gehirn. *Müller Arch. Anat. Physiol.* **289**.
- Rinne U.K. (1966) Ultrastructure of the median eminence of the rat. *Z. Zellforsch.* **74**: 98-122.
- Rodriguez E.M., Rodriguez S. and Hein S. (1998) The subcommissural organ. *Microsc. Res. Tech.* **41**: 98-123.

Rodriguez E.M., Oksche A., Hein S. and Yulis C.R. (1992) Cell biology of the subcommissural organ. *Int. Rev. Cytol.* **135**: 39-121.

Röhlich P., Vigh B., Teichmann I. and Aros G. (1965) Electron microscopy of the median eminence of the rat. *Acta Biol. Acad. Sci. Hung.* **15**: 431-457.

Rosenbaum J.L. and Witman G.B. (2002) Intraflagellar transport. *Nature Rev.* **3**: 813-825.

Ross A.J., May-Simera H., Eichers E.R., Kai M., Hill J., Jagger D.J., Leitch C.C., Chapple J.P., Munro P.M., Fisher S., Tan P.L., Phillips H.M., Leroux M.R., Henderson D.J., Murdoch J.N., Copp A.J., Eliot M.M., Lupski J.R., Kemp D.T., Dollfus H., Tada M., Katsanis N., Forge A. and Beales P.L. (2005) Disruption of Bardet-Biedl syndrome ciliary proteins perturbs planar cell polarity in vertebrates. *Nat. Genet.* **37**: 1135-1140.

Roth Y., Kimhi Y., Edery H., Aharonson E. and Priel Z. (1985) Ciliary motility in brain ventricular system and trachea of hamsters. *Brain Res.* **330**: 291-297.

Sapiro R., Tarantino L.M., Velazquez F., Kiriakidou M., Hecht N.B., Bucan M. and Strauss third J.F. (2000) Sperm antigen 6 is the murine homologue of the *Chlamydomonas reinhardtii* central apparatus protein encoded by the PF16 locus. *Biol. Reprod.* **62**: 511-518.

Sapiro R., Kostetskii I., Olds-Clarke P., Gerton G.L., Radice G.L., Strauss III J.F. (2002) Male infertility, impaired sperm motility, and hydrocephalus in mice deficient in sperm-associated antigen 6. *Mol. Cell. Biol.* **22**: 6298-6305.

Sarnat H.B. (1995) Ependymal reactions to injury. A review. *J. Neuropathol. Exp. Neurol.* **54**: 1-15.

## References

---

Sawamoto K., Wichterle H., Gonzalez-Perez O., Cholfin J.A., Yamada M., Spassky N., Murcia N.S., Garcia-Verdugo J.M., Marin O., Rubenstein J.L.R., Tessier-Lavigne M., Okano H., Alvarez-Buylla A. (2006) New neurons follow the flow of cerebrospinal fluid in the adult brain. *Science* **311**: 629-632.

Scott D.E., Krobisch D., Gibbs F.P. and Brown G.H. (1972) The mammalian median eminence, in *Brain-endocrine Interaction. Median Eminence: Structure and Function*. (Knigge K.M., Scott D.E. and Weindl A., eds.) pp 35-49. Karger, Basel.

Segal M.B. (1993) Extracellular and cerebrospinal fluid. *J. Inherit. Metabol. Dis.* **16**: 617-638.

Shi Y. (2002) Apoptosome: the cellular engine for the activation of caspase-9. *Structure* **10**: 285-288.

Shulman J.M. and St. Johnston D. (2000) Pattern formation in single cells. *Trends Genet.* **15**: 60-64.

Silva F.P., Hamamoto R., Nakamura Y. and Furukawa Y. (2005) WDRPUH, a novel WD-repeat-containing protein, is highly expressed in human hepatocellular carcinoma and involved in cell proliferation. *Neoplasia* **7**: 348-355.

Simons M., Gloy J., Ganner A., Bullerkotte A., Bashkurov M., Krönig C., Schermer B., Benzing T., Cabello O.A., Jenny A., Mlodzik M., Polok B., Driever W., Obara T. and Walz G. (2005) Inversin, the gene product mutated in nephronophthisis type II, functions as a molecular switch between Wnt signalling pathways. *Nature Genet.* **37**: 537-543.

Smith T.F., Gaitatzes C., Saxena K. and Neer E.J. (1999) The WD repeat: a common architecture for diverse functions. *Trends Biochem. Sci.* **24**: 181-185.

Sneath and Snokal (1973) Numerical Taxonomy. (Freeman W.H. and Co.) pp. 230-234. San Francisco.

## References

---

- Snell W.J., Pan J. and Wang Q. (2004) Cilia and flagella revealed: From flagellar assembly in *Chlamydomonas* to human obesity disorders. *Cell* **117**: 693-697.
- Sondek J., Bohm A., Lambright D.G., Hamm H.E. and Sigler P.B. (1996) Crystal structure of a G-protein beta gamma dimer at 2.1 Å resolution. *Nature* **379**: 369-374.
- Spassky N., Merkle F.T., Flames N., Tramontin A.D., Garcia-Verdugo J.M. and Alvarez-Buylla A. (2005) Adult ependymal cells are postmitotic and are derived from radial glial cells during embryogenesis. *J. Neurosci.* **25**: 10-18.
- Sterba G. (1969) Morphologie und Funktion des Subcommissuralorgans, in *Zirkumventriculäre Organe und Liquor* (Sterba G., ed) pp.17-27. G.Fischer, Jena.
- Strong L.C. and Hollander W.F. (1949) Hereditary loop-tail in the house mouse accompanied by imperforate vagina and with lethal craniorachischisis when homozygous. *J. Hered.* **40**: 329-334.
- Sumanas S., Larson J.D. and Miller-Bever M. (2003) Zebrafish chaperone protein GP96 is required for otolith formation during ear development. *Dev. Biol.* **261**: 443-455.
- Summerton J. and Weller D. (1997) Morpholino antisense oligomers: design, preparation, and properties. *Antisense Nucleic Acid Drug Dev.* **7**: 187-195.
- Takahashi S., Makita Y., Okamoto N., Miyamoto A. and Oki J. (1997) L1CAM mutation in a Japanese family with X-linked hydrocephalus: a study for genetic counseling. *Brain Dev.* **19**: 559-562.
- Takeda S., Yonekawa Y., Tanaka Y., Okada Y., Nonaka S. and Hirokawa N. (1999) Left-right asymmetry and kinesin superfamily protein KIF3A: new insights in determination of laterality and mesoderm induction by *kif3A*<sup>-/-</sup> mice analysis. *J. Cell Biol.* **145**: 825-836.



## References

---

Taylor J., Abramova N., Charlton J. and Adler P.N. (1998) Van Gogh: a new *Drosophila* tissue polarity gene. *Genetics* **150**: 199-210.

Verleysdonk S. (1994) Herstellung homogener astroglialer Zellkulturen aus Rattenhirn durch ein Mangelmedium und deren Charakterisierung (Diplomarbeit).

Verleysdonk S., Hirschner W., Wellard J., Rapp M., de los Angeles Garcia M., Nualart F. and Hamprecht B. (2004) Regulation by insulin and insulin-like growth factor of 2-deoxyglucose uptake in primary ependymal cell cultures. *Neurochem. Res.* **29**: 127-134.

Verleysdonk S., Kistner S., Pfeiffer-Guglielmi B., Wellard J., Lupescu A., Laske J., Lang F., Rapp M. and Hamprecht B. (2005) Glycogen metabolism in rat ependymal primary cultures: regulation by serotonin. *Brain Res.* **1060**: 89-99.

Voegtli W.C., Madrona A.Y. and Wilson D.K. (2003) The structure of Aip1p, a WD repeat protein that regulates cofilin-mediated actin depolymerization. *J. Biol. Chem.* **278**: 34373-34379.

Wall M.A., Coleman D.E., Lee E., Iniguez-Lluhi J.A., Posner B.A., Gilman A.G. and Sprang S.R. (1995) The structure of the G protein heterotrimer Gi alpha 1 beta 1 gamma 2. *Cell* **83**: 1047-1058.

Ward C.J., Yuan D., Masyuk T.V., Wang X., Punyashthiti R., Whelan S., Bacallao R., Torra R., LaRusso N.F., Torres V.E. and Harris P.C. (2003) Cellular and subcellular localization of the ARPKD protein; fibrocystin is expressed on primary cilia. *Hum. Mol. Genet.* **12**: 2703-2710.

Weibel M., Pettmann B., Artault J.C., Sensenbrenner M. and Labourdette G. (1986) Primary cultures of rat ependymal cells in serum-free defined medium. *Dev. Brain Res.* **25**: 199-209.

- Wellard J., Rapp M., Hamprecht B. and Verleysdonk S. (2003) Atrial natriuretic peptides elevate cyclic GMP levels in primary cultures of rat ependymal cells. *Neurochem. Res.* **28**: 225-233.
- Wellard J., de Vente J., Hamprecht B. and Verleysdonk S. (2006) Natriuretic peptides, but not nitric oxide donors, elevate levels of cytosolic guanosine 3',5'-cyclic monophosphate in ependymal cells ex vivo. *Neurosci. Lett.* **392**: 187-192.
- Westerfield M. (2000) *The Zebrafish Book. A Guide for the Laboratory Use of Zebrafish (Danio rerio)*. 4<sup>th</sup> ed., Univ. of Oregon Press, Eugene.
- Wheatley D.N., Wang A.M. and Strugnell G.E. (1996) Expression of primary cilia in mammalian cells. *Cell Biol. Int.* **20**: 73-81.
- Wilson J.E. (1997) Homologous and heterologous interactions between hexokinase and mitochondrial porin: evolutionary implications. *J. Bioenerg. Biomembr.* **29**: 97-102.
- Wittkowski W. (1967) Zur Ultrastruktur der ependymalen Tanyzyten und Pituizyten sowie ihre synaptische Verknüpfung in der Neurohypophyse des Meerschweinchens. *Acta Anat.* **67**: 338-360.
- Wittkowski W. (1998) Tanycytes and pituicytes: Morphological and functional aspects of neuroglia interaction. *Microsc. Res. Tech.* **41**: 29-42.
- Wolff T. and Rubin G.M. (1998) Strabismus, a novel gene that regulates tissue polarity and cell fate decisions in *Drosophila*. *Development* **125**: 1149-1159.
- Yamamoto T., Vukelic J., Hertzberg E.L. and Nagy J.I. (1992) Differential anatomical and cellular patterns of connexin 43 expression during postnatal development in the rat brain. *Dev. Brain Res.* **66**: 165-180.

## References

---

Zhang Z., Sapiro R., Kapfhamer D., Bucan M., Bray J., Chennathukuzhi V., McNamara P., Curtis A., Zhang M., Blanchette-Mackie E.J. and Strauss J.F. third (2002). A sperm-associated WD repeat protein orthologous to Chlamydomonas PF20 associates with Spag6, the mammalian orthologue of Chlamydomonas PF16. *Mol. Cell. Biol.* **22**: 7993-8004.

Zhengwei Y., Wreford N.G. and de Kretser D.M. (1990) A quantitative study of spermatogenesis in the developing rat testis. *Biol. Reprod.* **43**: 629-635.

## 6. Summary

- Screening of a subtractive ependymal cDNA library of ependyma minus brain and subcommissural organ minus brain revealed the wdr16 gene to be specifically transcribed in ependymal cells.
- Wdr16 is a WD40-repeat protein with two predicted covalently linked 7-bladed  $\beta$ -propellers.
- Wdr16 is evolutionary conserved and restricted to kinocilia-possessing organisms
- The rat ortholog is highly expressed in testis and ependymal primary culture as shown by Western blot analysis.
- RT-PCR studies demonstrate abundant transcription of the rat wdr16 gene in testis and ependymal primary culture, moderate Wdr16 mRNA levels in lung and brain, whilst kinocilia-free tissues are completely devoid of the Wdr16 message.
- In testis as well as in ependymal primary culture, levels for wdr16 transcript increase at approximately the same time and with practically identical time courses as the mRNA for the central apparatus constituent sperm-associated antigen 6 and the protein restricted to ciliated cells and associated with hydrocephalus, hydin.
- The expression of wdr16 is tied to the formation of kinocilia, as demonstrated for testis, ependymal primary culture and the respiratory epithelium.
- In-situ hybridisation experiments in zebrafish indicate that the gene orthologous to wdr16 is only transcribed in kinocilia-expressing cells.
- Blocking the translation of Wdr16 mRNA in zebrafish embryos via antisense morpholinos results in the generation of hydrocephalus, while the ependymal morphology and the ependymal ciliary beat remain unaltered.
- Wdr16 can be considered as a protein that is exclusively expressed in kinocilia-bearing cells, and therefore, considered as a marker for differentiated ependymal cells.
- The physiological relevance of Wdr16 may lie in the generation and/or maintenance of epithelial cell polarity.

---

Meine akademischen Lehrer waren:

Prof. Dr. E.K.F. Bautz  
Prof. Dr. H.-D. Behnke  
Prof. Dr. R. Beiderbeck  
Prof. Dr. K. Beyreuther  
Prof. Dr. P. Bock  
Prof. Dr. H. Bujard  
Prof. Dr. W. Buselmaier  
Prof. Dr. C. Clayton  
Prof. Dr. P. Comba  
Prof. Dr. B. Dobberstein  
Prof. Dr. W. Dröge  
Prof. Dr. D. Dubbers  
Dr. C. Erbar  
Prof. Dr. E. Fuchs  
Prof. Dr. U. Gehring  
Dr. D. Görlich  
Dr. S. Grafström  
Dr. I. Haas  
Prof. Dr. G. Hämmerling  
Prof. Dr. B. Hamprecht  
Prof. Dr. H. Herrmann-Lerdon  
Prof. Dr. U. Hilgenfeld  
Prof. Dr. K. Holmes  
Prof. Dr. E. Hurt  
Prof. Dr. G. Huttner  
Prof. Dr. W. B. Huttner  
Prof. Dr. H. Irngartinger  
Prof. Dr. D. Jeckel  
Prof. Dr. W. Just  
Prof. Dr. J. Knappe  
Dr. B. Knoop  
Prof. Dr. P. Krammer  
Prof. Dr. L. Krauth-Siegel  
Prof. Dr. J. Langowski  
Prof. Dr. P. Leins  
Prof. Dr. T. Leitz  
Prof. Dr. D. Manstein  
Prof. Dr. F. Marks  
Prof. Dr. H. F. Möller  
Prof. Dr. H. W. Müller  
Dr. G. Petersen  
Prof. Dr. T. Rausch  
Dr. K. Rippe  
Prof. Dr. H.U. Schairer  
Dr. G. Schilling  
Prof. Dr. H. Schneider  
Dr. M. Schnölzer  
Prof. Dr. Schölch

Prof. Dr. K. Simons  
Dr. D. Steverding  
Prof. Dr. M. Stitt  
Prof. Dr. V. Storch  
Dr. S. Verleysdonk  
Dr. G. Vogt  
Prof. Dr. H. Wiesinger  
Prof. Dr. R. Zwilling

---

# Lebenslauf

Name: Wolfgang Hirschner

Geburtsdatum: 14. 04. 1976

Geburtsort: Buchen (Odenwald)

1982 – 1986 Grundschule Rippberg

1986 – 1992 Konrad von Dürn Realschule Walldürn  
Abschluss: Mittlere Reife

1992 – 1995 Wirtschaftsgymnasium an der Frankenlandschule Walldürn  
Abschluss: Allgemeine Hochschulreife

1995 – 1996 Wehrdienst beim 4./ Rak.Art.Btl. 122 in Walldürn

1996 – 2001 Studium der Biologie an der Ruprecht - Karls - Universität in Heidelberg

Die Diplomarbeit mit dem Titel „Rolle der Cyclooxygenasen bei der Wundheilung in der Maushaut“ wurde am Deutschen Krebsforschungszentrum unter der Betreuung von Herrn Prof. Dr. F. Marks angefertigt.

Abschluss: Diplom

2001 – 2007 Anfertigung der Doktorarbeit unter der Anleitung von Prof. Dr. B. Hamprecht am Interfakultären Institut für Biochemie der Eberhard - Karls - Universität Tübingen mit dem Titel „ Identification and characterisation of ependyma-specific genes and their proteins.“

Tag der mündlichen Prüfung 13. 04. 2007

Tübingen, 20.04.2007